ABSTRACT

Title of Document: APPLICATION OF LASER SHEAROGRAPHY FOR DETECTING MICROCRACKS IN CONCRETE

Hung Khong, Master of Science, 2007

Directed By: Professor Amde M. Amde
Department of Civil and Environmental Engineering

Laser Shearography method (LSM) has shown a great potential for application in nondestructive testing (NDT) especially in the early detection of cracks in concrete. It is based on a refinement of electronic speckle pattern interferometry (ESPI) that records a sheared image of the speckle interferogram. The speckle interferograms are recorded before and after stressing and then compared to find the defects on the surface of tested object based on localized fringe irregularity.

In this research project, LSM was employed on 3" x 3" x 11.25" concrete prisms subjected to Duggan heat or freeze-thaw treatment prior to storage in limewater. Lasershearography images were taken at distinct intervals to detect the onset of cracking and to measure its subsequent propagation. Data analysis of the results after treatment revealed fine cracks at early ages in the concrete, with resolution better than 10 microns. The freeze-thaw treated concrete specimens exhibited more cracks over time compared to those subjected to the Duggan heat cycle.

APPLICATION OF LASER SHEAROGRAPHY FOR DETECTING THE CRACKS IN CONCRETE

By

Hung Khong

Thesis submitted to the Faculty of the Graduate School of the
University of Maryland, College Park, in partial fulfillment
of the requirements for the degree of
Master of Science
2007

Committee:
Professor Amde M. Amde, Advisor/ Chair
Professor Mohamad S. Aggour
Professor Chung C. Fu

Acknowledgements

First, I thank my adviser, Professor Amde M. Amde for his guidance, support and encouragement throughout my entire research.

Second, I thank Dr. Richard Livingston, Senior Physical Scientist at Turner-Fairbank Highway Research Center (FHWA) in McLean, Virginia for his advice during the course of the research.

I am very grateful to Mr. John Newman, President of Laser Technology, Inc. at Norristown, Pennsylvania for his technical support and assistance in the laser shearography image data processes and acquisitions.

Special thanks to Solomon Ben-Barka at National Ready Mixed Concrete Association Laboratory, College Park, Maryland for his assistance in sample preparations.

Finally, I thank my wife, Huyen, my parents and my good friend, Jorgomai for their support, encouragement and understanding.

Table of Contents

List of Tables

List of Figures

List of Abbreviations and Symbols

ASTM	American Society for Testing Materials
AFm	Monosulfate $C_3A.CaSO_4.12H_2O$
AFt	Ettringite $C_3A.3CaSO_4.32H_2O$
AAR	Alkali-Aggregate Reaction
ACR	Alkali–Carbonate Ractivity (ACR)
ASR	Alkali-Silica Reaction
CH	Calcium Hydroxide $Ca(OH)_2$
C-S-H	Calcium Silicate Hydrate
C_3S	Tricalcium Silicate $3CaO.SiO_2$ Alite
C_2S	Dicalcium Silicate $2CaO.SiO_2$ Belite
C_3A	Tricalcium Aluminate $3CaO.Al_2O_3$ Aluminate
C_4AF	Tetracalcium Aluminoferrite $4Ca.Al_2O_3.FeO_3$ Ferrite
DEF	Delayed Ettringite Formation
ESA	External Sulfate Attack
ESPI	Electronic Speckle Pattern Interferometry
ISA	Internal Sulfate Attack
LSM	Laser Shearography Method
NDT	Nondestructive Testing
W/C	Water to cement ratio by weight

Chapter 1: Introduction

1.1 General

Concrete has been considered a durable material for a long time in serviceability and utilized in many constructions due to its low maintenance cost. However, the formation of cracks in concrete due to physical and chemical factors reduces its ultimate strength and its durability. Understanding the deterioration of concrete related to the properties of the material and its interaction with the environment to which it is exposed is of great importance to the concrete industry.

The effect of temperature on concrete is that it changes its expansive behavior. Unfortunately, concrete is a heterogeneous material and formed by many types of materials with many different sizes. These features make concrete susceptible to uneven changes in volume due to temperature, thus causing cracks and leading to deterioration at a later stage. Two typical physical reasons which introduce cracks in concrete are heat treatment and freeze-thaw cycle.

Many investigations reported that the pre-existing cracks induced during the heat cycle could be the nuclear sites for the formation of ettringite in concrete exposed to moist conditions. The formation of ettringite at later ages in concrete is referred to as delayed ettringite formation (DEF). DEF is of interest due to its effect on the durability of concrete and its complexity. Many researches were conducted to study the effects of ettringite formation on the durability of concrete. DEF is mostly associated with expansion in concrete systems. However the relation between DEF and the expansive behavior of concrete is still a controversial issue. Some researchers blame DEF as the cause for expansion in concrete (Heinz, 1986, Heinz and Ludwig,

1989). These researchers tried to make a correlation between the expansions and weight changes of the examined concrete specimens. They concluded that the gap around the aggregate is a site where ettringite recrystallizes by a through - solution mechanism and this formation causes tensile stress in the concrete resulting in the formation of cracks. However, a contradicting hypothesis is also proposed to explain the expansive behavior of concrete. The researchers supporting this hypothesis provided evidence to show that the expansion of concrete is due to the movement of cement paste away from the aggregates to form the gaps around the aggregates. These gaps become larger because the aggregates do not expand (Skalny et al, 1996). These controversies have become the subject of many debates.

The presence of some new chemical compounds in hardened concrete due to sulfate attack, alkali–silica reactivity (ASR), alkali–carbonate reactivity (ACR), external sulfate attack (ESA), internal sulfate attack (ISA), and chloride attack is classified as chemical attack. The nature of chemical attack is that the chemical reactions will form products which occupy more space than available thus causing cracks in the concrete or that deleterious ions can react with the hydration products. This changes the physical properties of hydration products resulting in the loss of strength of the concrete. Both of the above reasons lead to later deterioration of the concrete. Understanding the chemical process in the concrete helps to mitigate the deterioration of the concrete due to external and internal attacks.

Finding the main reason causing the deterioration of concrete seems unsuccessful when the chemical and physical effects seem to be the combination of

attack mechanisms. Sometimes the physical factors facilitate and accelerate the deterioration induced by chemical factors and vice versa.

1.2 Research Approach

Pre-cast concrete has brought many advantages in applying concrete in structures such as quick installation, ease of controlling the quality of the pre-cast units, and low cost of construction. Concrete in the factory is cured before it is supplied to the construction sites. The temperature during curing has a big effect on the strength development of concrete. The increased early strength at high temperature is obtained because the rate of hydration of cement is accelerated. However, later strength decreases with time and reduces the durability of concrete. The reason is the formation of cracks due to tensile stresses caused by high temperatures during heat treatment. Cracks develop because of relative weakness in tensile strength. Controlling the variables that affect the formation of cracks can minimize later, weaker strength in the service life of concrete.

The formation of cracks in concrete during early states of the hardening process is classified as the main reason for the decrease in the later strength of concrete. It is at first due to the temperature and moist cycles. Apart from the physical factors, some chemical factors such as carbonation attack, sulfate attack, and alkali-silicate reaction also contribute to the formation of cracks. In some chemical attacks, the formation of ettringite due to sulfate attack is the reason for formation of cracks. Ettringite is a complex calcium sulfoaluminate hydrate. Ettringite forms during early states of the hydration process. This formation is not harmful to the

concrete, because at the early state of hydration the cement paste is still in the plastic phase and it can accommodate the change in volume due to the formation of ettringite. During the heat treatment the ettringite decomposes to lower sulfate content and then reforms in the hardened concrete. This reformation of ettringite, regarded as the delayed ettringite formation (DEF) in hardened concrete, causes tensile stress in concrete and extends the micro cracks introduced by the heat treatment. This process seems easily explained for the expansion of concrete because ettringite is observed during the early state of hydration and in the cracks and air voids of pre-cast concrete that exhibiting damage. The problems that emerge are whether DEF is the cause of the expansion of concrete and what exactly the mechanism of DEF is. Many investigations have been developed to give answers for this phenomenon but the results still seem unclear. The deterioration of concrete relates to many variables, therefore further study on this phenomenon need to be explored at a greater depth.

1.3 Problem Statement

The change in volume of concrete is always a problem in the pre-cast concrete industry because it directly affects the durability of concrete. Pre-cast concrete units in structures are expected to have no change in volume because changes in volume will cause cracks in concrete leading to the later deterioration of concrete. During the service life of concrete, structures have to go through many changes in the environment from high temperature in the summer to low temperatures in the winter. These factors will affect the strength development of concrete. Although it is known

that high temperature increases the rate of hydration of cement, the effect of this increase on the strength of concrete needs to be investigated.

The fully understanding of the deterioration process of concrete due to DEF is still controversial and needs further investigation. The correct mechanism of DEF and its effect on the expansion of concrete are not clear not only because of the physical factors but also that the chemical factors can affect the DEF. This study tries to make the correlation between the effect of temperature and the distribution of cracks in concrete. The relation between DEF and expansion of concrete is also addressed in this study.

1.4 Objective and Scope

This research aims to utilize the laser shearography method for detecting the cracks on the surface of concrete that is subjected to two different treatments. The first treatment used in this research is the simulation of the treatment used in the precast concrete industry to obtain high early strength. The other treatment is simulation of the environmental conditions that are common in North America, freeze-thaw cycles. The purpose is to study the effects of different treatments on the formation of micro-cracks and the deterioration of concrete due to delayed ettringite formation.

This study was conducted in two phases and Portland cement type III was used throughout the study. Two different treatments were applied for the two phases. The cement composition, the ratio of sand, aggregate, and water to cement, was kept constant for the two phases except the potassium content (K_2O) of total 1.5% by

weight of cement was added to study the effect of increased K_2O on the pretreatment for crack initiation in the phase II. concrete specimens

Two sets of concrete specimens were batched and then cured under laboratory temperatures for 24 hours. After that, the concrete specimens were stored in the water at room temperature for six days before applying two different treatments, Duggan heat and Freeze-Thaw cycles. All the concrete specimens were stored in the isothermal water bath, pH maintained at 12.5 after treatments, to study the effect of a high alkali level on the deterioration of concrete.

Laser shearography method (LSM) was utilized to detect the initial formation of cracks on the surfaces of the concrete specimens, for instance before and immediately after different treatments and at later stages. The DEF issue is addressed on some aspects such as formation, stability, properties and its effect on the expansion of concrete.

Chapter 2: Cement Chemistry

2.1 Introduction

Portland cement according to ASTM C150 has been defined as hydraulic cement due to its reaction with water to form the hydration products. There are eight types of cement: Types I, IA, II, IIA, III, IIIA, IV, and V used for different purposes. The classification of cement is based upon the proportions in compound composition of the different cements. Each type of cement has been classified by determining the properties of the environment in which the particular concrete has been used in order to resist their effects. The main minerals required in the production of Portland cement are lime (CaO) about 60 – 65 %, silica (SiO_2) about 20 – 25%, and alumina (Al_2O_3) and iron oxide (Fe_2O_3) about 7 – 12% (Atkins, 1997).

This chapter presents the role of cement in concrete, its effect on the durability of concrete and the change in volume. Volume change is the most important parameter of concrete because some deteriorations of concrete come from this factor. There are many types of cement with different compound compositions. Understanding the chemical properties of each component of cement is important in order to choose the right type of cement and the design mix of the concrete correctly, thereby reducing the deterioration of concrete at the later age.

2.2 Composition of Cement Portland

In the manufacture of Portland cement, raw materials, including limestone and clay, are heated in a kiln from 1400^0C to 1600^0C to form calcium silicates. Because of the impurity of the raw materials, there is also the presence of iron and alumina

contents of siliceous raw materials. The products, after heating, including some calcium silicates, iron and aluminum oxides has been called clinker. The presence of iron and alumina content in the clinker can lead to problems of durability and abnormal setting behavior of the cement. Therefore, gypsum is added to the clinker to control the rate of hydration and the setting of cement. The chemistry of cement has a great effect on the properties of concrete because concrete is actually the product of the hydrate reaction of cement. The typical composition of Portland cement includes tricalcium aluminate ($3CaOAl_2O_3$), tricalcium silicate ($3CaOSiO_2$), dicalcium silicate ($2CaOSiO_2$), and tetracalcium aluminoferrite ($4CaOAl_2O_3Fe_2O_3$). The amount of each chemical is determined by the desired properties of concrete such as compressive strength, resistance to sulfate attack, permeability, volume stability and crack control.

2.3 Hydration of Cement

Chemical reactions between cement and water have been named hydrate reactions and the products from these reactions are hydration products. These products are responsible for the hardening of concrete. All the later properties of concrete such as permeability, porosity, expansive behavior and strength development will be affected by the hydration process. The five compounds that constitute Portland cement are tricalcium silicate (C_3S), dicalcium silicate (C_2S), tricalcium aluminate (C_3A), and gypsum ($C\underline{S}H_2$) that is added to the composition of cement to control the flash setting. Hydration of cement includes the decomposing of the silicate, aluminate and ferrite compounds to form the hydration products in the

reaction with water. These products, gaining rigidity with time, are responsible for the development of the strength of concrete. The hydration reaction of cement can be devised into 5 stages depending on the release of heat from the hydration of cement, as shown in figure 2.1. The heat of hydration is proportional to the rate of reaction and is shown in the graph below.

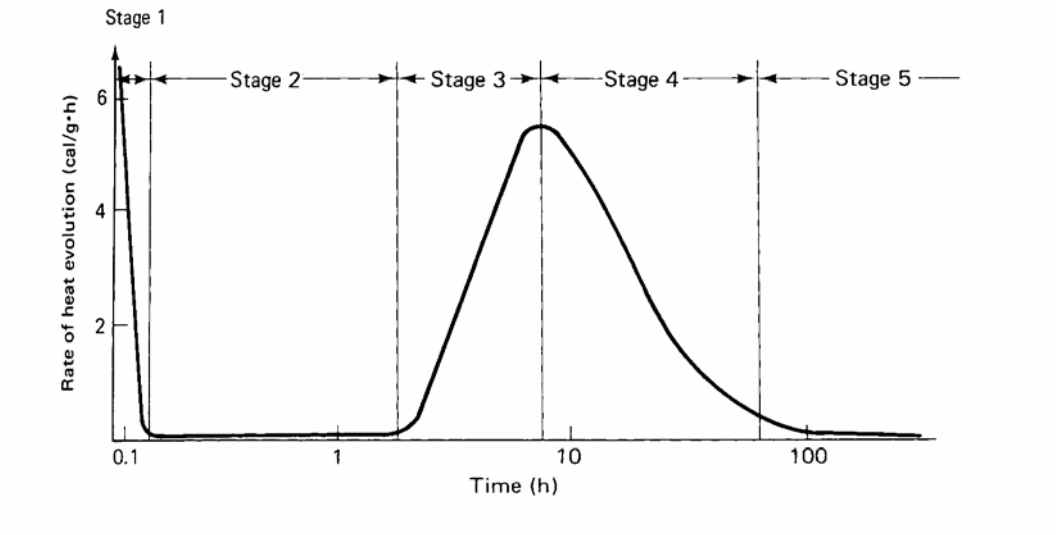

Figure 2.1: Heat of Hydration Stages

During the first 15 minutes, the period of rapid evolution of heat occurs (stage 1), and next, is the inactive period taking place for several hours (stage 2). Portland cement concrete remains in a plastic phase in the second period. After the 2nd period, a series of hydrate reactions occur and results with the release of heat of hydration, the third stage. The 3rd stage is marked by the maximum peak of heat release at the end of this stage. By this time the final set has been passed and early hardening has begun. In the next stage, 4th stage, the rate of hydration slows down until it reaches the stable stage, the 5th stage, within 12-24 hours (Young, 1981).

During the early stages of hydration, cement particles react directly with the water, the true hydrate reaction. This process comes along with the formation of the C-S –H gel. This gel has a low solubility in water as shown by the stability of the hardened concrete and it bonds firmly to the un-reacted cement particles at the later stage. The thickness of the hydrate layer increases and limits the contact between water and un-hydrated cement particles. So the movement of water through the C-S-H gel determines the rate of hydration and hydration becomes diffusion controlled. That is why the rate of hydration is very slow when there is a barrier of hydration products.

Hydration of cement can be seen as an interactive process because the reactions of cement compounds are affected by other processes such as the competition for the sulfate ions of C_3A and C_4AF. Therefore, the reactions of individual compounds must be assessed by referring to the presence of the other compounds. This phenomenon explains the properties of the concrete with different mix designs (Bogue, 1934).

2.3.1 Hydration of Calcium Silicates

Tricalcium silicate (C_3S) and dicalcium silicate (C_2S) are the two major compositions of Portland cement, together constituting 70 – 80% of Portland cement by weight. Therefore, these components contribute a major part of concrete strength and affect the strength development of concrete. The hydration reaction of these calcium silicates can be represented as following:

$$2C3S + 6H \rightarrow C_3S_2H_3 + 3CH \quad \text{….....2.1}$$

$$2C2S + 4H \rightarrow C_3S_2H_3 + CH \quad \text{….....2.2}$$

The productions of these two reactions are the same except for the different proportions of components. The main product, $3CaO.2SiO_2.3H_2O$, is calcium silicate hydrate or gel, C-S-H, which has an indefinite stoichiometry. The gels formed by the reaction of cement with water are almost amorphous, and do not have unique composition (Copeland, 1967). The Ca/Si (C/S) ratio varies between 1.5 and 2 or higher, depending on many factors: age of the paste, temperature of hydration, the water to cement ratio, and the amount and kind of impurity oxides (Chen, 2004).

2.3.2 Hydration of Tricalcium Aluminate and Ferrite Phases

The hydration reaction of tricalcium aluminate (C_3A) with water is violent and results in the undesired flash setting of the cement. So gypsum is added to retard the rate of this reaction. Because the added gypsum causes DEF, the amount of gypsum needs to be limited. The hydration is as follows:

$$C_3A + 3C\underline{S}H_2 + 6H \rightarrow C_6A\underline{S}_3H_{32} \quad \text{….....…2.3}$$

Ettringite forming from the above equation is only stable in an abundant supply of sulfate. With the formation of ettringite the concentration of sulfate decreases as gypsum is used in the equation (2.3). If the sulfate in the solution is

reduced, the ettringite will react with the excessive tricalcium aluminate to form monosulfoaluminate as in the following:

$$2C_3A + C_6A\underline{S}_3H_{32} + 6H \rightarrow 3C_4A\underline{S}H_{12} \quad \text{.....2.4}$$

It is noted that ettringite is only produced in the solution at a high concentration of sulfate ions. The formation of monosulfoaluminate occurs due to the lack of sulfate ions. Therefore, the ettringite will produce again in the hardened concrete when the new sources of sulfate become available, as following:

$$C_4A\underline{S}H_{12} + 2C\underline{S}H_2 + 16H \rightarrow C6A\underline{S}_3H_{32} \quad \text{.....2.5}$$

This delayed ettringite formation is the cause of deterioration of concrete named as sulfate attack.

The reaction of the ferrite phases in general is the same in comparison with that of tricalcium aluminate. The product from this reaction will be formed eventually because the rate of this reaction is lowest. Unlike the reaction of tricalcium aluminate, this reaction of the ferrite phases is lower and releases smaller amounts of heat compared to the heat released from the reaction of C_3A.

$$C_4AF + 3C\underline{S}H_2 + 21H \rightarrow C_6(A,F)\underline{S}_3H_{32} + (A,F)H_3 \quad \text{.....2.6}$$

Practical experience has shown that cement with low amounts of C_3A has the higher ability of sulfate resistance. It means that the transform action of C_3A to C_4AF can limit the reversion of monosulfate to ettringite.

2.3.3 Reaction of Gypsum

Gypsum, ($CaSO_4.2H_2O$) is added to cement during the final grinding to provide sulfate to react with C_3A to form ettringite (calcium trisulfoaluminate). This controls the hydration of C_3A. Without sulfate, cement would set rapidly. In addition to controlling the setting and early strength gain, the sulfate also helps to control drying shrinkage and can influence strength through 28 days. Sulfate can come from the other supplies such as hemihydrate ($CaSO_4.1/2H_2O$) and anhydrate ($CaSO_4$). The added Gypsum slows down the violent reaction between C_3A and water but later forms the ettringite related expansion (Famy, Scrivener and et al, 2001).

The greatest effect of gypsum on the hydration of cement must be its role in the retardation process. Without added gypsum, tricalcium alumanate reacts rapidly with water so that the quick set named flash set occurs. From the equation 2.3, we can see the reaction between gypsum and tricalcium aluminate in the presence of water. This reaction is seen as the retardation reaction in terms of limiting the reaction of tricalcium aluminate with water and gypsum as a retarding agent. This result comes from the dissolving of gypsum in the mixing water with the lime formed by the hydrolysis of the compounds present in the cement. The saturated lime –

gypsum solution depresses the solubility of alumina in the aqueous solution and therefore retards the hydration of the aluminate phases (Lerch, 1946).

2.4 The Properties of The Hydration Product

The products of the hydration reaction include calcium silicate hydrate (C-S-H gel), calcium hydroxide ($Ca(OH)_2$), and calcium sulfoaluminates. In these products, C-S-H gel is difficult to study due to its indefinite stoichiometry and unstable properties.

2.4.1 C-S-H

This is the most difficult product to examine due to its unspecific composition. The formula C-S-H is utilized to represent the main chemistry of the gel. The C/S ratio, varying in the range from 1.5 to 2, depends upon the age of the paste, the temperature of hydration, the ratio of water to cement (w/c), and the amounts and kind of impurity oxides in the clinker (Young, 1981).

The other variable content in the C-S-H gel is water. It can associate with the C-S-H gel in several different states. So water can be released from the C-S-H as the C-S-H is dried or the relative humidity is lowered from 100% due to the strong drying in a vacuum or on heating. The loss of water is completed after 24 hours of heating. Because of the variation in the composition, C-S-H gel does not have a definite stoichiometry. This property will be discussed specifically in the next chapter.

2.5.2 Calcium Hydroxide

Unlike C-S-H gel, Calcium hydroxide (CH) has a definite stoichiometry. It is a well crystallized compound, can be seen by the naked eye, and has distinctive hexagonal prism morphology. Calcium hydroxide grows in the voids formed in the concrete and constitutes about 20% to 25% of the volume of the solid phase in the hydrate products. Any solid material of a comparable stiffness filling in the air voids in the concrete must contribute to the strength of the concrete. Calcium hydroxide also affects the long term durability of concrete due to its high solubility. Leaching of CH facilitates the entry of deleterious ions into the concrete. The high alkalinity of CH contributes to the alkali-aggregate reaction resulting in the expansion of concrete (Cohen, 1982)

Chapter 3: Delayed Ettringite Formation

3.1 Introduction

In the mid 1990's, several cases of concrete deterioration relating to delayed ettringite formation (DEF) were recognized in the precast concrete industry. This phenomenon gained the attention of many researchers due to its uncertainty obout the cause of distress of concrete. Many hypotheses have been proposed to explain the mechanism of deterioration of concrete related to DEF but it is still unclear due to many variables classified as physical and chemical causes that can affect the deterioration process. The characteristic of precast concrete is that it has undergone high temperature curing and later may be exposed to moist conditions. The heat curing of concrete is a process used in the development of high early strength of precast concrete within a short time under normal curing conditions. Moisture condition is usually used to improve the strength gain of concrete after casting. However, this procedure of treatment causes some problem for concrete during its service life. It is believed that preexisting cracks in concrete, the sources of sulfate and moisture condition are the requirements for DEF. This belief is still being debated.

The cracks within concrete are caused by the tensile stress such as alkali silicate reaction (ASR), the high temperature during the heat cure, and freezing-thawing conditions. The ettringite which leads to concrete deterioration is normally found in the cracks and air voids. It is claimed that ASR is accelerated during the heat cure and is the cause of damage in concrete. Actually, ASR provides minor

expansions in concrete but that ASR is the cause of DEF is still unclear. The problem is whether the cracks are requirements for DEF or are formed due to the tensile stress caused by DEF.

Heat curing and subsequent exposure to moisture are the procedures that are applied in the pre - cast concrete industry to establish high early strength of concrete. However the negative effects of this treatment were recognized in the research study of Heinz and Ludwig (2001). Ettringite forms first in the early stage of hydration between C_3A and gypsum and then decomposes during the heat treatment to transform to the monosulfate. The conversion from ettringite to monosulfate releases sulfate ions into the pore solution. These sulfate ions are then absorbed into the CSH structure. Later, when moisture becomes available, metastable monosulfate combines with the released sulfate ions from the CSH structure to form the ettringite. This phenomenon also referred as internal sulfate attack comes along with the forming of cracks in concrete resulting in reduction in compressive strength.

The ability of CSH structure to absorb the aluminum and sulfate ions into the CSH structure is still debatable. It is claimed that, during heat cures, the released sulfate ions from the conversion from ettringite to monosulfate and aluminum ions become available due to the presence of monosulfate. It is then incorporated into the CSH structure which is eventually leached out to the storage solution. The low temperature and alkalis content of the pore solution decrease the solubility of ettringite. During this stage, the other result is that the sulfate gradient, which causes the "chemical force," released sulfate ions from the CSH structure. This is the requirement for DEF resulting in further expansion of concrete.

The DEF phenomenon is mostly associated with the expansive process of concrete. Many researchers have blamed DEF for the deterioration of concrete due to its ability to cause the deleterious expansion of concrete, which is still debatable. Therefore, this problem needs to be further investigated to provide some answers.

3.2 Formation of Etringite

Ettringite forms during the early age of hydration after a few hours mixing with water. At first, Ca ions and Hydroxide ions released from the surface of the cement particles raise the pH to over 12. This is required for the chemical reaction in the pore solution to occur (Young, 2002). Tricacium aluminate will quickly react with the gypsum to form ettringite. This expansive formation is not harmful since the concrete at this stage is still in the plastic phase and can accommodate the change in volume. The rate of this reaction is accelerated in the high pH concentrate solution and the abundant supply of sulfate. However, the early formation of ettringite is innocuous to the durability of concrete because it does not cause any problem to concrete. The ettingite crystals formed are stable at high pH levels of the pore solution in the abundant presence of sulfate ions. With the hydration process, the sulfate level reduces when gypsum is consumed from the reaction to form ettringite and causing the unstable phase of ettringite. At this stage, ettringite tends to transform to another form of a lower sulfate content chemical known as monosulfoaluminate. Monosulfoaluminate is known as a metastable phase and easy to convert to ettringite at a later age. The greatest effect of the formation of ettringite comes from the delayed ettringite formation (DEF) in the hardened concrete. At this

stage, concrete attains a certain rigidity, so it cannot accommodate any change in volume. That is the first step in deterioration of concrete and this deterioration seems easy to explain. However, the condition for the reaction to form the ettringite is under great debate. Many researchers have conducted experimental studies on the DEF problem and have tried to address the condition. Generally, there are three conditions for DEF: the pre-existing cracks are induced by high temperatures during the heat treatment, wetting-drying cycles, freezing-thawing cycles, ASR and mechanical results such as (1), the internal or external supply of sulfate (2), and the moisture conditions (3).

3.2.1 Pre-existing Cracks

Pre-existing cracks in concrete may be provided in many ways including heat cure, ASR with the formation of the gaps around aggregate, freeze-thaw cycles, wetting-drying cycles (Fu et al, 1996, Shayan, 1995, Oberholster et al, 1992 and Tepponen and Eriksson, 1987 and Collepardi, 1999). The presence of cracks tended to cause distress of concrete and facilitate the later formation of ettringite.

Fu et al. (1996) conducted a research study to investigate the effects of micro-cracks induced by heat cure, wetting-drying cycles, freeze-thaw cycles, and loading-unloading cycles on DEF. Only heat treated concrete specimens showed expansion right after the treatment. The expansion can be attributed to the formation of micro - cracks in the cement paste or the interface between cement and aggregate. The conclusion was that the pre-existing cracks were the precursor of DEF. Further growth of DEF in these microcracks will act as sources of expansive pressure. The cracks will extend to become macrocracks as the induced stress increases. The

widening of the cracks increases with the growth of ettringite. The more etttingite that forms in the cracks, the wider the cracks.

However, by comparing the ultimate expansion of the concrete with different treatments after the heat cure, Petrov and Tagnit (2004) confirmed that higher expansion is achieved for concrete returned to the room temperature at the slow rate of 2^{o}C/hour when compared to the expansion of concrete put in the limewater. They concluded that ettringite in microcracks induced by heat cure does not cause any expansion. Actually, the micro-cracks in the heat-cured concrete only accelerate the expansion. The cracking system facilitates the DEF-related expansion. It is reasonable to assume that the cracking systems weaken the cement aggregate bond. The weakened cement paste easily changes the volume resulting in more cracking formation. This is expected to provide more space for DEF-related expansion. The cracking system helps to transport deleterious chemicals that can react with hydrate products and is necessary for DEF.

3.2.2 Supply of Sulfate Ions

Sulfate is present in cement from the manufacturing of cement during the burning process of sulfur rich fuels or organic residues (Miller and Tang, 1996). Some of this sulfur is slowly present as soluble sulfate. This kind of sulfate supply is not helpful for the early formation of ettringite but later it becomes available for the formation of ettringite in the hardened concrete (Hime, 1996). The supply of sulfate provides the sulfate ions for the DEF and is known as internal sulfate attack (ISA). The other supply of sulfate comes from the soils, groundwater, and sea water. These sulfate ions go through concrete by permeable channels to form the ettringite known

as external sulfate attack (ESA). In the presence of calcium hydroxide (CH), water, tricalcium aluminate (C_3A) and the monosulfate (Afm), sulfate ions can react with these chemicals to form ettringite. The products of this reaction occupy larger volume than the reactants and thus cause expansion in concrete and the tensile stress in hardened concrete (Tikalsky, 1989).

The formation of ettringite will be quicker when cement with higher sulfate content is used. Collepardi evaluated the DEF in the laboratory-prepared specimens subjected to different conditions and found that DEF only occurs in the concrete specimens with a high sulfate content of 4% after steam cure at 90^{o}C (1999). No DEF occurs in concrete specimens independently using the cement with total sulfate content of 2 %. He also found that the DEF related to the late sulfate release can occur only if the pre-exiting microcracks are available. This result confirmed the important relationship between late sulfate release and pre-exiting microcracks in the DEF phenomenon.

3.2.3 Moisture Condition

Moisture condition or saturated air condition facilitates the DEF-related expansion to occur. Heinz and Ludwig found that concrete exposed to an environment below 59% R.H could reduce the ultimate degree of expansion (1989). It is noted that the reformation of ettringite needs the full supply of water from the ambient environment for the reaction. Due to the high water content in the structure of ettringite, water absorbed in the concrete reacts with monosulfate, tricalcium aluminate, calcium hydroxide, and unhydrated cement grains to reform the delayed ettringite resulting in a higher degree of expansion (Odler, 1995). Water fills up the

cracking systems in concrete and helps to transport sulfate ions from the external environment and other chemicals necessary for the DEF-related expansion. The degree of expansion still continues as long as concrete is exposed to the moisture condition (Yan, 2004). Field experience showed more severe damage occurs in concrete ties exposed to rain and sun than those exposed to the rain but permanently in shadow conditions (Thaulow et al, 1996, Mielenz et al, 1995). Other researchers studied the effect of moisture condition on concrete ties made with the same cement composition and found that DEF only occurs in wet concrete ties, while there is no DEF in the ones protected from contact with water. These studies confirmed the important role of moisture condition in helping the migration of reactant ions from the cement paste up to the stage where ettringite can be formed.

3.3 Stability of Ettringite

The formation of ettringite is the result of reaction between gypsum and tricalcium aluminate. By using the X-ray diffraction (XRD) analysis, ettringite can be found for the first few hours of hydration and increases in the first few days. After this stage, the amount of ettringite seems to be reduced or increased depending upon some factors. The factors that affect the stability of ettringite can be the composition of cement and environmental conditions.

3.3.1 Cement Composition.

The formation of ettringite comes from the reaction between the chemicals of cement. Thus, the cement composition must control the formation of ettringite.

Many researchers have confirmed that using cements with a high content of sulfate from gypsum and tricalcium aluminate facilitates DEF. The relationship between composition of cement and DEF has been studied by many researchers. However, it is believed that the cement that generates high heat evolution and includes high sulfate content from gypsum will be susceptible to damage related to DEF. Fu and Beaudoin studied concrete made with the cement types I, III and IV and found that concrete made with cement type III was easy to be deteriorated due to DEF (1996). Later, Fu et al (1997) confirmed that the concrete made with cement of high fineness of 5000 cm^2/g and/or high sulfate content of 3.5% or more will expand more than other concretes made with different cement compositions. Obviously, the fineness of cement during hydration will liberate more heat than cement of lower fineness due to the high rate of hydration and the high sulfate content that help to form more ettringite. Some researchers also get the same result when examining the DEF in concrete made with different cement compositions. It is suggested that the concrete with cement of SO_3/Al_2O_3 ($\underline{S}/A$) greater than 0.7 is susceptible to DEF and subsequent deterioration related to DEF. Cement with C_3A content of 10.3% and $\underline{S}/A$ ratio of about 0.85 will exhibit maximum expansion in concrete. Higher content of C_3A and sulfate would result in higher expansion of concrete (Older and Chen, 1996). Heinz and Ludwig believed that the cement with the molar ratio of $\underline{S}/A > 0.67$ or $\underline{S_2}/A$ ratio > 2 is required for damage of concrete related to DEF (1986). So, the composition of cement plays a key role in the deterioration of concrete related to DEF.

3.3.2 High Temperature

Heat treatment is used in the precast concrete industry to provide high early strength concrete and accelerate the hydrate reaction at the early stage. However, excessive heat treatment at temperatures over 70^{o}C will result in expansion related DEF (Taylor, 1997, Lawrence, 1995). Taylor showed that concrete cured at high temperature developed lower strength than those cured at room temperature (1994). It is widely accepted that high temperature over 70^{o}C is the critical temperature for DEF (Day, 1992, Heinz, 1987). At the temperature of 70^{o}C the formation of ettringite will be stopped and the already existing ettringite decomposes to form monosulfate. Monosulfate is a metastable phase in hardened concrete and forms at temperature over 70^{o}C (Heinz and Ludwig, 1998). The decomposing of ettringte at high temperature raises the sulfate content in the pore solution facilitating the formation of monosulfate. Kalousek‘s study showed that the amount of “missing” sulfate ions increases when the concrete was cured at higher temperature (1985). He believed that the missing sulfate ions could be substituted in the CSH gel and these sulfate ions later become the source for DEF.

Many researchers found that there is a wide range of temperatures lower than 60^{o}C at which ettringite is stable. Ettringite can be found in cement paste curing at 25^{o}C after a few hours by X-ray analysis (Taylor, 1990). It can be stable up to 65^{o}C in a dry atmosphere and partially decomposes at 93^{o}C. However, in moist condition, ettringite will decompose to monosulfate at 149^{o}C and to hydrogarnet at 232^{o}C (Mehta, 1972). These results were later confirmed by Satava and Veprok (1975). They found that under hydrothermal condition with the temperature rise of

10^{o}C/minute ettringite will decompose at 111^{o}C to form monosulfate and hemihydrate.

3.3.3 Alkali Condition.

After it is mixed with water, the pH level of pore solution increases due to the dissolution of clinker so that the hydrate reaction can progress. A high pH level is required for hydrate reaction (Young, 1981). Alkalis in clinker come from sulfates such as Na_2SO_4, K_2SO_4 and are responsible for a high pH level of a pore solution. Alkalis content in the pore solution increases ettringite solubility and decreases lime solubility (Daerr, 1977).

In their study on the phase changes of C_3A hydration as a function of pH degree, Gabrisova et al. changed the pH degree of pore solutions by adding $Ca(OH)_2$ or H_2SO_4 and found that the ettringite coexists with monosulfate at pH 11.6 and higher (1991). When the pH decreases, ettringite is unstable at pH lower than 10.7 and then decomposes to form hydrogarnet and gypsum.

Damidot et al. studied the phase changes in the CaO-Al_2O_3-$CaSO_4$-H_2O system at various pH values and found that the upper limit of pH range for the stability of ettringite is expanded by the addition of Na_2O from 12.5 to 13.23 (1993). They concluded that the alkalis increase the stability of ettringite.

3.3.4 The Presence of CO_2.

The effects of CO_2 on the stability of ettringite have been studied by Kuzel using X-ray diffraction analysis (1996). He observed that the increase in ettringite

and monocarbonate comes with the reduction in monosulfate in the cement paste exposed to atmospheric CO_2 under moisture conditions. The presence of CO_2 also prevents the conversion of ettringite to monosulfate. The substitution of SO_4^{2-} by CO_3^{2-} in the monosulfate releases sulfate ions in the pore solution. With the addition of sulfate from carbonation process, monosulfate can react with these sulfate ions to form ettringite. Many researches confirmed the deterioration of concrete due to carbonation process (Taylor, 1997, Sylla, 1988). These researchers also found the evidence that the carbonation process of concrete is contributed to not only by DEF but also by the formation of Thaumasite, the product from the substitution of molecules water by CO_3^{2-}. In fact, Taylor revealed that the replacement of sulfate ions can occur with CO_3^{2-} (1997). It is noted that during the heat treatment there is an amount of sulfate ions absorbed into the gel structure. The sulfate ions can be replaced by CO_3^{2-} into the gel structure which releases sulfate ions into the pore solution to facilitate DEF.

3.4 Mechanism of Expansion Related to DEF

Expansion of concrete during its service life attracts much attention due to many variables that can affect the expansive behavior of concrete. So, there are many views concerning the expansive mechanism of concrete related to DEF. Cohen classified two main streams of hypothesis that can be used to explain the expansive behaviour of concrete (1983). These are the ettringite crystal growth and homogeneous paste expansion hypothesis.

3.4.1 Crystal Growth Hypothesis

This view considers the stress due to the ettringite crystal growth in cracks and the gap between cement paste and aggregate as the cause of expansion. It was first proposed by Heinz and Ludwig in 1986 and later supported by other researchers (Sylla, 1988, Diamond, 1996, Fu et al., 1996, Zhang et al., 2002). These researchers tried to make the correlation between the weight change and the expansion accompanied by the peak in the ettringite formation using XRD analysis. With the result from SEM method, it is concluded that the presence of the pre-existing cracks and the gap between cement paste and aggregate is required for DEF. These cracks and gaps occurred where ettringite recrystallized exerting crystallization pressure. As this pressure is larger than the tensile strength of the cement paste the expansive process occurs.

To cause the expansive pressure, ettringite crystals in the confined space must dissolve into the solution and recrystallize as larger ettringite crystals in the larger space. This process will continue until all the ettringite in the system attains the same level of crystal growth pressure. Furthermore, the ettringite must fill up the cracks and the gaps before it can generate the crystal growth pressure. It is impossible because there are many cracks and gaps in the cement system and not every crack is filled with ettringite crystal. Based on this hypothesis, pre-existing cracks must be present for crystal growth to develop. In properly cured cement, however, where there are no gaps and microcracks may not occur, DEF expansion still occurs (Scrivener and Taylor, 1993).

Deng and Tang in their study calculated the stress caused by the recrystalization phenomenon (1994). They concluded that a higher degree of supersaturation of the

pore solution with respect to ettringite results not only in a larger crystallization pressure but also in a higher rate of ettringite formation. The requirement for DEF expansion is that the concentration of the etttringite in the pore solution must exceed its normal concentration in the saturated pore solution. Then the crystallization pressure will depend on the degree of supersaturation with respect to the ettringite.

3.4.2 Cement Paste Expansion Hypothesis

This hypothesis points out that the width of the gap formed around aggregate particles is always proportional to the size of aggregate particles and the gaps formed in the aggregate (Johansen et al, 1993). Later, many researchers also agreed that cement paste expands while aggregate does not change its volume. Then the cement paste moves away from the surface and contacts with the aggregate. This movement causes the cracks and the gaps around aggregate where ettringite recrystallizes (Shayan, 1992, Skalny, 1996, and Famy, 1999).

The width of the gaps around aggregate has a linear relation with the size of aggregate particles. In his study, Pade et al. pointed out that the relationship between the gap width and the aggregate diameter revealed a linear relationship with slope of 0.008 (1970). This result was measured in one dimension of the mortar sample corresponding with the length change of the mortar samples. For the total expansion this value will be corrected by multiplying it by 2 to account for the expansion of the volume of the mortar samples. So the final result of 0.016 is similar to the real expansion value of 0.0154.

It is easy to imagine that concrete is an inhomogeneous material with many types of constituted materials varying in scale of size. Some factors that can

contribute to the overall expansion of concrete include variation of the local strength of cement paste, the difference in the rate of reaction and the effect of reinforcement. Each component will contribute in different ways in respect to the overall expansion of concrete. So this hypothesis seems more convincing than the previous hypothesis.

3.5 Structure of Ettringite

Ettringite refers to the product of reaction between tricalcium aluminate, sulfate and water. It has the chemical formula is $C_6A\underline{S}_3H_{32}$. Ettringite crystal has the form of needle hexagonal prisms consisting of parallel columns. The sulfate and remaining water molecules lie between the columns (Taylor, 1997).

Figures 3.1 and 3.2 showed clearly the crystal structures of ettringite which consist of four columns in a trigonal structure and channels running parallel to the c-axis of the hexagonal prisms. The composition of the columns is $[Ca_6Al(OH)_6.24H_2O]^{6+}$ and the composition of channels is $[SO_4^3.2H_2O]^{6-}$. Each column includes the chain of polyhedra with one aluminum and three calcium.

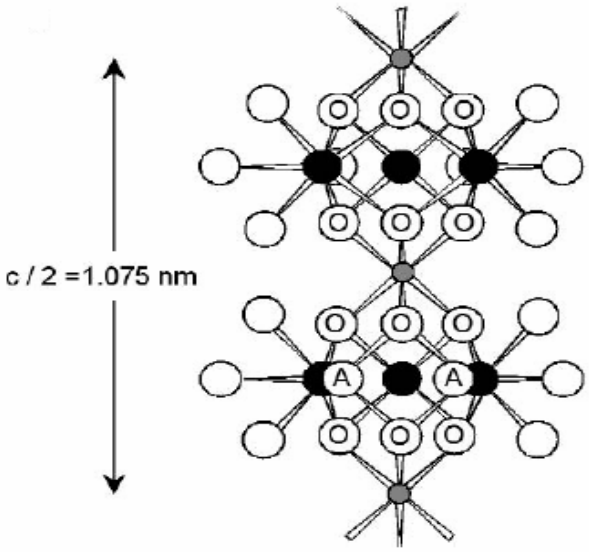

Blank Circles are Water Molecules

Structure of Columns in Ettringite Crystal

(Extracted from Taylor,1997)

Figure 3.1: Sulfate – Ettringite Structure (Molecules)

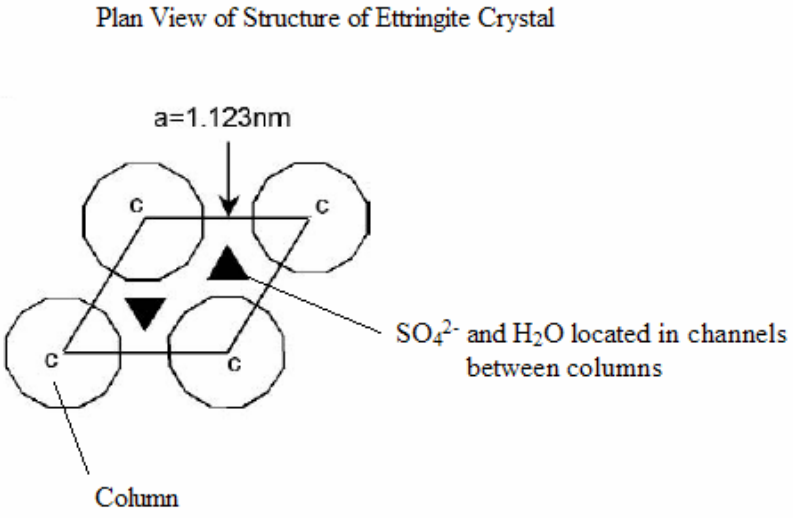

Figure 3.2: Sulfate-Ettringite Structure (Columns and Channels)

3.6 Some Controversies on DEF

The formation of ettringite related to the expansive behavior of concrete is explained in many research studies. However, there are various hypotheses proposed to reveal the mechanism of expansion of concrete. This section discusses recent investigation relating to the DEF phenomenon.

3.6.1 Alkali Silicate Reaction (ASR)

There are many controversies in the coexistence of ASR and DEF especially when the DEF is still unclear. These controversies come from the difficulties encountered when isolating and defining the participation and contribution of each mechanism in the deterioration of concrete. In heat-cured concrete railway ties, improper heat treatment was found to be the main cause of premature deterioration. However, in these deteriorated concretes, ASR and DEF can occur stimulaneously. This poses some difficulty when evaluating the reasons which caused the distress and loss of bond in the concrete.

In their study, Tepponen and Ericksson reported that the damage of concrete railway concrete ties in Finland is due to DEF (1987). Later, Shayan and Quick evaluated the same damage in the prestressed precast railway ties and found that ASR was the cause of damage (1994). They also believed that DEF can only occur at a later stage of deterioration and it would be the consequence of the cracking formation rather than the cause of deterioration of concrete. Some other researchers have also found similar conclusions from their work (Heinz et al., 1986, Sylla, 1988, and Oberholster et al., 1992).

In 1980, Pettifer and Nixon in their study on sulfate attack reported that the rate of ASR increases as the alkalinity of the pore solution increases. Their research confirmed that ASR occurs at the same time with DEF. However, the later research studies suggest that ASR may occur without DEF. Diamond and Ong showed that ASR is accelerated by the heat treatment followed by crystallization of ettringite in the cracks (1994). Later, Shayan and Ivanusec confirmed that ASR accelerated by heat curing is the primary cause of damage in the field concrete (1996). However, the subsequent formation of ettringite in the cracks or the gaps between cement paste and aggregate only cause minor expansion. They also noted that ASR plays a key role in providing cracks in concrete when a maximum curing temperature of 75^{o}C was used. At this temperature, ettringite was destroyed during the heat treatment in a relatively short period of 8 hours. They concluded that the large expansion during and after the heat treatment is due to the ASR and the DEF only provides minor expansion.

3.6.2 The Role of Calcium Silicate Hydrate in DEF

It is noted that the formation of ettringite needs an adequate supply of sulfate ions. These sulfate ions can be provided by the external sulfate supply or internal sulfate supply. During the hydration of cement, there is a large number of ettringite ions from the reaction of tricalcium aluminum with gypsum and water. Then, during the heat treatment, these ettringites decomposed to transform to monosulfate. This transformation releases the free sulfate ions in the pore solution. Many researchers reported that the released sulfate ions will be incorporated into the CSH structure.

Later, during the cooling process these sulfate ions are released from the CSH structure to become the sulfate supply for the delayed ettringite formation.

The role of CSH in the formation of ettringite was studied early by Copeland (1967). In his study, C_3S was treated with various ions to measure the substitution for silicon ions in the CSH structure by these ions. It was reported that aluminum, iron, and sulfate ions can be incorporated into the CSH structure by substituting them for silicon ions into the CSH structure during the heat treatment. In 1987, Odler et al. confirmed that the ettringite disappeared after three days of hydration. The aluminum, iron and sulfate are incorporated in the CSH structure and this phenomenon increases with the high temperature of cement hydration. Similar results were obtained from the study of Fu et al., (1994). When studying the disappearance of gypsum in a mixture by using the different temperature heat treatment for hydration of C_3S, they found that the rate of sulfate adsorption was accelerated at higher temperatures. However, the rate of sulfate adsorption decreased with an increase in temperature. They also concluded that the critical temperature above which sulfate adsorption accelerates is 65^oC.

3.6.3 Freeze-Thaw Conditions and DEF

The correlation between DEF and freeze-thaw condition are still unclear in some studies of damaged field concrete. There are many researches with contracting views on the correlation between DEF and freeze-thaw condition. Some researchers point out that air voids filled with ettringite can contribute to the damage due to the tensile stress exerted by DEF and reduces the freeze-thaw resistance of concrete (Stark and Bollman, 1997, Shao et al, 1997). However, Detwiler gave an opposing

view on the role of DEF (1997). He believed that the deposition of ettringite in air voids may not cause expansion on concrete and the cracks formed by freeze-thaw conditions provide the space for DEF. The study on the correlation of DEF and freeze-thaw resistance for concrete with different cementitious materials was conducted by Ouyang and Lane (1997). In their study, concrete is treated in three cycles, each cycle consisted of wetting at 21^{o}C and drying at 49^{o}C in an oven. They found that the concrete specimens with extensive filling of ettringite in the air voids are more likely to suffer freeze-thaw damage. The moisture condition along with the extent of wetting and drying are the right conditions for DEF in the air voids. Bollman suggested that the action of the wetting and drying process is sufficient for DEF in the air voids and cracks (1997). DEF is facilitated if the concrete is heated at high drying temperature.

Shao et al. conducted the research on the effects of delayed period of concrete before it is subjected to freeze-thaw condition (1997). The length of delayed period seems to be influential in determining the level of deterioration of concrete. The concrete samples of 0.4, 0.5, 0.7 water to cement ratio were subjected to 2 hours precure period at 20^{o}C and followed by heat curing at 70^{o}C or 90^{o}C, then stored in water at 20^{o}C. Expansion measurements were taken and he found that the longer the specimens were stored in the water, the greater the expansion. SEM analysis taken for these concrete specimens shows the presence of ettringite within the cracks and the gap between cement paste and aggregate. It was possible that the heat cure provided some microcracks in the concrete specimens. These cracks and air voids

were then filled with DEF and reduced the freeze-thaw resistance especially for the specimens stored longer in water before applying the freeze-thaw conditions.

In a different view, Detwiler investigated the pavement quality concrete in accordance with ASTM C 666 (1997). The concrete prisms were cast with cement types I and III, air entrain 2 to 6 %. He concluded that ettringite deposited in the air voids could not cause any expansion or contribute to the cracking but the cracks formed due to freeze-thaw condition provided the spaces for DEF to grow.

3.7 Detecting DEF

The visual techniques that are used most for detecting the materials in the cracks, gaps or cavities of the damaged concrete are a scanning electron microscope (SEM) equipped with energy dispersive analyzer x-ray (EDXA), differential scanning calorimetry (DSC), quantitative X-ray diffraction (QXRD), and X-ray computed tomography (X-ray CT). In these methods, SEM seems to be the most powerful technique for detecting materials in terms of shape and position. With the help from chemical analysis, ettringite can be easily detected by using this method (Livingston et al, 2006).

Many researchers have used SEM and EDXA for detecting DEF in the deteriorated concrete (Amde et al, 2005 , Hime, 1996). SEM help to detect the form of DEF and the place where ettringite can be found, EDXA method can provide exactly the chemical content of ettringite in the concrete. Each element is identified on its spectrum by the position of the peak. The chemical composition of ettringite is 6 calcium to 3 sulfur and 2 aluminum.

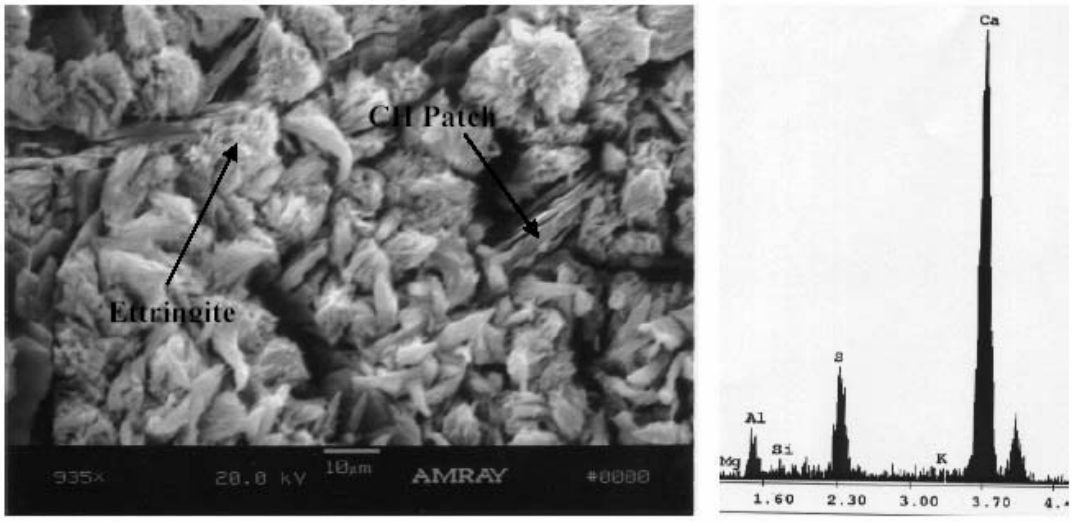

SEM picture of ettringite

EDXA chemical analysis result of ettringite.

Figure 3.3: The SEM image and EDXA chemical analysis of ettringite (Adopted from Ceesay, 2004)

Chapter 4: Laser Shearography Method and Image Analysis Software

4.1 Laser Shearography Method

Laser Shearography Method has been shown to be a great application for non-destructive evaluation (NDE) of integrity of materials. This method is widely used for detecting the flaws on the surface of materials, especially in the automotive and aircraft industries. Finding cracks with the size of a micron unit seems to be difficult. However, with the development of Laser shearography Method (LSM), this difficulty can be overcome. It is an optical method for measuring surface deformation. It is noted that composite materials will deform when stressed. The surface with defects will react weaker with the stressing load. So each position on the surface with defects will be deformed differently with the external stressing sources. The associated change in speckle interference patterns will be compared to find defects within the examined material. This method gains impressive results in non-destructive testing method (NDT) because of its advantages, such as getting high solution images, having quick results, reducing the cost of maintenance, and being applied at the same position over time to monitor the propagation of defects.

For its application in detecting cracks in concrete, the LSM is suitable for detecting and characterizing fine cracks at a very early age. If the cracks are detected when they are still small, the crack formation can be mitigated to eliminate the penetration of water and deleterious chemicals that are necessary for the formation of ettringite.

4.2 Theory of Laser Shearography Method

Laser Shearography Method (LSM) is based on the optical interference technique and uses random pattern of speckles produced by interference of laser light reflected from the optically rough surface (Steinchen, 2003). It is based on the sense of interferometry which occurs when two laser lights with the same wavelength interfere with each other. The laser lights reflect off the object through a shearing device into a camera. The distinguishing feature of this optical method is that because it uses only one laser light and the shearing device, the interference occurs inside the laser shearography device. So this method is not being affected by the environment and is applicable in the field.

Each of the two laser lights can be seen as a spherical wave so the interference of these laser lights will be consistent with Huygens's principle. The interference of these laser lights on the surface of the image device produces the bright speckle pattern if in phase or a dark speckle pattern if out of phase. However, the laser shearography method only records the change in a speckle interference pattern if the first derivative of surface displacement is not zero.

Figure 4.1 shows a typical laser shearography setup in which the modified Michelson Interferometer is utilized as a shearing device. The purpose of the shearing device is to bring two reflected lights from two points on the surface of the tested object into one point on the surface of an image device such as a photography film or device electronic imager. It will form the speckle interferogram. Assuming

that the two laser lights from two points can be represented by the two following equations:

$$U_1 = A_1 e^{i\phi_1} \quad \text{.....4.1}$$

$$U_2 = A_2 e^{i\phi_2} \quad \text{.....4.2}$$

Where: A_1 and A_2 are the light amplitudes.

ϕ_1 and ϕ_2 phase angle of the light wave from two point

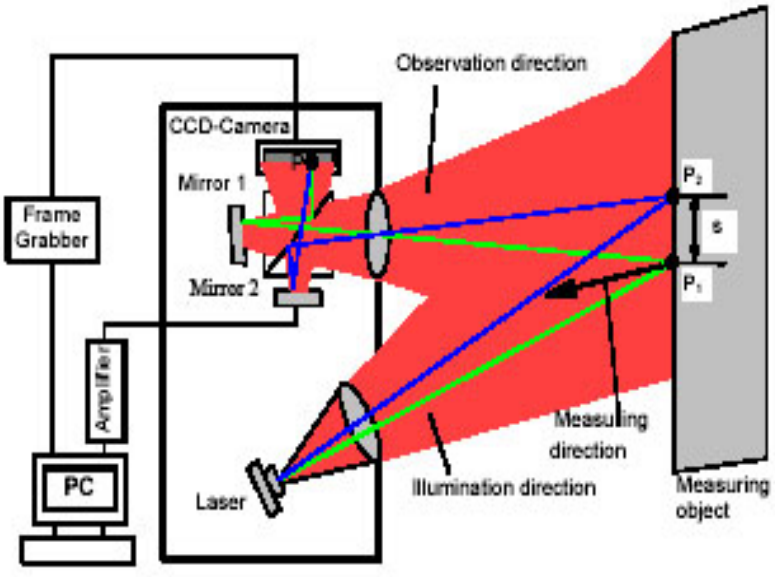

Figure 4.1: The schematic diagram of laser shearography
(Adapted from Yang et al., 2003)

The total light U_t at the point on the surface of the CCD camera can be represented by the following equation:

$$U_t = U_1 + U_2.$$

The intensity at the point P on the surface of the CCD camera can be calculated and that is what the camera can register.

$I = U_t.U_t^* = (A_1 e^{i\phi_1} + A_2 e^{i\phi_2}).(A_1 e^{-i\phi_1} + A_2 e^{-i\phi_2})$

Where : U_t^* is conjugate – complex from U_t.

$$I = (A_1^2 + A_2^2) + 2A_1A_2\cos(\phi_1 - \phi_2)$$

The difference $\theta = \phi_1 - \phi_2$ is the phase difference between the two light waves. After being stressed, the object is deformed resulting in changing the phase difference. It now becomes $\theta' = \theta + \Delta$. The relative phase change, Δ that is related to the relative deformation between two points can be determined from two values θ' and θ (Yang et al, 2003).

In practice, the laser shearography setup is arranged so that the two following equations can be applied.

$$\Delta_x = \frac{4\pi\delta x}{\lambda}\frac{\partial w}{\partial x} \quad \text{..... (4.3)}$$

$$\Delta_y = \frac{4\pi\delta y}{\lambda}\frac{\partial w}{\partial y} \quad \text{..... (4.4)}$$

Where Δx and Δy are the observed relative phase differences in the x and y directions respectively: δx and δy are the actual magnitudes of the introduced shifts; λ is the laser wavelength and w is the magnitude of the displacement vector normal to the surface. The shear displacement δx and δy are known from the properties of the shearing device; it is then possible to extract the spatial first derivatives from the observed relative phase differences (Livingston et al., 2006).

If there is any crack on the surface of the object, this material will be weakened at the position of cracks and will react easier to the stress applied on the surface. At this position the displacement of the materials will be larger. Then, the cracks can be detected due to the localized fringe irregularity.

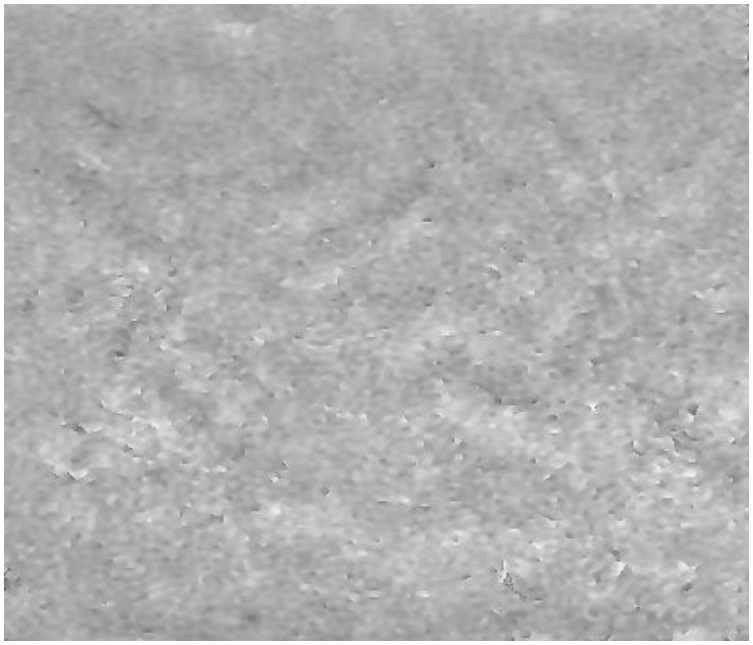

Figure 4.2: Laser Shearograph Image of Concrete Prism Surface –
1 Day After Casting.

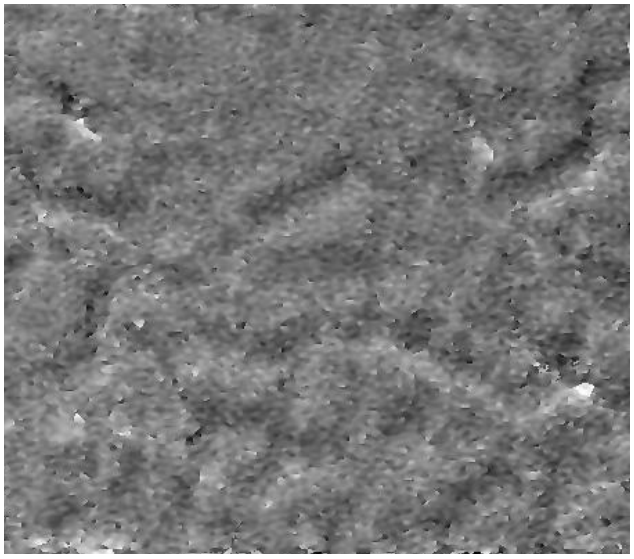

Figure 4.3: Laser Shearograph Image of Concrete Prism Surface After 120 Days in Limewater.

4.3 Method to Cause Stress on The Surface of Materials

Before using the optical interference technique, the surface of the object needed to be stressed to cause the deformation on the surface during the inspection process. There are some methods to cause the stress on the surface of the object such as pressure or thermal, mechanical, and vibration methods. This research uses the shearogaphy device with mounted thermal stressing device. When the object is stressed the surface of the object deforms. The purpose of the stressing process is to cause the laser beam path length used to illuminate the object to change. The associated change pattern in the phase of the laser light also causes the speckle interference pattern to change. Two speckle interferences produced before and after stress will be compared to identify the flaws on the surface of the object.

4.4 Description of Laser Shearography Device

The laser shearography device includes a digital camera, shearing unit, laser device for illumination and a vacuum system for attaching the unit to the surface of the tested object. Choosing the right laser shearography device depends on applications and maintenance cost.

The camera is the device to record the intensity by means of gray level. There are some kinds of commercial cameras with different spatial resolutions. Normally, the camera with a resolution of 700 pixels in horizontal and 600 pixels in vertical direction is suitable for most practical applications.

The shearing unit is the key device for the laser shearography system. The purpose of this unit is to split the reflected light from the object into two laser lights and then recombine them on the plane of the camera where the speckle interference fringes are recorded. So, the most important thing for LSM is to choose the right shearing device. With most laser shearography devices, the modified Michelson Interferometer is used. It helps to change the shearing amount and the direction by changing the tilting angle of mirror M2 (from Figure 4.1).

4.5 Image Analysis Software

Image –Pro® Plus Version 5.0: The Proven Solution for Image is the primary software that is chosen to analyze the concrete's laser shearography pictures. The software, which is designed for Microsoft® Windows 32-bit systems, possesses the advances in acquiring, enhancing and analyzing all kinds of standard image file formats such as TIFF, JPEG, BMP and TGA from a variety of sources including

cameras, microscopes, VCRs and scanners. Beside the properly basic capabilities for such an ideal Image Analysis Software, Image-Pro® Plus Version 5.0 provides an easy-to-use advantage for its users. It is powerful, advanced and, yet, very simple to use.

The ability of the software varies and some of its features are counted as follows:

- Work with gray scale data (8, 12, 16 or 32-bit floating-point depths) and color data (palletized or 24-, 36-, or 48-bit format)
- Trace and count objects manually or automatically.
- Measure object attributes (area, angle, perimeter, etc.)
- View collected data in numerical, statistical or graphic form.
- Sort and classify measurement data according to personalized criteria.
- Collect intensity data and measure intensity by the standard intensity or Optical Density curves.
- Create composite in-focus images from partially focused source images.
- Extract features with spatial tools.
- Manage images using Media Cybernetics' new IQbase product.

Such features created for Image-Pro® Plus Version 5.0 have advantages for the practice of analyzing concrete images.

4.5.1 Major Concepts about the Software

4.5.1.1 Define Image Processing

Image processing manipulates information within an image to make it more distinct to use for each purpose. Digital image processing is a specific type of image processing that is performed with a computer. The first stage in digital image processing is converting the images into numeric form, then all other kinds of processing techniques may take place.

4.5.1.2 Pixel Depth

The digitization process divides an image into a horizontal array of very small regions called picture pixels. Each pixel in the bitmap (which represents the image) is identified based on its position. Pixel depth is the number of bits used to represent the pixel values in an image. Pixel depth also can be called bits-per-pixel (BPP). Each pixel value can be stored from 1 to 32 bits anywhere within the image. A single bit is used for black and white images and 24 bits are used for color images.

4.5.1.3 Image Class

Image is class is determined by the number of bits per pixel (BPP) used to represent each pixel value. However, while the bit depth (BPP) informs how many unique colors an image can possess, it does not inform what colors are actually contained within the image. Image-Pro refers color interpretation as image class and this software supports 8 classes in two models: Gray Scale Models and Color Models.

- Gray Scale Models: Gray Scale pixel values represent a level of grayness or brightness, ranging from completely black to completely white. This class is also referred as “monochrome”.
    - Gray Scale 8: the most common gray scale images because of its advantage from simple 1-byte-per-pixel size and ability to represent any gray scale image, includes 8 BPP, provides 256 distinct levels of gray.
    - Gray Scale 12: a gray scale format generated by many specialized imaging systems and equipment such as infrared camera and medial imaging devices, includes 12 BPP, provides 4096 levels of gray, used for specialized operations and applications.
    - Gray Scale 16: a gray scale generated by many specialized imaging systems and equipment such as infrared camera and medial imaging devices, includes 16 BPP, and provides 65,536 levels of gray, used for specialized operations and applications.
    - Floating Point: a gray scale format that is not native to any device or image format, but is useful for certain arithmetic and filtering operations, includes 32 BPP and provides virtually unlimited number of gray levels.
- Color Models: A color model is a standard way to represent color in mathematic models. Most color models use a 3D-coordinate system and each point within the system’s subspace represents a unique color.

- RGB 24 (RGB stands for Red, Green, Blue): also called True Color bitmap, includes 24 BPP, made up of three separate 8-bit samples. Each sample represents the level of brightness of its respective color channel which ranges within a 256-level scale.
- RGB 36: includes 36 BPP, made up of three separate 16-bit samples, each color channel ranges within a 4095-level scale.
- RGB 48: includes 48 BPP, made up of three separate 16-bit samples, each color channel ranges within a 65535-level scale
- Palette: a convenient way to store images that have fewer than 256 colors, includes 8 BPP, does not represent a brightness value, able to change the color of all pixels with a certain value by simply redefining the contents of entry that certain value in the palette.
- HIS (HIS stands for Hue, Saturation, Intensity): represents a color in terms of how it is perceived by the human eyes, useful for comparing two colors while processing image or for changing a color from one to another.
- HSV (HSV stands for Hue, Saturation and Value): most frequently used in digital image processing, similar to HIS model but in HSV model a pixel's brightness (V) is determined from the mean of the minimum and maximum value of its three color values.
- YIQ (YIQ stands for Y-axis, In-phase and Quadrature): designed to take advantage of the human visual system's greater sensitivity to change in luminance rather than changes in hue or saturation.

4.5.1.4 Spatial Filtering

Filtering operations reduce or increase the rate of change that occurs in the intensity transitions within an image. This is done by detecting and modifying the rate of change at edges which causes sudden or rapid changes in intensity in certain areas of the image. It can increase the intensity differences in a soft edge to make it appear sharper or reduce it in a hard edge to smooth and soften it.

The basic act of filtering operations is to modify a pixel's value based on the values of the pixels around it and then reduce variation among neighboring pixels. Filtering techniques include 2 categories: Convolution/Enhancing Filters and Nonconvolution/Morphological Filters.

- Convolution/Enhancing Filters: Convolution filters process image neighborhoods by multiplying the values within them by a matrix (kernel) of filtering coefficients (integer values). There are three stages in the process:
  - Stage 1: Each pixel in the image neighborhood is multiplied by the contents of the corresponding element in the filtering kernel.
  - Stage 2: The results from the multiplication are summed and divided by the sum of the kernel.
  - Stage 3: The result is scaled and boosted, and used to replace the center pixel in the image neighborhood.

  Image-Pro provides such convolution filters as Lo-pass, Hi-pass, Sharpen, Gauss, Higauss, Local Equalize, Flatten, Median, Rank and many other kinds of Edge Filters.

- Nonconvolution/ Morphological Filters: Nonconvolution filters work with pixel neighborhood only by the data in the neighborhood itself. They use either a statistical method or a mathematic formula to modify the pixel upon which it is focused.

  Image-Pro provides such nonconvolution filters as Erode, Dilate, Open, Close, Tophat, Well, Watershed, Thinning, Pruning, Reduce and Branch/Endpoints.

4.5.1.5 Intensity Analysis

Intensity analysis operations help collect data from the image based upon the intensity values it contains. Image-Pro provides three kinds of intensity analysis tools on the measure menu and they are:

- Histogram Analysis: Measure and illustrate the intensity characteristics of an image in a graph form, can be used to manipulate the image for enhancement purposes or for data gathering purposes to measure the area associated with a specific intensity value.
- Line Profile Analysis: Collect actual index values along a defined line (a profile plot which shows the pixel positions of the line along the X-axis which represents the spatial scale and on the Y-axis that measures the index value for each position along the line).
- Bitmap Analysis: It views the pixel values of the active window in numeric format; pixel values can be displayed as they actually exist in the image or in their calibrated form.

4.5.1.6 Measuring and Counting

Measuring and counting are two of the most powerful capabilities of Image-Pro. There are 3 basic ways to perform measurements by Image-Pro:

- Manually measuring single objects: Measure the length of defined lines or polylines, area of polygons and angles of arcs, automatically trace and measure the edge of an object or feature in the image, measure distance between 2 features and perform tolerance testing.
- Automatically counting and measuring multiple objects: Collect multiple measurements of multiple objects within a single image, count the number of cells in a sample, measure the area, roundness or perimeter of cells and visualize the classified date by plotting it on a scattergram.
- Manually counting and measuring multiple objects: Collect multiple measurements of multiple objects within a single image, select the number of objects in a class (up to 256) and the number of classes in a single image (up to 16) as well as color, symbol and name to identify each class.

4.5.2 Basic Steps

There are 7 basic steps that should be considered to properly perform works with Image-Pro:

- Loading the Image
- Copying and Pasting
- Enhancing the Image
- Working with Filters

- Defining an AOI
- Zooming in on the Image
- Printing and Saving the Image.

4.6 Application of Image Pro Software for Detecting the Cracks

The laser shearography image is digital image that would be analyzed by using the Image Pro Software. The steps for analyzing the data include:

- Cropping the image to get the exact area needed to be analyzed.
- Applying the Gauss filter command to focus on the dark area that represent the cracks.
- Using the trace command to place the black line on the cracks.
- Using the calibration system to facilitate the measuring steps.
- Getting the data from the analyzing process.

Here are some images that illustrate the steps in the Image Pro Software to get the result.

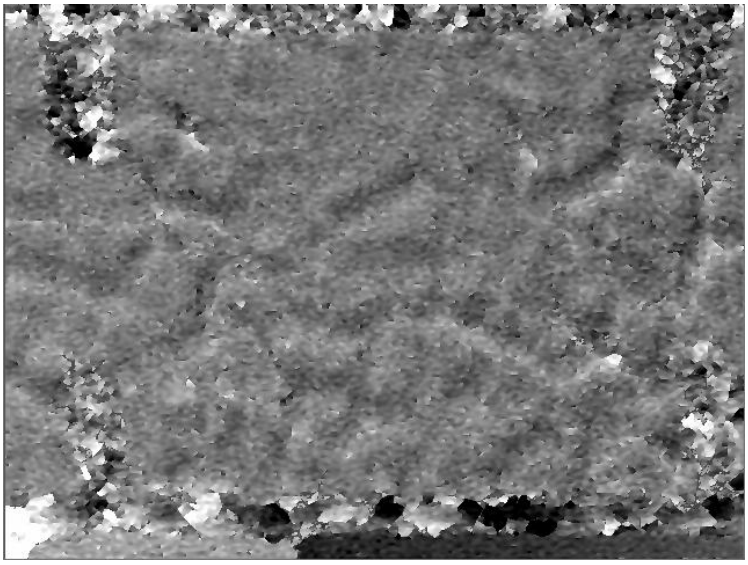

Figure 4.3: Shearography Image before Cropping.

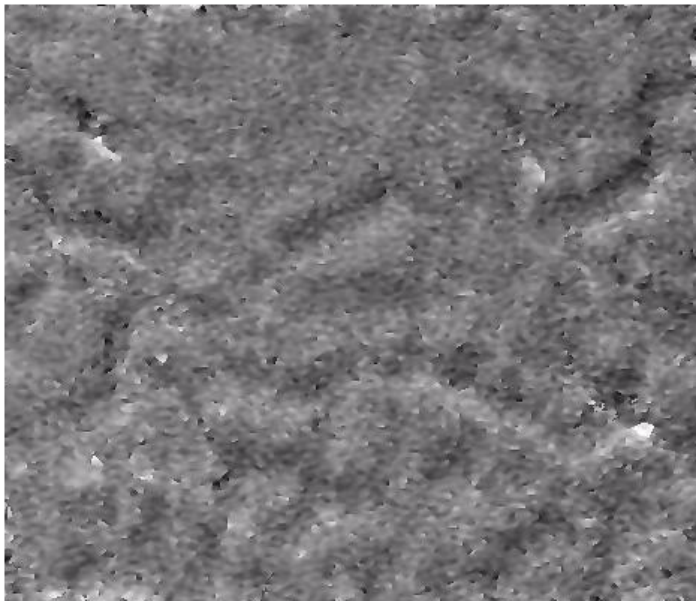

Figure 4.4: Shearography Image after Cropping.

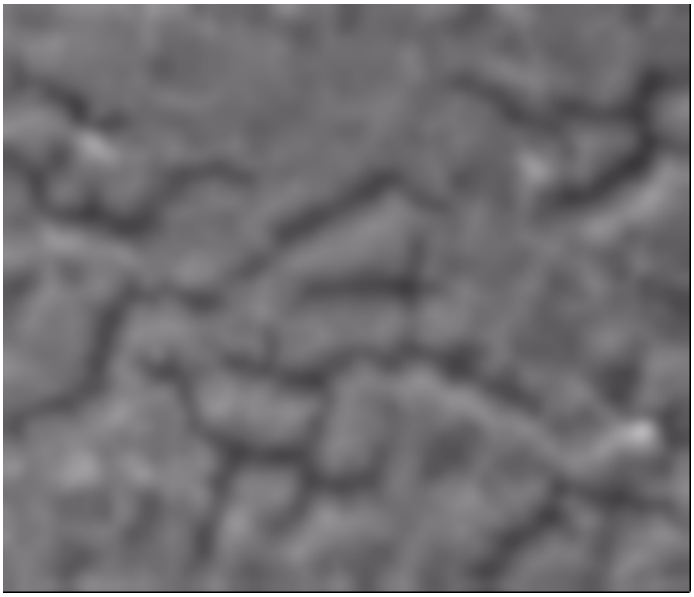

Figure 4.5: Shearography Image after using the Gauss Filter Command.

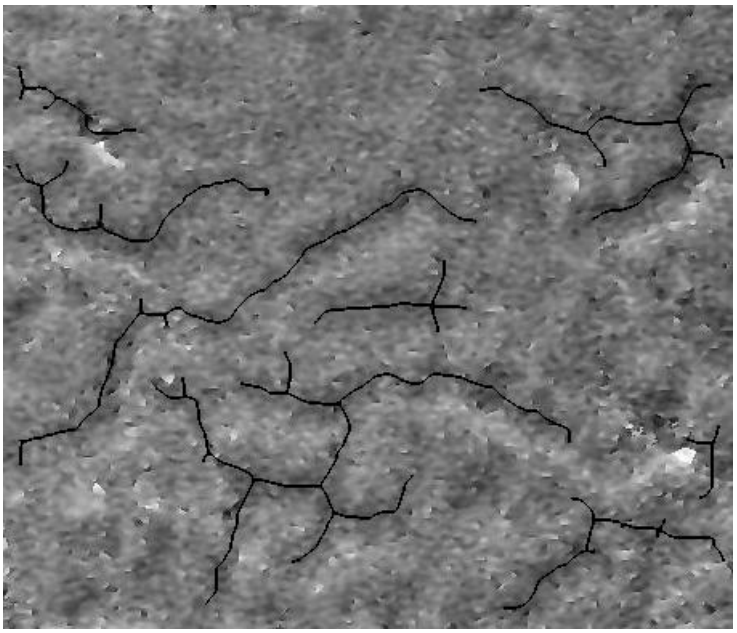

Figure 4.6: Shearography Image with the black line placed on the dark area.

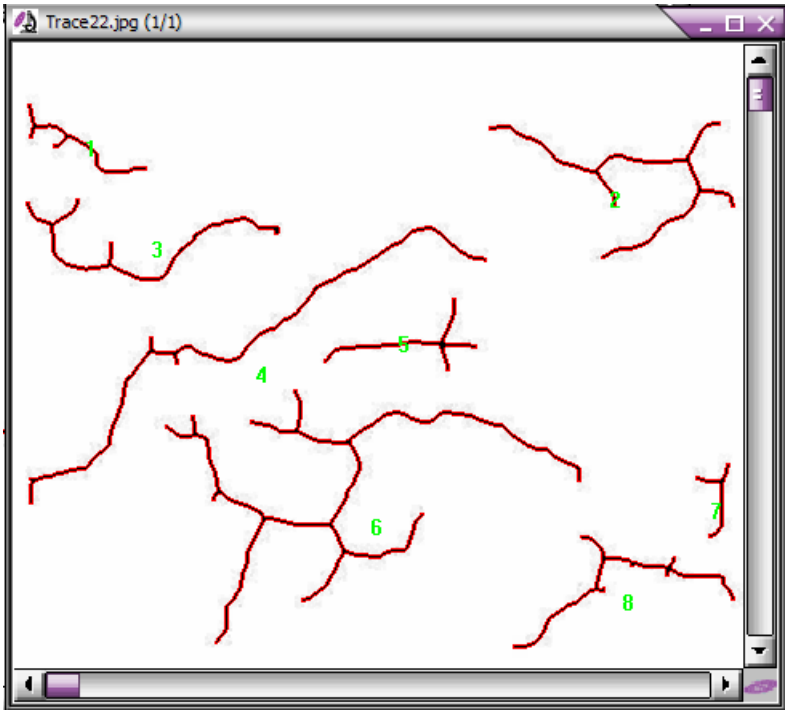

Figure 4.7: Image for crack on the surface of prism.
(After being analyzed by Image Pro Software)

Chapter 5: Sample Preparation and Materials

5.1 Introduction

This chapter details the procedures used in the preparation of the concrete specimens for laser shearography work. After casting for one week, the specimens were subjected to either Duggan heat or freeze-thaw cycles to accelerate DEF and its deleterious expansions.

5.2 Laboratory Specimens

This research study was taken into two series with some variable on the treatment and materials to evaluate the effect of these factors on the cracking phenomenon of concrete. The mixing and casting of the concrete specimens were done according to ASTM C109-99 (ASTM 2001).

Series one concrete specimens were used as a control with no varying parameters. All specimens were cured under ambient temperature and then de-molded after 24 hours of casting. Then, the specimens were stored under water at room temperature for 6 days before subjecting them to the Duggan heat cycle or Freeze-Thaw cycle. After the Duggan heat treatment or Freeze-Thaw cycles, all specimens were stored in the Isothermal water bath with pH maintained at 12.5. This is to evaluate the effect of alkali exposure conditions on the formation of cracks in concrete.

Series two concrete specimens were cured the same as Series one but with additional potassium carbonate (K_2CO_3) added to the mixing water to accelerate the

expansion and DEF. The total potassium (K_2O) content of all the batch mixes was adjusted to 1.5%. All specimens were cured under ambient temperature and then de-molded after 24 hours of casting. Then, all specimens were stored under water at room temperature for 6 days before the Duggan heat treatment or freeze-thaw cycles were applied.

5.2.1 Duggan Heat Cycle

Many researchers confirm that the heat treatment for the first few days after casting has a major effect on the long term durability of concrete. With the excessive heat treatment at high temperature, micro-crack can be produced during the heat treatment. These micro-crack systems will then accelerate the deterioration of concrete at a later age. So the heat treatment (Duggan heat cycle) was used to reveal damage in the laboratory-prepared samples in the shortest amount of time and is intended to accelerate DEF and its associated deleterious expansion.

The Duggan heat cycle consists of three cycles as shown in figure 5.1. The first two cycles included subjecting the specimens to 1 day in a dry oven at 82^{o}C followed by about $1^{1}/_{2}$ hour cooling and 1 day soaking in water at room temperature. In the third cycle, the specimens were left in the oven for 3 days at 82^{o}C. At the end of the third cycle, the specimens were allowed to cool for 2 days at room temperature in the laboratory, and then stored in the isothermal water tank with constant pH of 12.5.

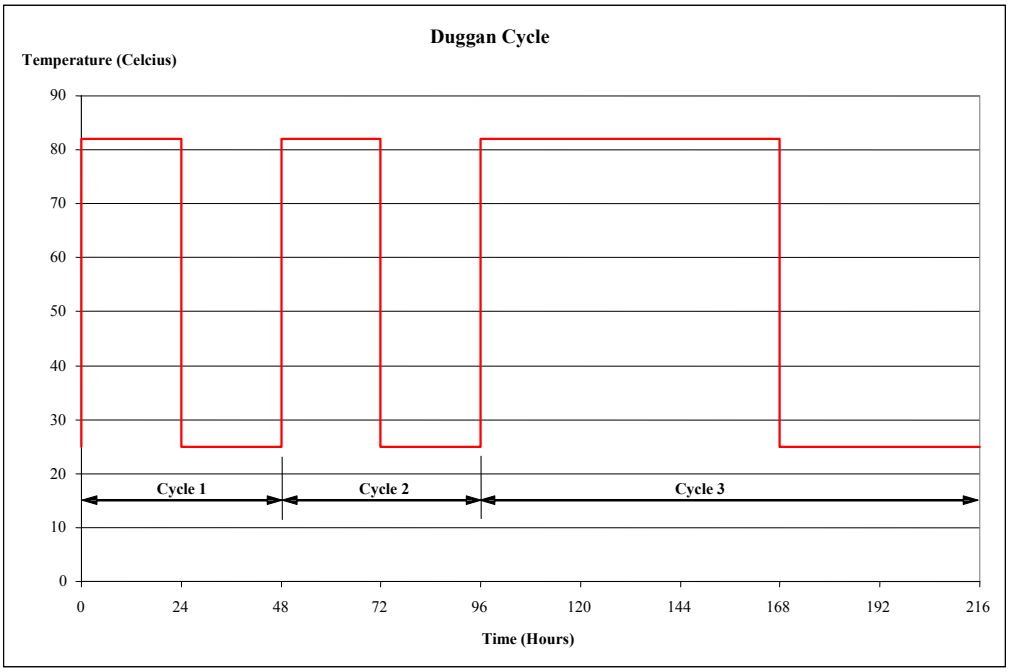

Figure 5.1: Duggan Heat Cycle for Mortar and Concrete Specimens

5.2.2 Freeze-Thaw Cycle

For concrete exposure to the freeze-thaw condition, it is confirmed that there are two factors affecting the durability of concrete. At low temperature, some of monosulfate in the cementious system is transformed to ettringite. The other factor is that the freeze-thaw cycles facilitate the formation of microcracks in concrete (Ludwig, 1992). However, some researchers also reported that the ettringite deposited in the microcracks introduced by the freeze-thaw cycle does not contribute to the cracking phenomenon (Detwiler et al, 1997).

The freeze-thaw cycles employed took 9 days to complete. Then, the concrete specimens were stored in saturated calcium hydroxide solution for the duration of the

research study. The freeze-thaw cycles were employed to initiate micorcracks in the concrete specimens. Figure 5.2 below shows the freeze-thaw cycles used for the pretreatment of the concrete specimens.

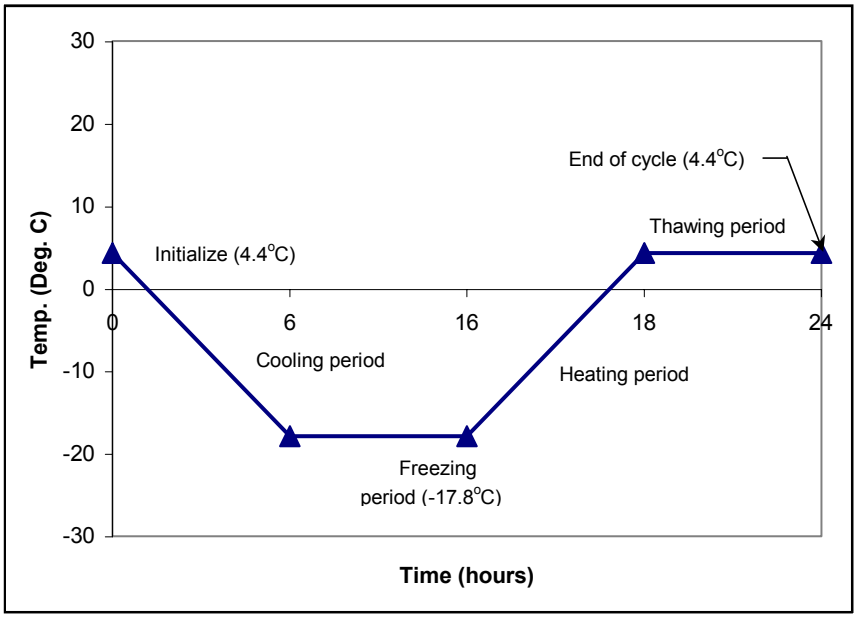

Figure 5.2: Freeze-Thaw Cycle for Concrete Specimens

5.3 Materials

5.31 Potassium Carbonate

Potassium Carbonate is a chemical admixture added to change the concrete to increase its alkali level. In this study the effects of added alkali content on the formation of cracks is monitored. Anhydrous granular reagent grade potassium carbonate (K_2CO_3) was added. Potassium carbonate was added to the mixing water to increase the potassium content of the mix. Potassium carbonate was used because

the high alkali solution could be attained without change in other parameters of the concrete mixture.

5.3.2 Calcium Hydroxide

Hydrated lime, chemically known as calcium hydroxide, $Ca(OH)_2$, or caustic lime, a white powder, was used to provide a required storage condition. The hydrated lime was dissolved in water at room temperature to produce a saturated solution with a pH of 12.5.

5.3.3 Storage Condition

A plastic rack was built to hold the concrete specimens in storage containers of 5 gallons. The limewater in these buckets was maintained at a constant pH of 12.5. This storage condition was obtained by having a saturated solution of calcium hydroxide, $Ca(OH)_2$, and water at room temperature. This made a 12.5 pH value aqueous solution and the specimens were all totally immersed throughout the research.

5.4 Sample Preparation

The concrete specimens were 3" x 3" x 11.25" prisms for laser shearography (non-destructive testing). These concrete specimens were prepared in the laboratory in accordance with ASTM C305-99. They were then cured at room temperature for 24 hours. Then the specimens were kept for 6 (six) days before exposing them to either Duggan or Freeze and Thaw cycles.

5.4.1 Series One

All the mix materials and proportions were kept the same for Series one and Series two. The chemical analysis of the cement indicated 0.82% potassium content (K_2O). The cement was used without changing the potassium content throughout Series one as the control. Two concrete batches were prepared with all the mix materials and proportions kept the same. The specimens were prepared according to ASTM C305-99 and cured at room temperature before subjecting them to either the Duggan cycle or Freeze-Thaw cycles. The specimens were then stored under water at room temperature for six (6) days. After storage under water, the specimens were subjected to Duggan or Freeze-Thaw cycles.

5.4.2 Series Two

Again, all batches were mixed and prepared similar to Series one in terms of cement composition, sand, aggregate, w/c ratio. The chemical analysis of the cement indicated 0.82% potassium content (K_2O). So, an addition of 0.68% potassium carbonate by weight of cement was added to the mixing water to achieve the desired 1.5%. Again, additional concrete batches were mixed to compare curing conditions and their influence on DEF and associated damage variables.

5.5 Laser Shearography Test

Concrete prisms - 3" x 3" x 11.25" were prepared and then were either subjected to heat (Duggan cycle) or freeze and thaw cycles before subsequently storing them in isothermal water, pH maintained at 12.5. Laser shearography work

was done before and after the curing of the specimens to determine surface crack density. Statistical analysis of the collected image data will help in the detection of cracking, quantify crack growth over time and observation of crack patterns due to delayed ettringite formation.

Chapter 6: Discussion of Results

6.1 General

This chapter details the results from laser shearography method and Image Pro Analysis software. As mentioned before, the laser shearography images are stored in digital format and later processed with a computer. These data can be easily analyzed by using the Image Pro Analysis software (IPAS). Some parameters can be extracted from the list of information about an image such as the length, width, perimeter, area and orientation of cracks. This information will help to evaluate the level of damage of concrete at an early stage of deterioration. Comparisons of the results were also employed during this research study.

This experimental research was divided into two series to evaluate the effects of different parameters on the crack formation and development. For series one and two, after casting for seven days, the concrete specimens were then subjected to Duggan heat or Freeze-Thaw cycles. The laser shearography images were taken to reveal the cracks after treatment and later to anticipate the crack development.

6.2 Experimental Research Observation

The concrete specimens used in series one and two show no crack on the surface of concrete prism before treatment program. After subjecting the concrete specimens to either the Duggan heat or Freeze-Thaw cycles, all of them show cracks on the surface at different levels. The laser shearography later showed the trend of crack development for all of the concrete specimens.

6.2.1 Series One (Control)

6.2.1.1 Duggan Heat Cycle Treatment

Concrete specimens for series one (1) were prepared without additional potassium carbonate and then subjected to the Duggan heat cycle. The laser shearography images after treatment showed significant changes in the surfaces of the examined concrete prisms. All the dark spots represent the cracks in concrete. The laser shearography testing was again employed at 100 days after treatment and subsequently storing in limewater. These shearography images were then compared to find the changes in crack density and crack development. The purpose of using Duggan treatment is to simulate similar procuring methods used in the pre-cast concrete industry. The heat treatment program is used to establish a high early concrete strength. However, the period not being delayed enough or excessive heat treatment will cause the initial cracks in concrete. These cracks later will become larger and raise the permeable property of concrete. This helps to transport water and chemicals into concrete and results in reducing its strength. The results from this research showed that before treatment there was no crack on the surface of concrete prism. Immediately after treatment, cracks can be seen from the laser shearography images analysis. Figures 6.1 through 6.6 show the laser shearography images over time on the concrete prism surfaces.

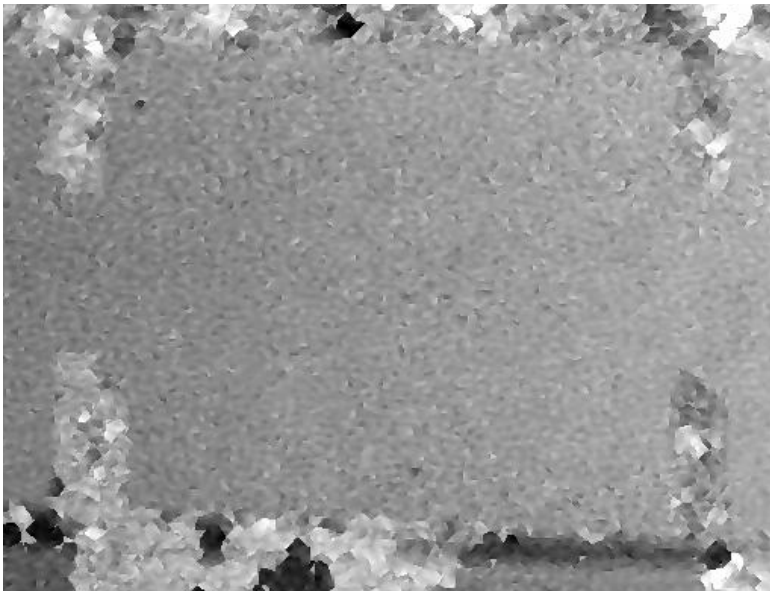

Figure 6.1: Shearography Image of Face 1 Section 2 for Concrete Prism Surface-Series One 7 Days After Casting

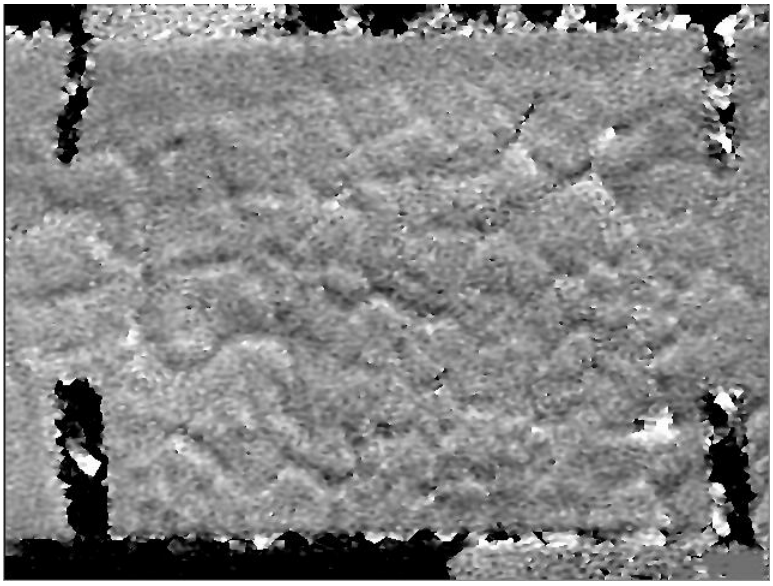

Figure 6.2: Shearography Image of Face 1 Section 2 for Concrete Prism Surface-Series One After Duggan Treatment

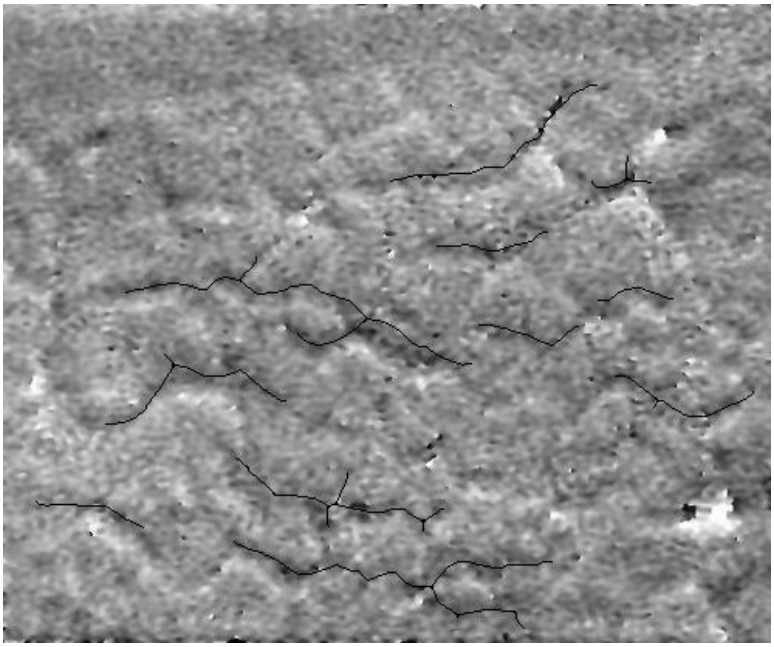

Figure 6.3: Enhanced Shearography Image Face 1 Section 2 for Concrete Prism Surface - Series One After Duggan Treatment

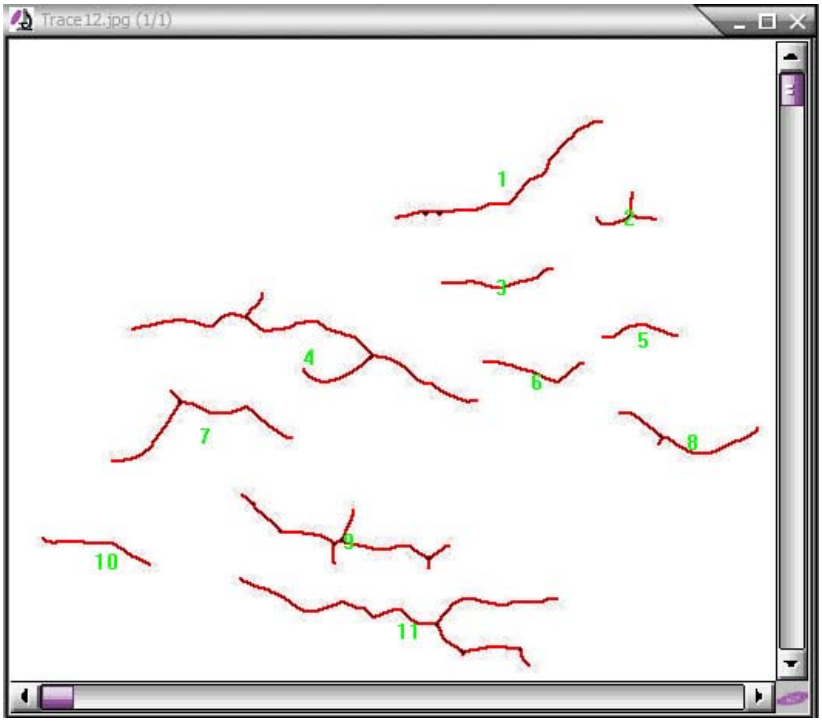

Figure 6.4: Analysis Image of Face 1 Section 2 for Concrete Prism Surface – Series One After Processing Using Image Pro Plus Software (After Treatment)

Table 6.1: Image Pro Plus Measurement Data Sheet of Face 1 Section 2 for Series One After Duggan Treatment

Object # 12	Area (in^2)	Aspect Ratio	Angle	Perimeter (inch)	Length (inch)
1	0.02	5.84	62.84	2.31	1.16
2	0.01	2.08	76.94	0.81	0.41
3	0.01	8.07	84.58	1.10	0.55
4	0.04	5.61	104.80	4.38	2.19
5	0.01	5.09	87.93	0.77	0.39
6	0.01	5.40	97.13	1.05	0.53
7	0.02	2.92	79.62	2.21	1.11
8	0.01	4.09	100.68	1.52	0.76
9	0.02	6.13	103.08	2.75	1.37
10	0.01	8.56	101.22	1.10	0.55
11	0.04	5.02	97.12	4.30	2.15
Total	0.18			22.32	11.16

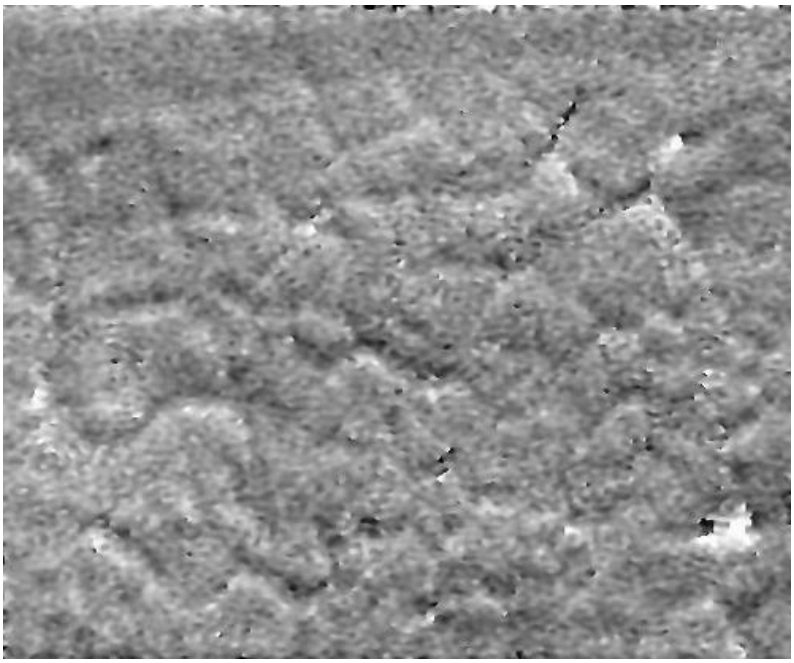

Figure 6.5: Shearography Image of Face 1 Section 2 for Concrete Prism Surface - Series One 100 Days After Duggan Treatment

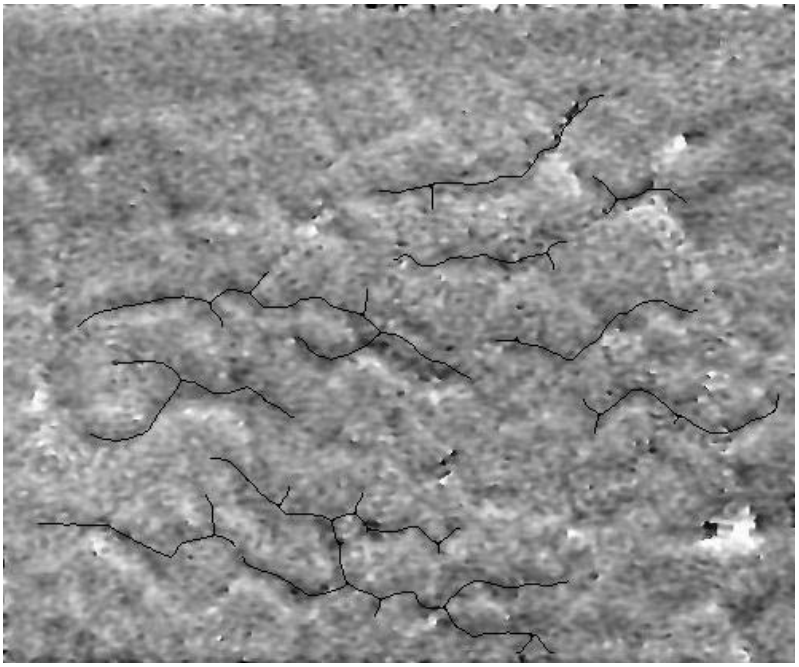

Figure 6.6: Enhanced Shearography Image Face 1 Section 2 for Concrete Prism Surface – Series One 100 days After Duggan Treatment

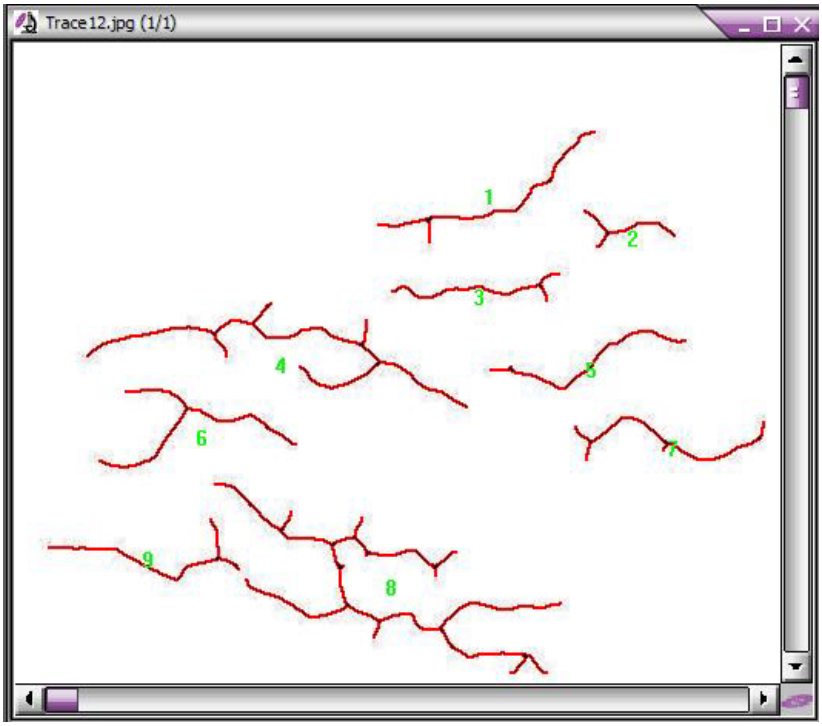

Figure 6.7: Analysis Image of Face 1 Section 2 for Concrete Prism Surface – Series One After Processing Using Image Pro Plus Software (100 days after Duggan Treatment)

Table 6.2: Image Pro Plus Measurement Data Sheet of Face 1 Section 2 for Series One 100 Days After Duggan Treatment

Object # 12	Area (in^2)	Aspect Ratio	Angle	Perimeter (inch)	Length (inch)
1	0.02	5.57	65.99	2.70	1.35
2	0.01	3.36	91.30	1.20	0.60
3	0.02	9.88	86.98	1.94	0.97
4	0.05	5.24	99.18	5.38	2.69
5	0.02	5.29	73.69	2.19	1.09
6	0.02	2.22	83.80	2.99	1.50
7	0.02	5.01	94.08	2.49	1.25
8	0.07	3.06	112.72	7.82	3.91
9	0.02	4.30	92.22	2.42	1.21
Total	0.25			29.12	14.56

It is obvious that the initial crack system after Duggan treatment is larger than before treatment in term of crack length, area and perimeter of cracks. Table 6.1 and 6.2 provide the information about the area, aspect ratio, angle, length, and perimeter of cracks. These acquired data are analyzed and then evaluated for each of the concrete prism surfaces.

Table 6.3 Image Pro Plus Measurement Data Sheet Summary for Series One After Duggan Treatment

Duggan Heat Cycle (Series One) After Treatment			
Face # Sec #(*)	**Crack Density**	**Crack Length (in)**	**Area of Crack (in^2)**
11	0	0.00	0.00
12	11	11.16	0.02
13	13	5.03	0.09
21	6	5.12	0.13
22	8	5.11	0.01
23	8	3.11	0.07
31	0	0.00	0.00
32	13	6.38	0.01
33	12	6.23	0.01
41	0	0.00	0.00
42	8	4.78	0.10
43	0	0.00	0.00
5	12	3.99	0.08
6	9	3.55	0.07
Total	100	54.46	0.59

(*): 1^{st} digit is face #, 2^{nd} digit is section #.

Table 6.4 Image Pro Plus Measurement Data Sheet Summary for Series One After Duggan Treatment and 100 Days in Lime Water

Duggan Heat Cycle (Series One) 100 days after treatment			
Face # Sec #(*)	**Crack Density**	**Crack Length (in)**	**Area of Crack (in^2)**
11	0	0.00	0.00
12	9	14.56	0.26
13	17	7.13	0.15
21	7	6.83	0.18
22	8	7.27	0.21
23	8	4.31	0.09
31	0	0.00	0.00
32	10	8.46	0.02
33	12	8.04	0.17
41	0	0.00	0.00
42	8	4.83	0.13
43	0	0.00	0.00
5	13	5.30	0.11
6	10	5.30	0.10
Total	102	72.04	1.44

(*) : 1^{st} digit is face #, 2^{nd} digit is section #.

Two tables, 6.3 and 6.4, provide the summary data for the information in terms of crack density and crack length of every crack on the six surfaces of the concrete specimens, for series one right after treatment and 100 days in lime water after treatment. The tables show significant changes in the crack length.

6.2.1.2 Freeze-Thaw Cycle Treatment

The concrete samples were again prepared with no additional potassium carbonate and then subjected to Freeze-Thaw cycles. This type of treatment was chosen to simulate weather conditions normal in North America. Many researches

confirm that the Freeze-Thaw cycles treatment process contribute to the expansion of concrete. In this research, the data showed that the cracks occur immediately after the Freeze-Thaw cycles treatment. By comparing the data after treatment and 100 days after treatment, the rate of crack development on these concrete prism surfaces is much more than that subjected to Duggan Heat cycle treatment. Figures 6.8 through 6.17 showed laser shearography images of series one (1) concrete prism surfaces subjected to Freeze-Thaw cycles treatment.

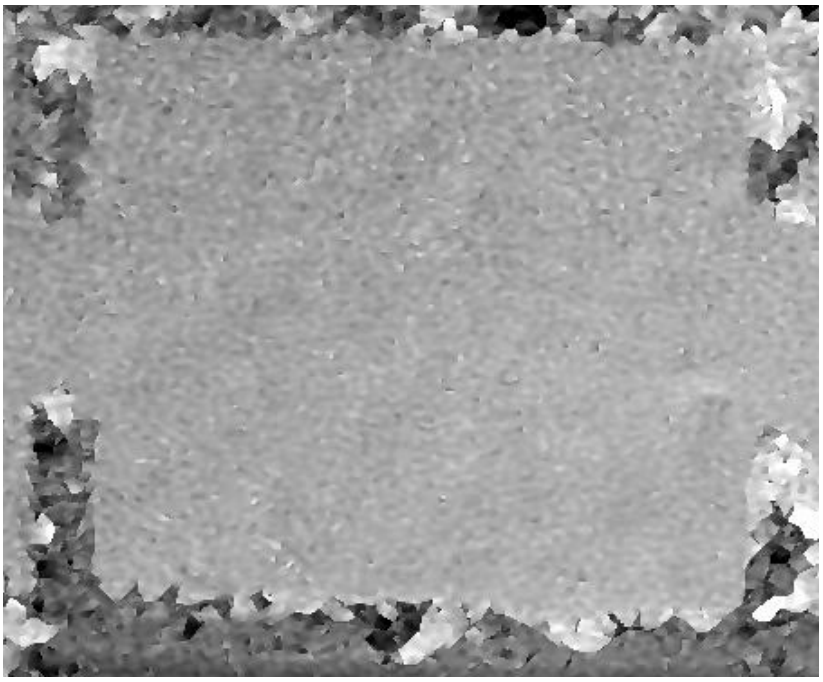

Figure 6.8: Shearography Image of Face 1 Section 2 for Concrete Prism Surface – Series One 7 Days After Casting (Freeze-Thaw Treatment)

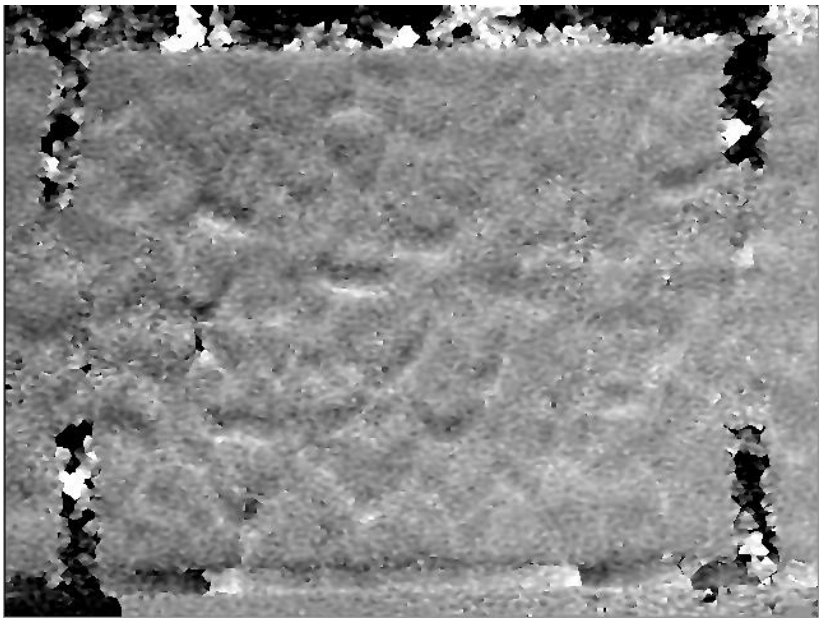

Figure 6.9: Shearography Image of Face 1 Section 2 for Concrete Prism Surface - (Series One) After Freeze-Thaw Treatment

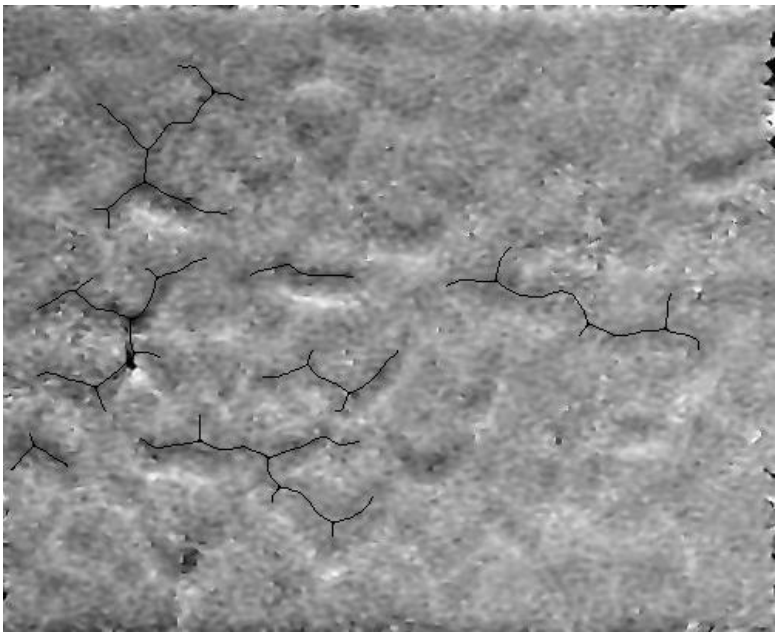

Figure 6.10: Enhanced Shearography Image Face 1 Section 2 for Concrete Prism Surface - Series One After Freeze-Thaw Treatment

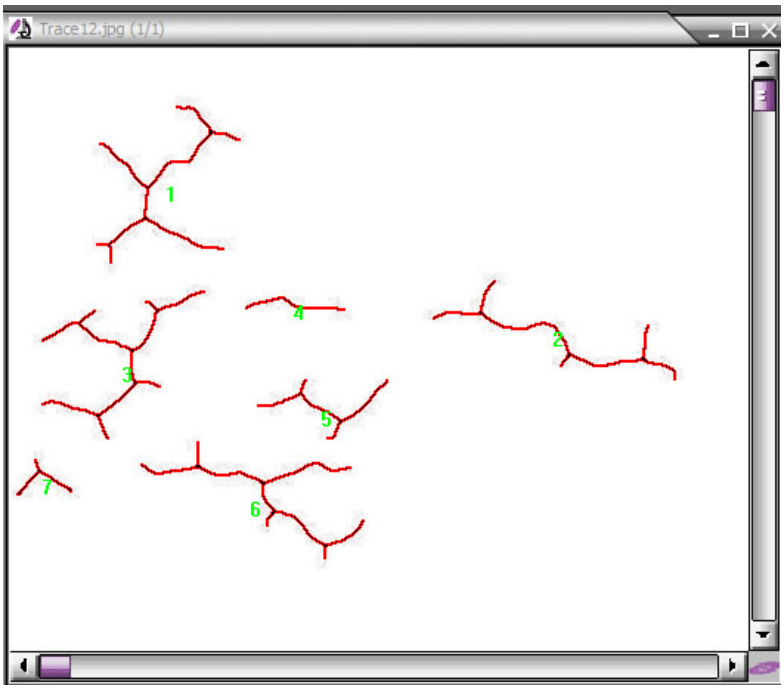

Figure 6.11: Analysis Image of Face 1 Section 2 for Concrete Prism Surface After Processing Using Image Pro Plus Software After Freeze-Thaw Treatment

Table 6.5: Image Pro Plus Measurement Data Sheet of Face 1 Section 2 for Series One After Freeze-Thaw Treatment

Object # 12	**Area (mm^2)**	**Aspect Ratio**	**Angle**	**Perimeter (mm)**	**Size (length) mm**
1	0.03	1.57	30.96	3.81	1.90
2	0.03	5.68	106.15	3.39	1.69
3	0.03	1.57	42.19	3.95	1.98
4	0.01	9.70	94.66	1.04	0.52
5	0.02	2.48	90.70	1.90	0.95
6	0.03	2.78	109.26	3.84	1.92
7	0.01	1.77	93.43	0.81	0.40
Total	0.16			18.75	9.37

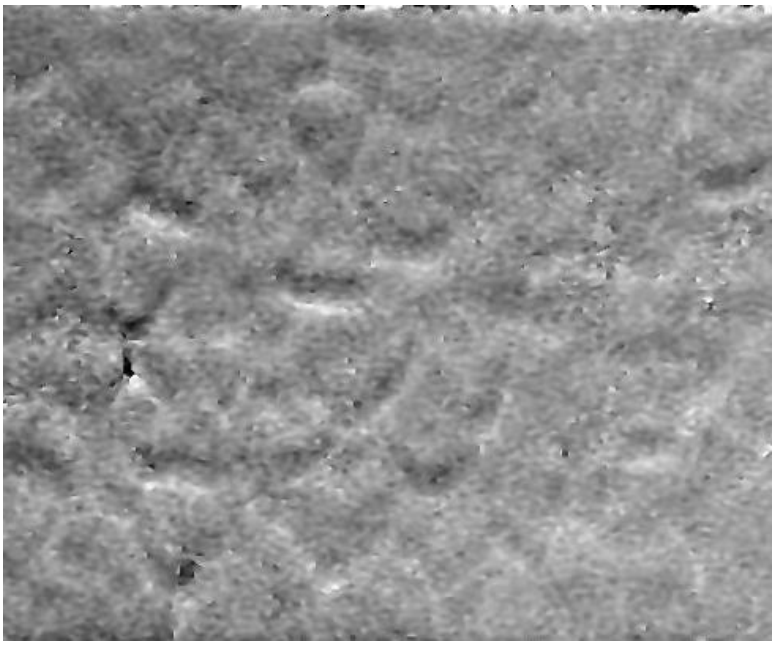

Figure 6.12: Shearography Image of Face 1 Section 2 for Concrete Prism Surface - Series One 100 Days After Freeze-Thaw Treatment

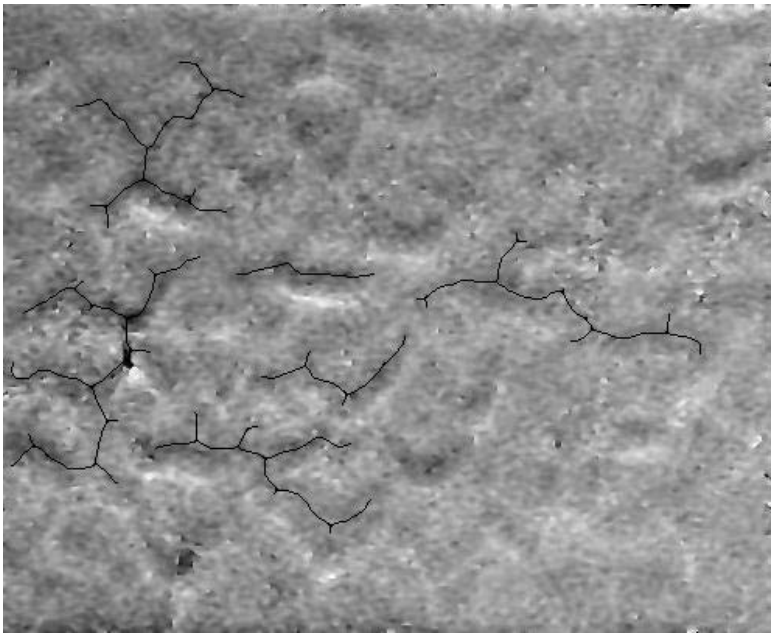

Figure 6.13 Enhanced Shearography Image Face 1 Section 2 for Concrete Prism Surface - Series One 100 Days After Freeze-Thaw Treatment

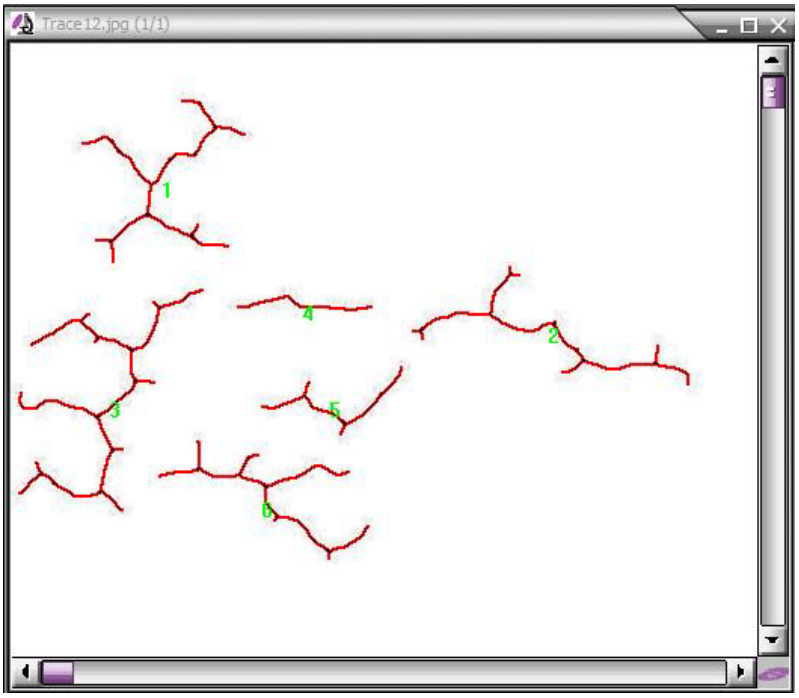

Figure 6.14: Analysis Image of Face 1 Section 2 for Concrete Prism Surface After Processing Using Image Pro Plus Software (100 Days After Freeze-Thaw Treatment)

Table 6.6: Image Pro Plus Measurement Data Sheet of Face 1 Section 2 for Series One 100 Days After Freeze-Thaw Treatment

Object # 12	Area (mm^2)	Aspect Ratio	Angle	Perimeter (mm)	Size (length) mm
1	0.04	1.34	30.47	4.31	2.15
2	0.04	4.31	106.16	4.04	2.02
3	0.06	1.90	24.04	5.77	2.88
4	0.01	11.89	93.24	1.41	0.70
5	0.02	2.87	83.13	1.99	1.00
6	0.03	2.68	113.39	3.92	1.96
Total	0.19			21.43	10.71

Again, it is obvious that the initial crack system after Freeze-Thaw treatment is larger than before in terms of crack length, area and perimeter of cracks. It shows

that the effects of Freeze-Thaw treatment make cracks on the surface of concrete specimen become larger when considering crack length, area and perimeter of cracks.

Table 6.7: Image Pro Plus Measurement Data Sheet Summary for Series One After Freeze-Thaw Treatment

Freeze-Thaw Cycle (Series One) After Treatment			
Face # Sec #(*)	**Crack Density**	**Crack Length (in)**	**Area of Crack (in^2)**
11	10	3.65	0.07
12	7	9.37	0.16
13	11	6.52	0.13
21	0	0.00	0.00
22	12	7.73	0.19
23	0	0.00	0.00
31	12	4.36	0.09
32	8	4.67	0.10
33	8	3.97	0.09
41	10	3.41	0.08
42	9	4.51	0.11
43	7	2.72	0.05
5	4	1.74	0.04
6	12	3.98	0.08
Total	110	56.61	1.19

(*): 1^{st} digit is face #, 2^{nd} digit is section #.

Table 6.8: Image Pro Plus Measurement Data Sheet Summary for Series One 100 Days After Freeze-Thaw Treatment

Freeze-Thaw Cycle (Series One) 100 Days After Treatment			
Face # Sec #(*)	**Crack Density**	**Crack Length (in)**	**Area of Crack (in^2)**
11	7	4.16	0.10
12	6	10.71	0.19
13	12	8.36	0.17
21	0	0.00	0.00
22	15	9.38	0.24
23	5	3.85	0.08
31	9	8.84	0.12
32	8	6.29	0.14
33	9	5.01	0.12
41	10	3.96	0.10
42	11	5.89	0.14
43	8	3.19	0.07
5	7	3.33	0.08
6	13	5.23	0.10
Total	120	78.21	1.66

(*) : 1^{st} digit is face #, 2^{nd} digit is section #.

6.2.1.3 Discussion of Series One Results

The results for series one came from the analysis process by Image Pro Plus software showing the change in the total number of cracks on each concrete specimens and the cracks length. The comparison was taken to highlight the trend of crack development in concrete subjected to Duggan or Freeze-Thaw treatment. As expected, the cracks occur on the surface of every specimen at a different level. Two parameters, crack length and crack density were chosen to be compared.

Cracks appeared on all of the six surfaces of the concrete specimens except for a few sections where no cracks were detected. This indicates that the concrete originally was not structured homogeneously. These cracks became larger in size, length and area after treatments were implemented. A few new cracks appeared after a period of 100 days from the completion of the treatments. More cracks appeared on the concrete specimen after Freeze-Thaw treatment than after Duggan treatment. At the 100th day after treatments, the overall lengths of these cracks also showed a tremendous increase from Freeze-Thaw compared to Duggan. This means that the permeability of the concrete specimens that was caused by Freeze-Thaw also is greater than by Duggan.

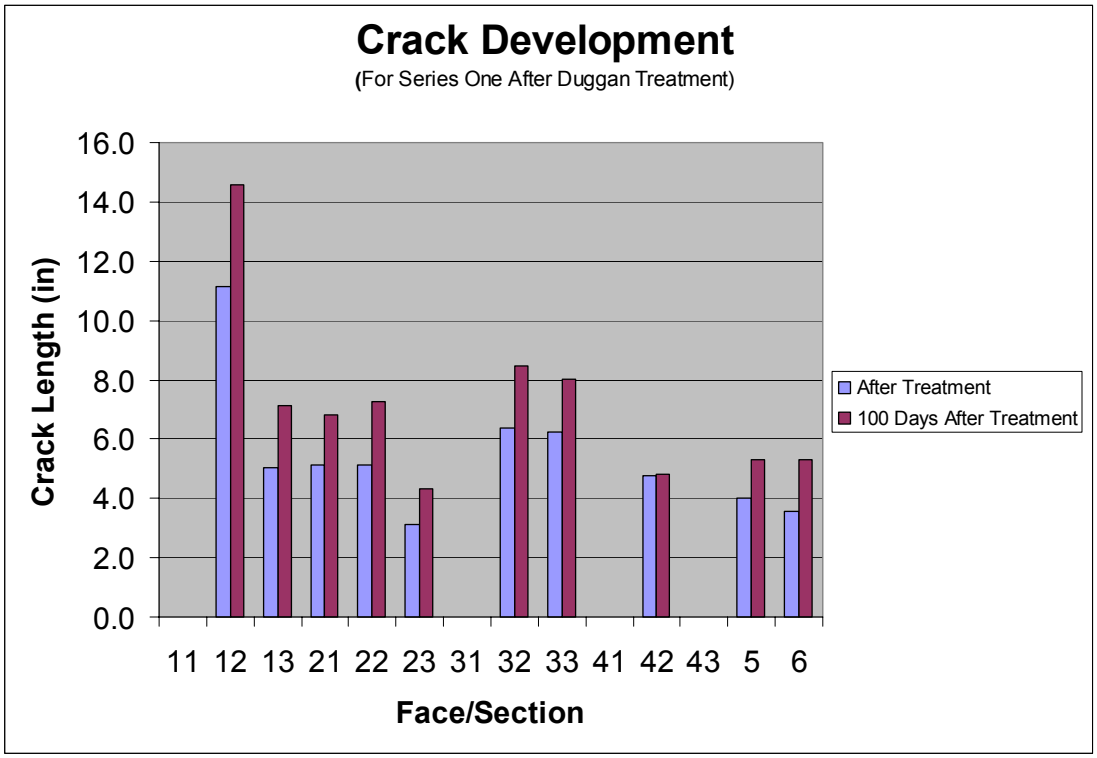

Figure 6.15: Crack development for series one after Duggan Treatment

As illustrated on Figure 6.15, before the Duggan treatment, all of the image data had not shown any trace of cracks. Right after treatment, the cracks appeared on all the surfaces of the concrete specimens but, to some of the sections, this process didn't take place. However, in general, the sum of the lengths of cracks on each section showed the increasing trend later, after 100 days and there was no new crack development. This means only that the existing cracks were expanding during the sampling process.

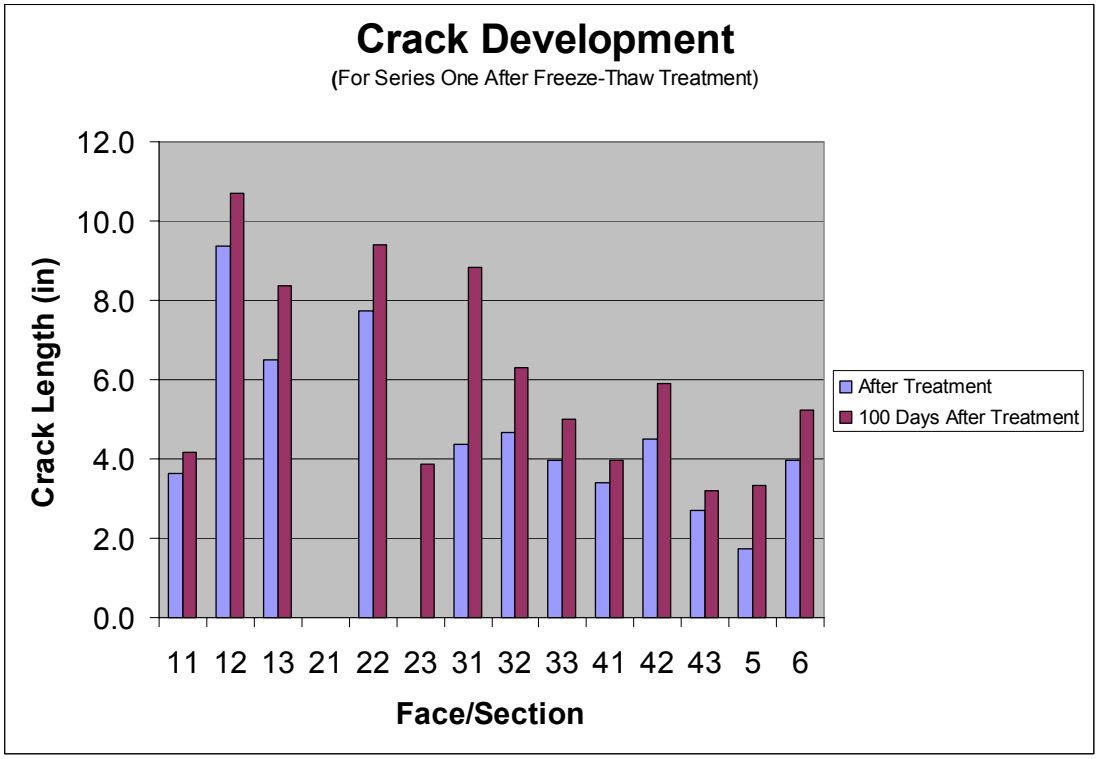

Figure 6.16: Crack development for series one after Freeze-Thaw Treatment

Similar to the Duggan treatment's results, cracks appeared on all surface of the concrete specimen after Freeze-Thaw treatment although there was no crack before. And the existing cracks kept growing within 100 days after that. Figure 6.16 shows the differences between crack growths on every section. Particularly, on face 2

section 3, there was no crack right after the Freeze-Thaw treatment (no blue column showed on figure); but after 100 days submerged in limewater, some new cracks appeared on this section of the specimen.

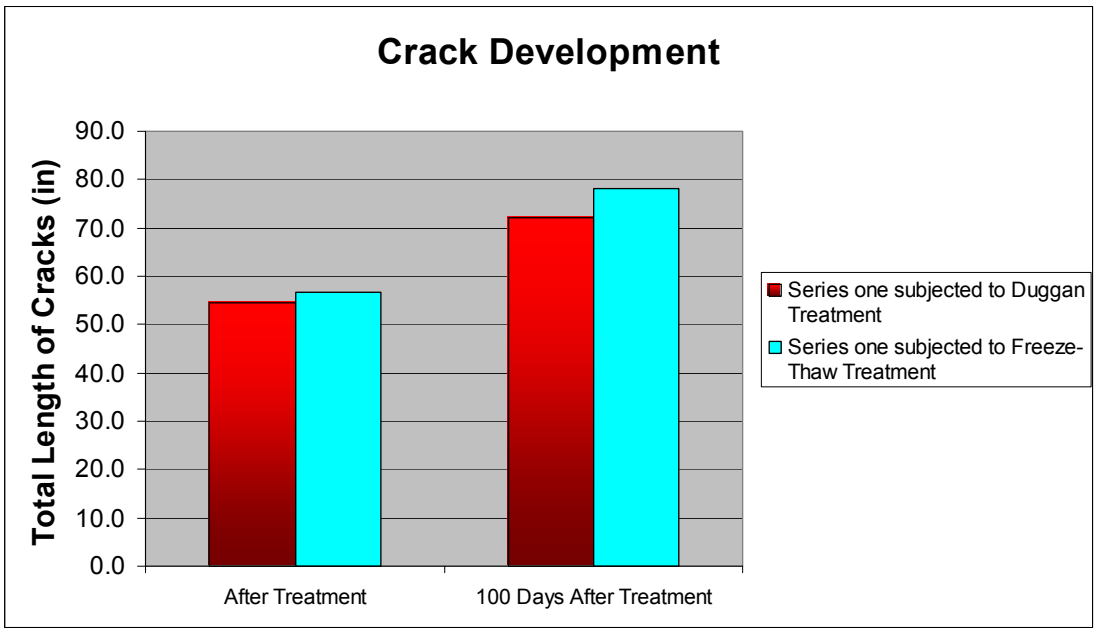

Figure 6.17: Crack development for series one after Duggan and Freeze-Thaw Treatments

As illustrated in figure 6.17, the sums of length of the cracks in both concrete specimens (in Duggan and Freeze-Thaw treatments) were nearly equal to each other when they were measured right after the treatments. However, the rate of crack development of the concrete specimen subjected to Freeze-Thaw treatment was larger than that of concrete specimen subjected to Duggan treatment. This means the effect of Freeze-Thaw treatment to the concrete made of the same parameter is more severe than that of Duggan treatment.

In terms of crack density, the data also show the change in total number of cracks in every surface of specimens (but not every section). However, for the whole surface, there were always cracks appearing. The sum of crack numbers on each

section numerically differs due to the connection among these cracks. If two cracks are connected together, they form one crack; the image analysis software will show the larger length for this newly formed crack.

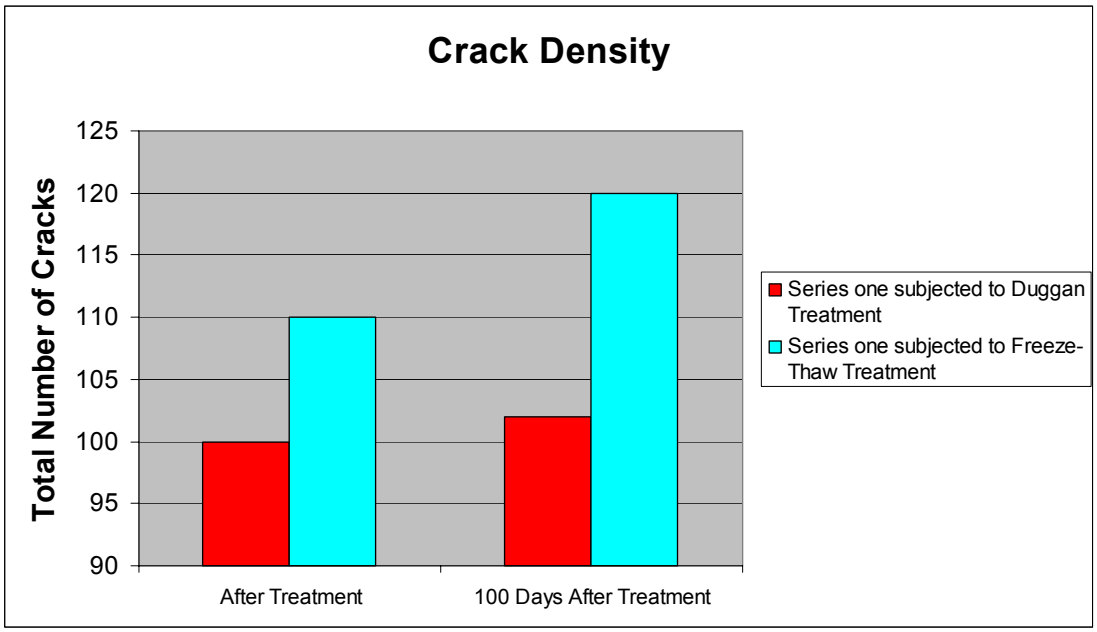

Figure 6.18: Crack density for series one after Duggan and Freeze-Thaw Treatments

The figure above shows that the Freeze-Thaw Treatment immediately resulted in a higher number of cracks appearing on the concrete specimen than Duggan treatment did (110 cracks on the Freeze-Thaw specimen and 100 cracks on the other). Moreover, during 100 days of the sampling process, the increase of crack numbers in the specimen subjected to Freeze-Thaw treatment was faster than that in the specimen subjected to Duggan treatment (approximately 10% in Freeze-Thaw and 2% in Duggan).

6.2.2 Series Two.

6.2.2.1 Duggan Heat Cycle Treatment

The concrete specimens in this series were prepared with the same cement content, sand and gravel as series one except that additional potassium was added to the mixing water. The purpose of using this chemical is to favor the formation of ettringite resulting in larger expansion values. After casting, laser shearography images do not show any cracks on the surfaces of the concrete prisms. After treatment, there are many cracks occurring on the surfaces of the concrete prism and much more than for series one. This confirms that the additional potassium carbonate affects the crack density and development.

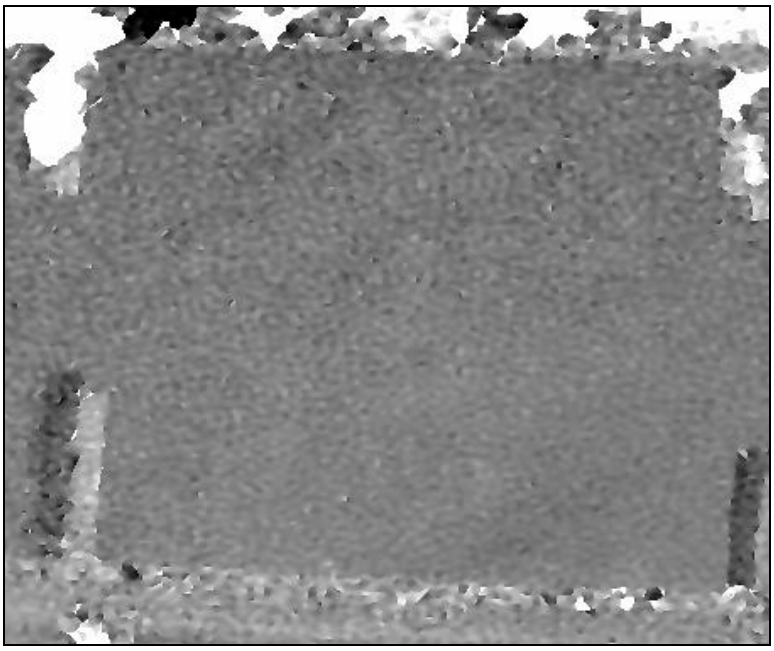

Figure 6.19: Shearography Image of Face 1 Section 2 for Concrete Prism Surface - Series Two After Casting (Duggan Heat Cycle Treatment)

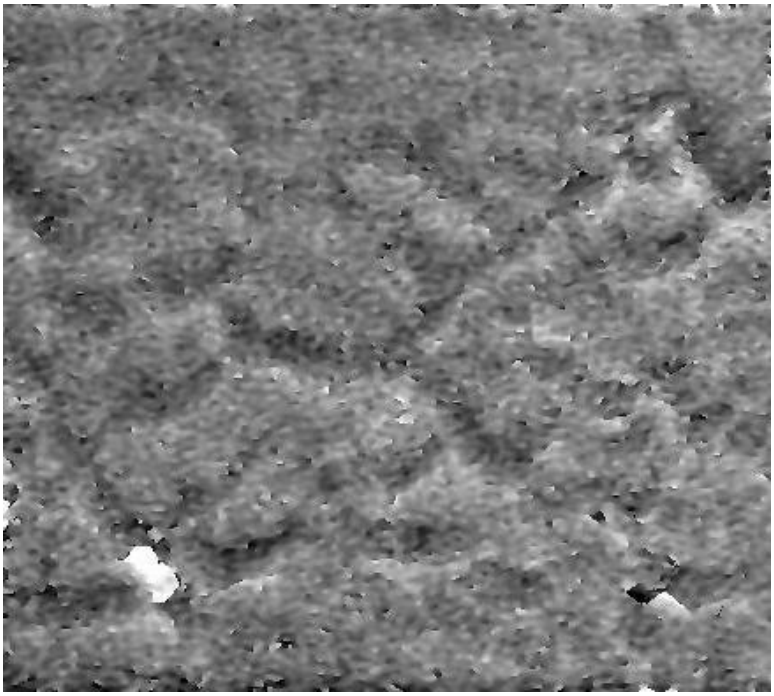

Figure 6.20: Shearography Image of Face 1 Section 2 for Concrete Prism Surface Series Two After Duggan Heat Cycle Treatment

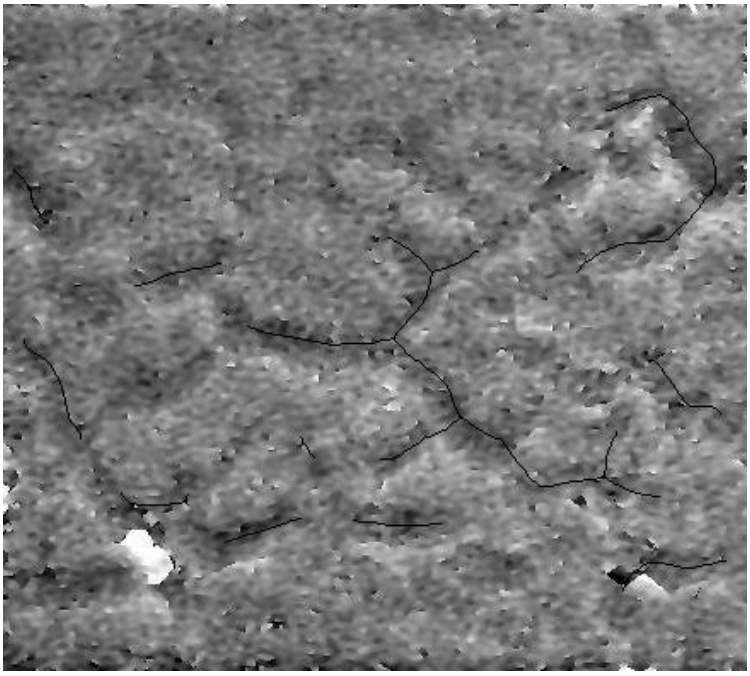

Figure 6.21 Enhanced Shearography Image Face 1 Section 2 for Concrete Prism Surface - Series Two After Duggan Heat Cycle Treatment

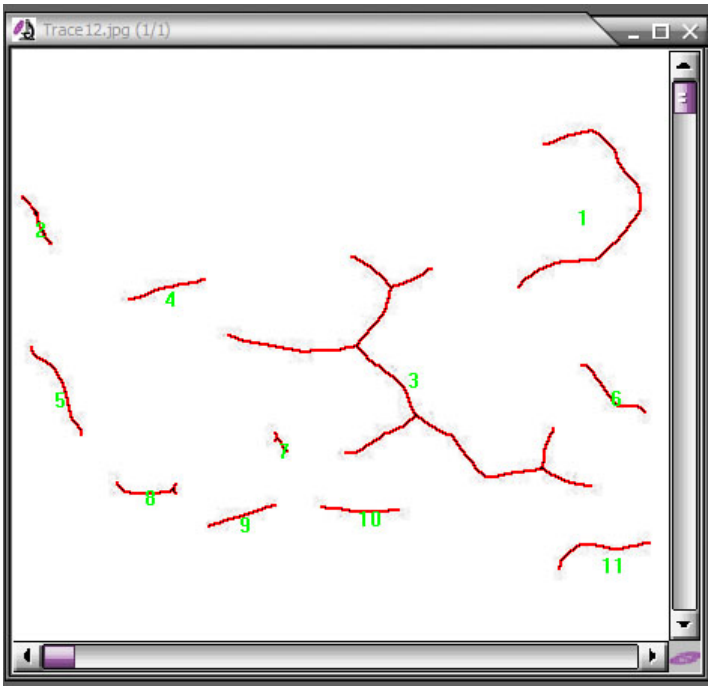

Figure 6.22 Analysis Image of Face 1 Section 2 for Concrete Prism Surface – Series Two After Processing Using Image Pro Plus Software (After Duggan Heat Cycle Treatment)

Table 6.9: Image Pro Plus Measurement Data Sheet of Face 1 Section 2 for Series Two After Duggan Treatment

Object # 12	Area (in^2)	Aspect Ratio	Angle	Perimeter (inch)	Length (inch)
1	0.02	1.67	18.04	3.01	1.51
2	0.01	10.00	152.16	0.59	0.29
3	0.06	2.27	125.80	6.72	3.36
4	0.01	17.35	75.08	0.81	0.40
5	0.01	7.82	151.51	1.06	0.53
6	0.01	5.59	129.85	0.88	0.44
7	0.00	4.61	145.06	0.25	0.13
8	0.01	6.33	91.20	0.71	0.36
9	0.01	21.28	72.44	0.72	0.36
10	0.01	17.25	92.43	0.79	0.40
11	0.01	6.06	81.20	1.06	0.53
Total	0.14			16.62	8.31

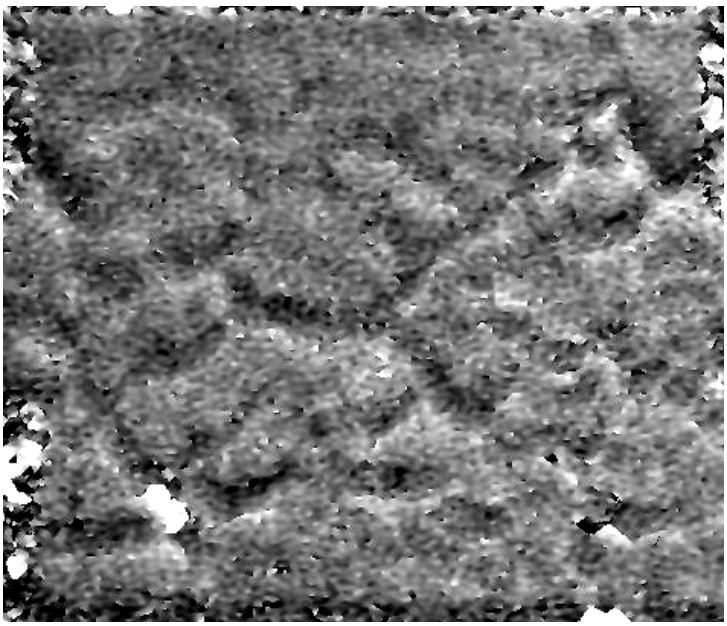

Figure 6.23: Shearography Image of Face 1 Section 2 for Concrete Prism Surface - Series Two 100 Days After Duggan Heat Cycle Treatment

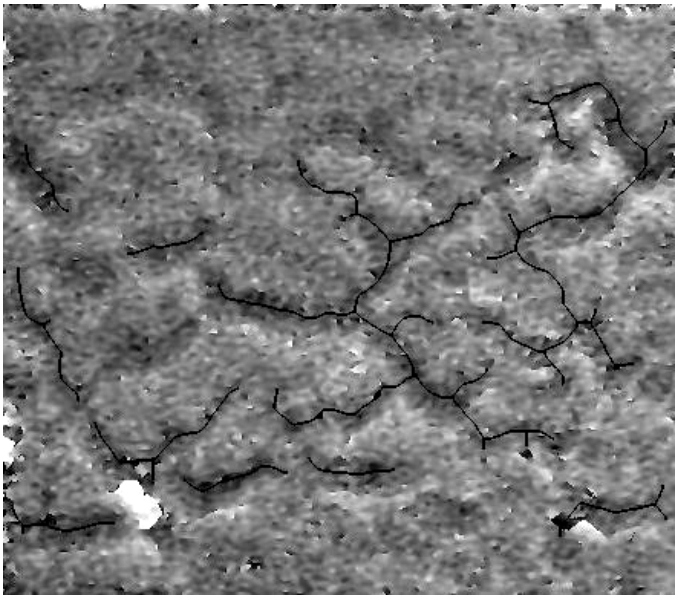

Figure 6.24: Enhanced Shearography Image Face 1 Section 2 for Concrete Prism Surface - Series Two 100 Days After Duggan Heat Cycle Treatment

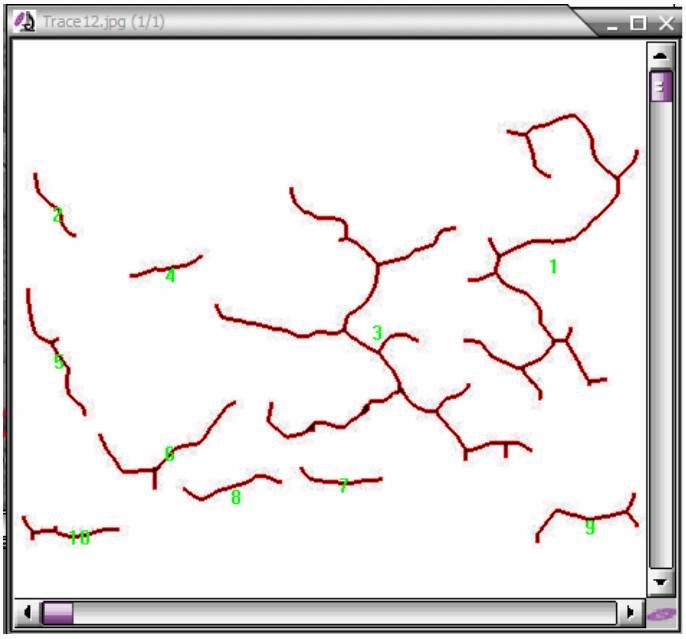

Figure 6.25: Analysis Image of Face 1 Section 2 for Concrete Prism Surface – Series Two After Processing Using Image Pro Plus Software (100 Days After Duggan Heat Cycle Treatment)

Table 6.10: Image Pro Plus Measurement Data Sheet of Face 1 Section 2 for Series Two 100 Days After Duggan Treatment

Object # 12	Area (in^2)	Aspect Ratio	Angle	Perimeter (inch)	Length (inch)
1	0.09	2.29	10.41	7.29	3.65
2	0.01	9.74	145.90	0.87	0.43
3	0.11	1.40	140.53	9.20	4.60
4	0.01	12.59	76.81	0.82	0.41
5	0.02	9.33	152.88	1.65	0.83
6	0.02	2.81	66.79	2.14	1.07
7	0.01	7.55	94.04	0.95	0.48
8	0.01	8.15	77.09	1.16	0.58
9	0.02	4.67	80.31	1.60	0.80
10	0.01	6.63	92.09	1.24	0.62
Total	0.30			26.92	13.46

Table 6.11: Image Pro Plus Measurement Data Sheet Summary for Series Two After Duggan Treatment

Duggan Heat Cycle (Series Two) After Treatment			
Face # Sec #(*)	**Crack Density**	**Crack Length (in)**	**Area of Crack (in^2)**
11	7	5.23	0.11
12	11	8.31	0.14
13	17	8.64	0.19
21	12	6.28	0.13
22	11	6.99	0.15
23	9	5.31	0.12
31	0	0.00	0.00
32	8	4.80	0.09
33	10	6.75	0.13
41	0	4.32	0.00
42	11	6.59	0.13
43	13	6.59	0.12
5	6	2.64	0.05
6	6	3.74	0.08
Total	121	76.19	1.44

(*) : 1^{st} digit is face #, 2^{nd} digit is section #.

Table 6.12: Image Pro Plus Measurement Data Sheet Summary for Series Two 100 Days After Duggan Treatment

Duggan Heat Cycle (Series Two) 100 Days After Treatment			
Face # Sec #(*)	**Crack Density**	**Crack Length (in)**	**Area of Crack (in^2)**
11	7	6.88	0.25
12	10	13.46	0.30
13	11	8.52	0.31
21	13	8.28	0.26
22	8	9.42	0.35
23	12	6.22	0.19
31	0	0.00	0.00
32	10	6.93	0.27
33	10	7.08	0.28
41	6	4.65	0.16
42	0	0.00	0.00
43	0	0.00	0.00
5	9	5.78	0.16
6	11	6.69	0.19
Total	107	83.91	2.73

(*): 1^{st} digit is face #, 2^{nd} digit is section #.

6.2.2.2 Freeze-Thaw Cycles Treatment

Similarly, the concrete specimen for this series two with additional potassium carbonate was subjected to Freeze-Thaw treatment. Laser shearography images were taken before subjecting the specimen to Freeze-Thaw treatment and after the treatment. The shearograpphy images at 100 days after treatment show more crack than the shearography images after treatment. It confirmed that the initial cracks provided by this treatment developed over time. Figures 6.26 through 6.32 show the laser shearography images before and after treatment.

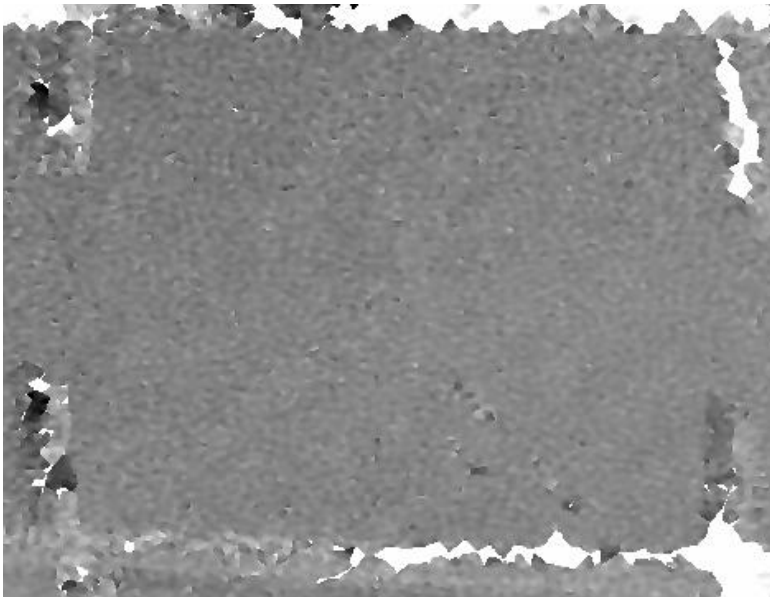

Figure 6.26: Shearography Image of Face 1 Section 2 for Concrete Prism Surface – Series Two 7 Days After Casting (Freeze-Thaw Cycle Treatment)

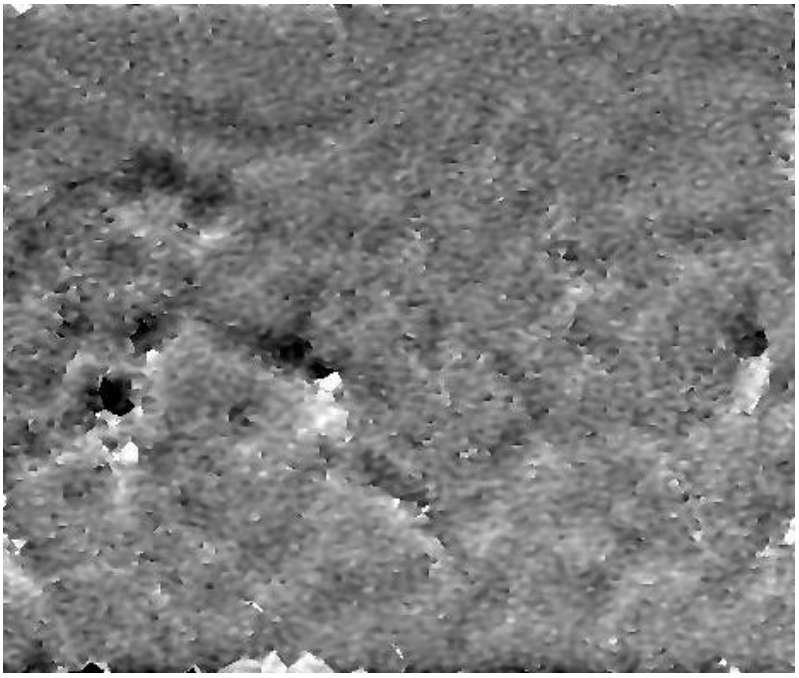

Figure 6.27: Shearography Image of Face 1 Section 2 for Concrete Prism Surface Series Two After Freeze-Thaw Treatment

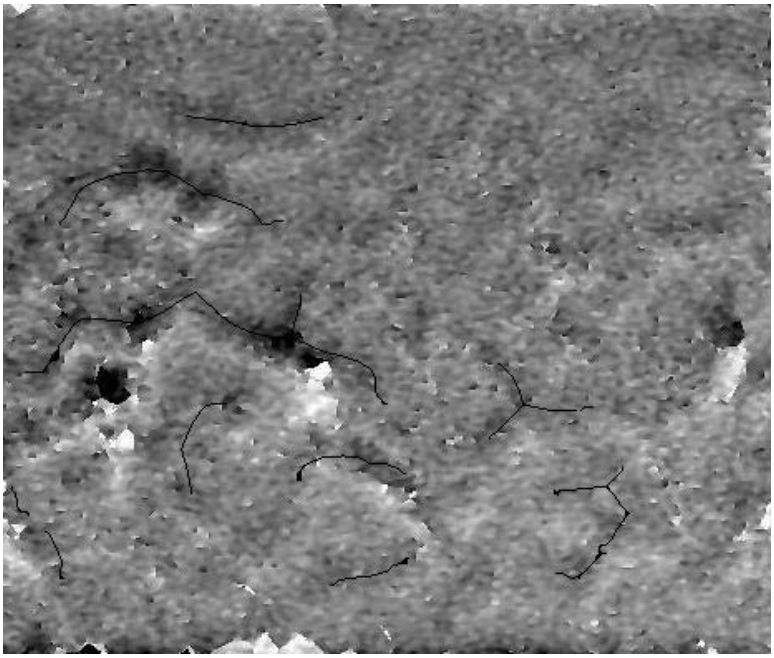

Figure 6.28: Enhanced Shearography Image Face 1 Section 2 for Concrete Prism Surface- Series Two After Freeze-Thaw Cycle Treatment

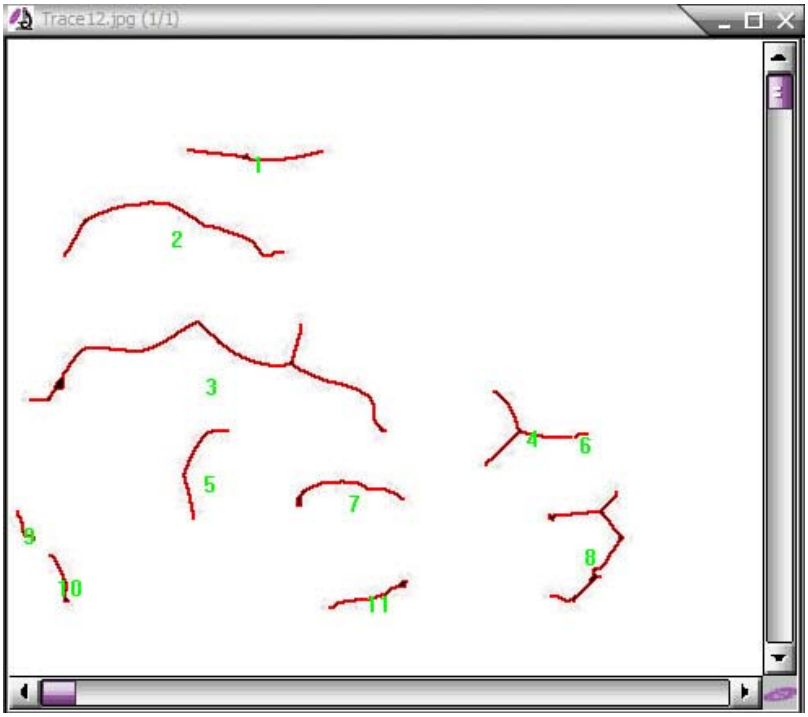

Figure 6.29: Analysis Image of Face 1 Section 2 for Concrete Prism Surface – Series Two After Processing Using Image Pro Plus Software (After Freeze-Thaw Cycle Treatment)

Table 6.13: Image Pro Plus Measurement Data Sheet of Face 1 Section 2 for Series Two After Freeze-Thaw Treatment

Object # 12	Area (mm^2)	Aspect Ratio	Angle	Perimeter (mm)	Size (length) mm
1	0.01	13.22	91.95	1.24	0.62
2	0.02	4.25	95.93	2.31	1.16
3	0.04	4.39	93.63	4.19	2.09
4	0.01	1.20	99.13	1.34	0.67
5	0.01	3.67	17.21	1.04	0.52
6	0.00	3.63	76.09	0.13	0.06
7	0.01	5.10	88.21	1.14	0.57
8	0.02	1.76	13.71	1.99	1.00
9	0.00	4.48	151.72	0.34	0.17
10	0.00	7.00	162.81	0.50	0.25
11	0.01	11.51	73.17	0.78	0.39
Total	0.12			14.99	7.49

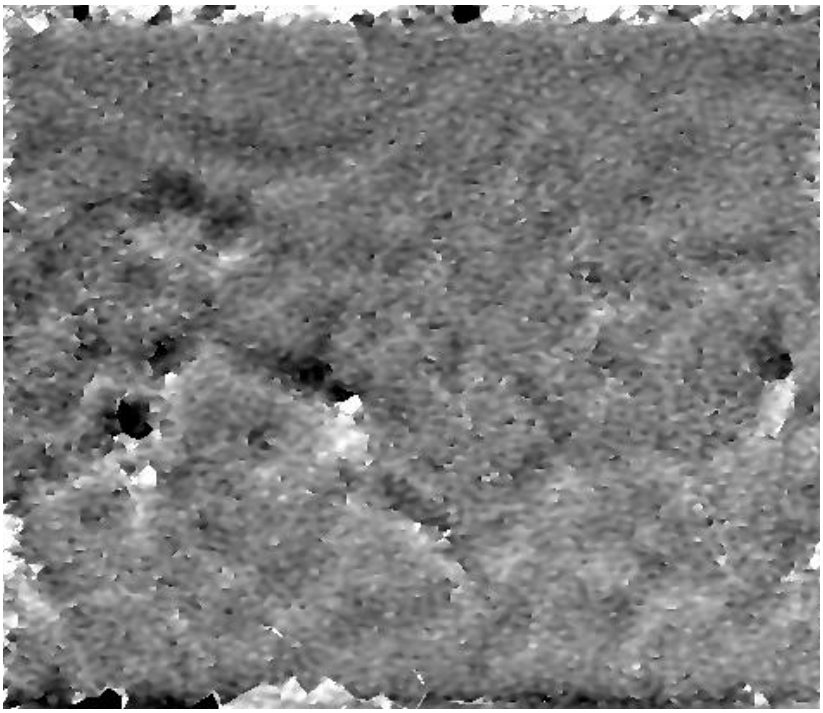

Figure 6.30: Shearography Image of Face 1 Section 2 for Concrete Prism Surface Series Two 100 Days After Freeze-Thaw Treatment

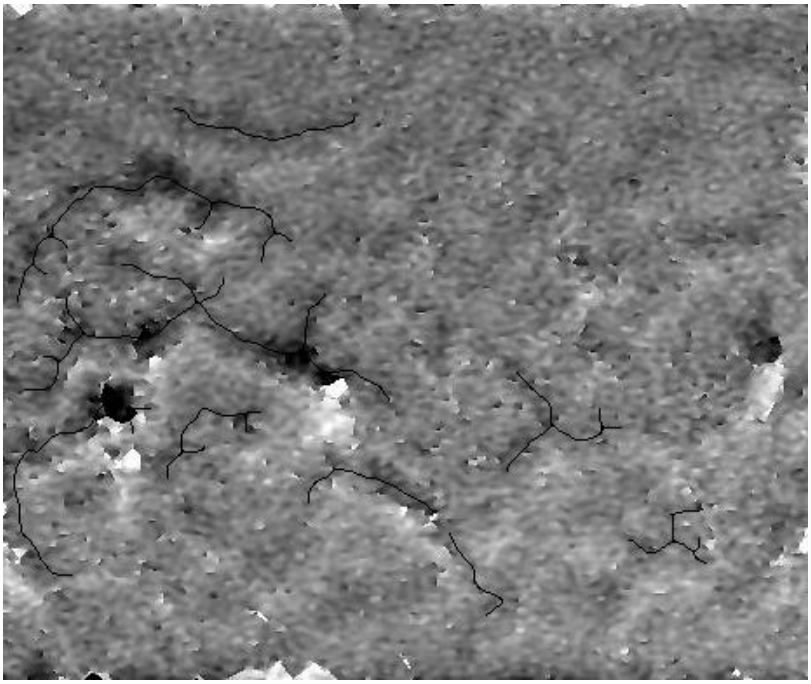

Figure 6.31: Enhanced Shearography Image Face 1 Section 2 for Concrete Prism Surface - Series Two 100 Days After Freeze-Thaw Cycle Treatment

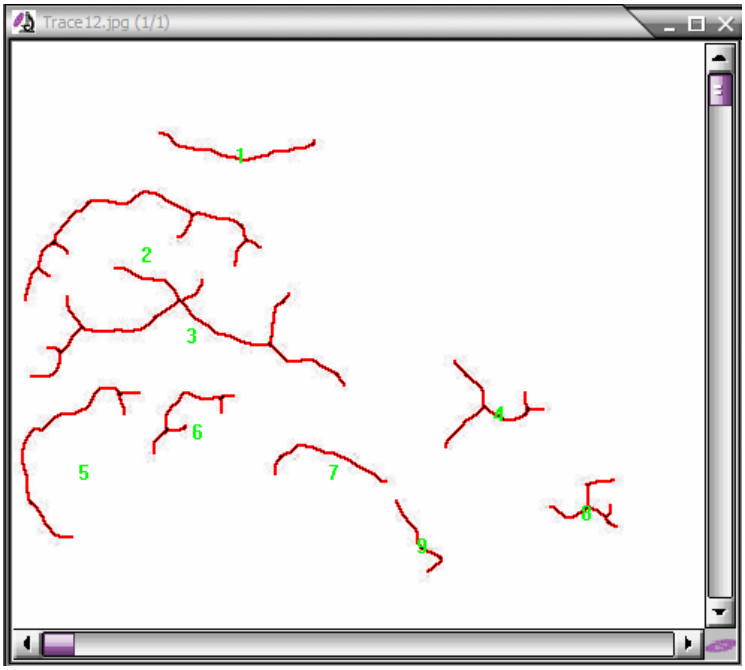

Figure 6.32: Analysis Image of Face 1 Section 2 for Concrete Prism Surface – Series Two After Processing Using Image Pro Plus Software (100 Days After Freeze-Thaw Treatment)

Table 6.14: Image Pro Plus Measurement Data Sheet of Face 1 Section 2 for Series Two 100 Days After Freeze-Thaw Treatment

Object # 12	Area (mm^2)	Aspect Ratio	Angle	Perimeter (mm)	Size (length) mm
1	0.01	7.35	92.98	1.76	0.88
2	0.04	3.09	82.16	3.99	2.00
3	0.05	3.05	93.52	5.72	2.86
4	0.02	1.39	91.82	2.04	1.02
5	0.02	2.29	31.91	2.90	1.45
6	0.01	2.73	56.56	1.62	0.81
7	0.01	4.21	100.38	1.44	0.72
8	0.01	1.30	76.95	1.48	0.74
9	0.01	6.45	147.01	1.02	0.51
Total	0.20			21.97	10.99

Table 6.15: Image Pro Plus Measurement Data Sheet Summary for Series Two After Freeze-Thaw Treatment

Freeze-Thaw Cycle (Series Two) After Treatment			
Face # Sec #(*)	Crack Density	Crack Length (in)	Area of Crack (in^2)
11	5	4.14	0.11
12	11	7.49	0.12
13	6	2.11	0.04
21	0	0.00	0.00
22	8	5.35	0.18
23	7	2.90	0.06
31	0	0.00	0.00
32	16	6.93	0.16
33	10	4.51	0.08
41	7	4.00	0.07
42	7	5.07	0.09
43	20	9.31	0.24
5	5	2.74	0.05
6	3	2.61	0.07
Total	105	57.15	1.26

(*) : 1^{st} digit is face #, 2^{nd} digit is section #.

Table 6.16: Image Pro Plus Measurement Data Sheet Summary for Series Two 100 Days After Freeze-Thaw Treatment

Freeze-Thaw Cycle (Series Two) 100 Days After Treatment			
Face # Sec #(*)	**Crack Density**	**Crack Length (in)**	**Area of Crack (in^2)**
11	9	7.07	0.24
12	9	10.99	0.20
13	8	4.30	0.10
21	0	0.00	0.00
22	8	6.65	0.26
23	15	7.26	0.22
31	0	0.00	0.00
32	20	10.71	0.30
33	17	8.30	0.19
41	13	9.43	0.20
42	12	9.14	0.22
43	21	12.41	0.39
5	7	5.63	0.13
6	8	4.71	0.15
Total	147	96.60	2.60

(*) : 1^{st} digit is face #, 2^{nd} digit is section #.

6.2.2.3 Discussion of Series Two Results

Similar to the results of series one, the results of series two came from the analyzing process of Image Pro Plus software showing the changes in the total number of cracks and cracks' length on each concrete specimen. The comparison was taken to highlight the trend of crack development in concrete subjected to Duggan or Freeze-Thaw treatment. As expected, the cracks occur on the surface of every

specimen at different level. Two parameters, crack length and crack density, were chosen to be compared.

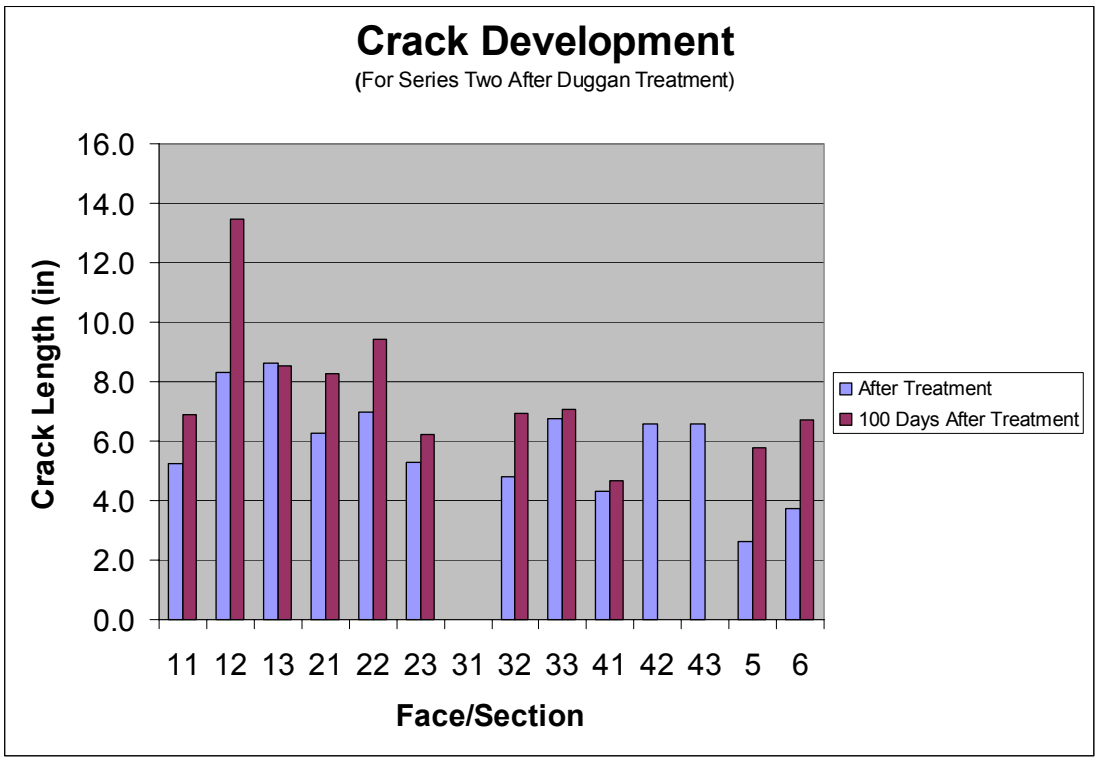

Figure 6.33: Crack development for series two after Duggan Treatment

Cracks appeared on all of the six surfaces of the concrete specimens except for a few sections. These cracks became larger in the overall sizes in lengths and areas after treatments were implemented. A few new cracks appeared after a period of 100 days from the completion of the treatments.

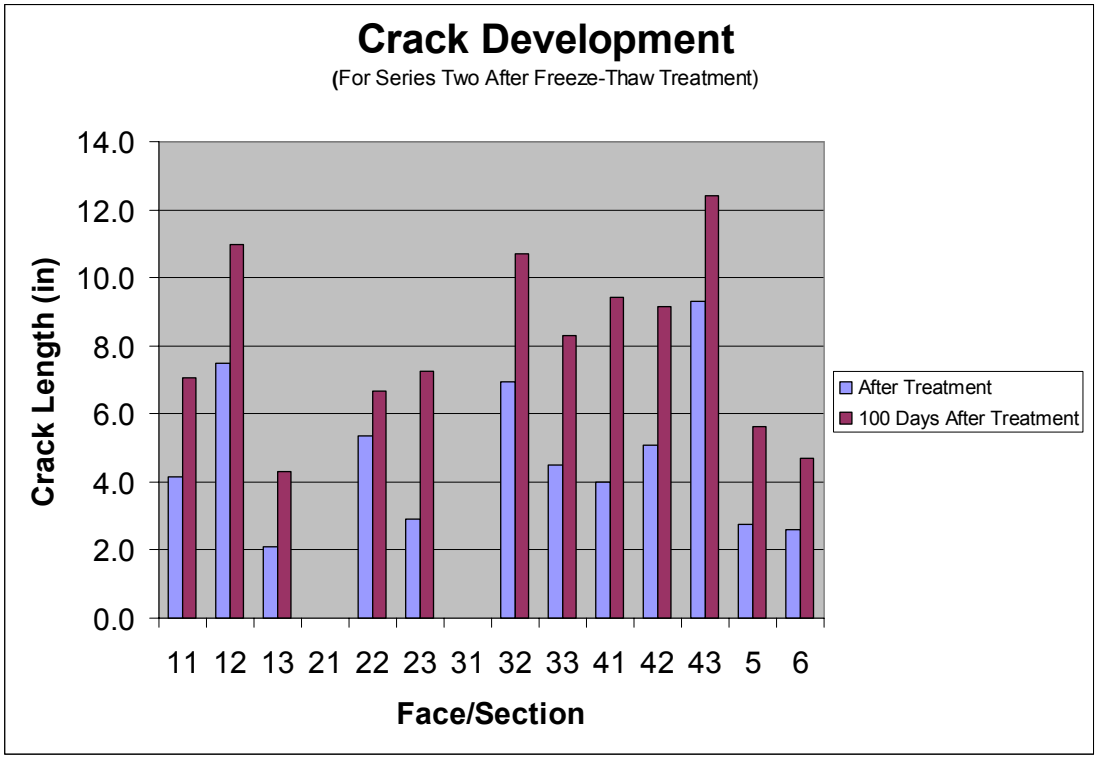

Figure 6.34: Crack development for series two after Freeze-Thaw Treatment

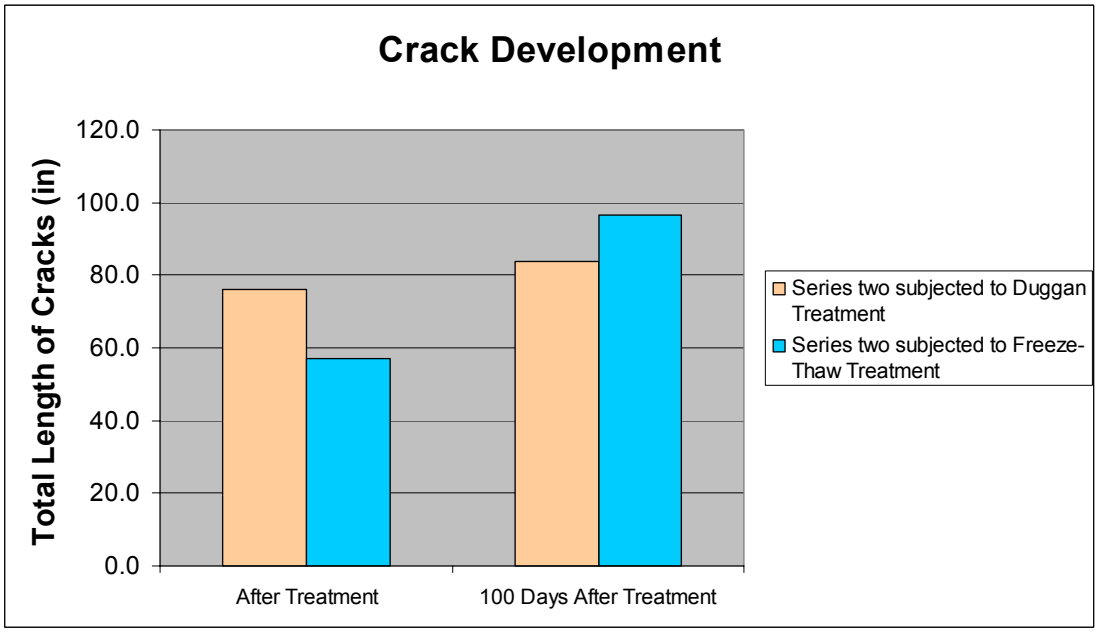

Figure 6.35: Crack development for series two after Duggan and Freeze-Thaw Treatments

Right after treatments, the total length of cracks in concrete specimens subjected to Duggan treatment appeared to be larger than that in concrete specimens subjected to Freeze-Thaw treatment. However, as the sampling process went on, the rate of expansion of crack length in those two specimens showed an opposite relationship: about a 10% increase in Duggan treated specimen and 80% increase in Freeze- Thaw treated specimens. So the conclusion that can be drawn is that Freeze-Thaw treatment affected the concrete specimens more severely than the Duggan treatment did.

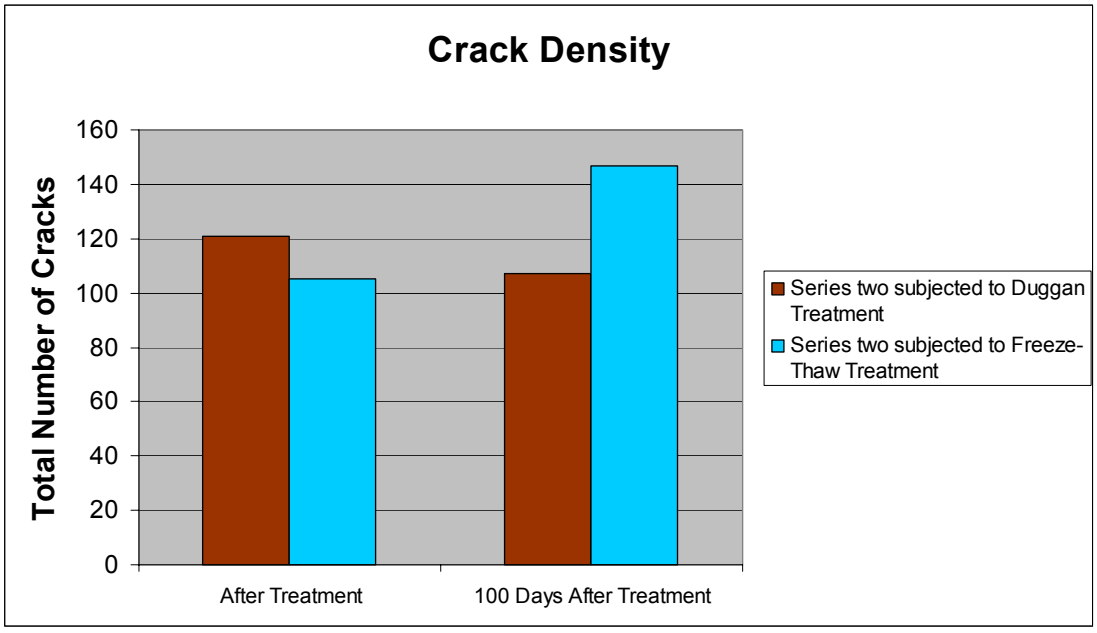

Figure 6.36: Crack density for series two after Duggan and Freeze-Thaw Treatments

The Duggan treatment resulted immediately in a larger number of cracks in the concrete specimen than the Freeze-Thaw treatment did. After 100 days, due to the process of merging existing cracks (two or more cracks merged to form in one new

crack), there was a decline in the total number of cracks in the Duggan treatment specimens. Nevertheless, in the same time period, several new cracks continued to appear on the concrete specimen subjected to Freeze-Thaw treatment.

6.3 Discussion

Comparison was made to highlight the trend of crack development in concrete subjected to Duggan or Freeze-Thaw treatment. As expected, the cracks occurred on the surfaces of every specimen at different levels. Two parameters, crack length and crack density, were chosen to be compared.

6.3.1 Crack Development over Time

Cracks appeared on all of the six surfaces of the concrete specimens except for a few sections where no cracks have shown. This indicates that the concrete originally was not structured homogeneously. These cracks became larger in overall size in lengths and areas, after treatments were implemented. A few new cracks appeared after a period of 100 days from the completion of the treatments. More cracks appeared on the concrete specimen after Freeze-Thaw treatment than Duggan treatment. At the 100^{th} day after treatments, the overall lengths of these cracks also showed a tremendous increase from Freeze-Thaw as supposed to Duggan. This means that permeability of the concrete specimens that was caused by Freeze-Thaw is also greater than Duggan.

Obviously, the total lengths of cracks expanded quicker with series two where potassium carbonate was added. This proves that there is a high influence of

potassium carbonate in crack development, which shows that potassium carbonate does have effects on the delayed etringite formation. This process leads to changes in expansive behaviors in concrete specimens.

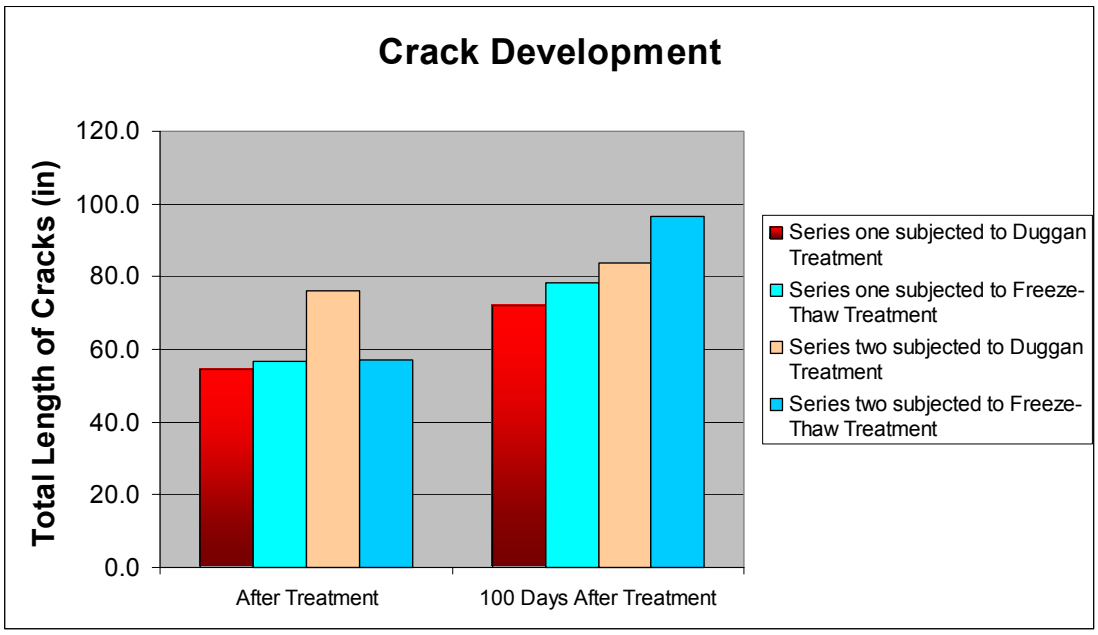

Figure 6.37: Crack development of series one and series two after Treatments

6.3.2 Crack Density

There are increases in lengths and amount of cracks on the surfaces. Like total lengths, the number of cracks appeared to increase a lot more with the concrete that was subjected to Freeze-Thaw treatment than it that subjected to Duggan. Potassium Carbonate also has an effect on the amount of cracks though not as great as the effect on the lengths of cracks.

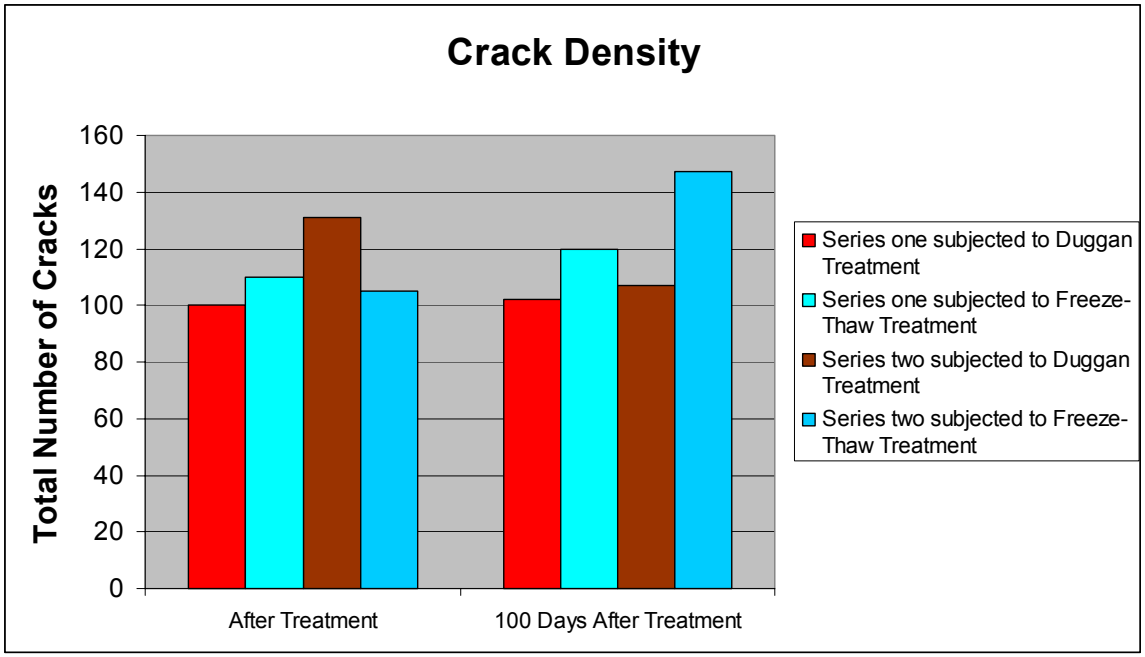

Figure 6.38: Crack Density of series one and series two after Treatments

Chapter 7: Summary and Conclusion

7.1 Summary

Concrete is a commonly used material in the construction industry due to its strength and serviceability. Nevertheless, the effects of physical and chemical elements in the external environment and cement contents in reality limit the practical use of concrete. One of the elements from the external environment that usually affects the durability of concrete in the Northeast U.S. is the Freeze-Thaw process. Besides the Freeze-Thaw cycles, the heat treatment used in the pre-cast concrete industry could also be the cause of poor quality after production of the concrete. Excessive heat could be the problem that allows cracks to form immediately after production. Moreover, this kind of problem is hard to determine at the beginning when the cracks are not visible. Laser Shearography method has been used widely in other industries such as automobiles and aircrafts. Today, this method is also used in detecting cracks on the surfaces of building materials. This research was performed using Laser Shearography Method to explain the different effects of both Duggan and Freeze-Thaw treatments on the initiation of cracks on surfaces of concrete prisms.

7.2 Conclusion.

This research aimed to utilize the Laser Shearography Method to detect cracks on the surfaces of concrete specimens. These cracks occur in the concrete due to many factors such as alkali-silica reaction, delayed ettringite formation and freeze-thaw cycles. However, at the first stage of cracking formation, these cracks are not

visible. There are many methods used to detect the cracks in concrete. However, LSM has many advantages for application in non-destructive testing methods. It is noted that if the cracks in concrete structures are detected when they are still small maintenance for the structures will be easier and will reduce the cost of maintenance. Furthermore, LSM has many advantages such as low cost, provides quick results with high resolution images and is not affected by the external environment. From this research study, the following conclusions can be drawn:

- Laser Shearography Method is successful in detecting the cracks in concrete even when these cracks are invisible to the naked eye.
- The cracks occur in concrete right after the concrete specimens are exposed to either the Duggan Heat Cycle or Freeze-Thaw cycles.
- The additional potassium content in concrete accelerates the rate of cracking formation in both treatments.
- The amount of cracks developed in the concrete specimens treated in the Freeze-Thaw cycles is greater than in those of the Duggan Heat cycle treated.
- The rate of crack development in the Freeze-Thaw cycles treated concrete prisms is also faster than those in the Duggan Heat cycle treated.

7.3 Recommendation.

The LSM is very helpful for the application in NDT of building materials. However, for the application in detecting cracks in concrete, it is not sensitive with the thermal stressing source like with the other materials. The results from the laser shearography image analysis have the limitation of not providing the correct width of

cracks. The stressing source needs to be improved for better laser shearography images.

The Image Analysis Software provides good analysis results from the laser shearography image. It reduces significantly the time of counting and measuring steps. Based on the analysis results, more improvement is needed in reducing noises especially around the edges of the laser shearography images.

References

ASTM, 2001 Annual Book of Standards. Volume 04.02 Concrete and Aggregate. American Society for Testing and Materials, Philadelphia.

Amde, A.M., Ceary, M. and Livingston, R. A., "Investigation of Maryland Bridges for DEFAnd ASR," ICACS 2005 Int. Conf., Chennai, India, January 2005, 809-816, **(*Keynote Paper*).**

Amde, A.M., Williams, K. and Livingston, R.A., "Influence of Fine Aggregate Lithology on DEF In High Early Strength Concrete," *Indo US workshop (sponsored by NSF) on High Performance Cement- based Concrete Composites*, *American Ceramic Society*, Chennai, India, January 2005, 199-209.

Amde, A.M. and Livingston, R.A., "UMD/FHWA Studies on Delayed Ettringite Formation," *International Conference on Advances in Concrete and Construction* (ICACC2004), Hyderabad, India, December 2004, 425-434 (***Keynote Paper***).

Amde, A.M., Ceary, M. and Livingston, R.A., "Investigation of Maryland Bridges for DEF and ASR," J of Structural Engineering, Vol. 32, No. 1, Apr.-May 2005, 33-36.

Amde, A.M., Azzam, A. and Livingston, R.L., "Mitigation of DEF using Class F Fly Ash or Mix Water Conditioner," OWICS 05-Engaging the Future, Singapore, August 2005, 191-198, (**Bauchemie Award 2005 for Best Paper**).

Amde, A.M., Livingston, R. L. and Azzam, A., "Influence of Alkali Content and Development of Accelerated Test Method for Delayed Ettringite Formation," *Proceedings of the International Innovative world of Concrete Conference*, Pune, India, 2003.

Amde, A.M., Ceary, M. and Livingston, R., "Measurement of Expansion Associated with DEF," *106th Annual meeting & Exposition of the American Ceramic Society*, Indianapolis, 2003.

Amde, A.M., Ceary, M. and Livingston, R., "Correlation Between Map Cracking and DEF in Field Specimens," *The 11th Int. Conf. on Fracture*, Turin, Italy, Sec.15, #4526, Mar. 2005.

Amde, A. M., K. Williams, et al. (2004). Influence of Fine Aggregate Lithology on Delayed Ettringite Formation in High Early Strength Concrete:MD-04-SP. Baltimore, Maryland State Highway Administration.

Batic, O.R., Milanesi, C.A., Maiza, P.J., Marfil, S.A., [2000], "Secondary ettringite formation in concrete subjected to different curing conditions," *Cement and Concrete Research*, Vol. 30, 2000, p. 1407-1412.

Bisle, W.J., Scherling, D., Tober, G., [1994], "Phase Stepping Shearography for Testing Commercial Aircraft Structures", *Rev. of og. In Pr QNDE* Vol. 15, Seattle.

Bonen, D. and Diamond, S., [1995], "Characteristics of delayed ettringite deposits in ASRaffected steam-cured concretes," *Proceedings of the Material Research Society's Symposium on Mechanisms of Chemical Degradation of Cement-Based Systems*, Boston, USA, 27-30 November, 1995, p. 297-304.

Campbell, G.M. and Detwiler, R.J., [1993], "Development of mix designs for strength and durability of steam-cured concrete," *Concrete International*, July 1993, Vol. 20, p. 37-39.

Cao,Y. and Detwiler, R.J., [1995], "Backscattered electron imaging of cement pastes cured at elevated temperature," *Cement and Concrete Research*, Vol. 25, No. 3, 1995, p. 627-638.

Ceesay, J., [2004], "The Influence of Exposure Conditions on Delayed Ettringite Formation in Mortar Specimens," *Master Thesis,* University of Maryland, 2004.

Chatterji, S., Thaulow, N. and Jensen, A.D., [1987], "Studies of the alkali-silica reaction Part 4: effect of different alkali salt solutions on expansion," *Cement and Concrete Research*, Vol. 17, 1987, p. 777-783.

Cohen, M.D. and Richards, C.W., [1982], "Effects of the Particle Sizes of Expansive Clinker on Strength – Expansion Characteristics of Type K Expansive Cements," Cement and Concrete Research, Vol. 12, No. 6 pp. 717-725.

Cohen, M.D., Campbell, E. and Fowle, W., [1985], "Kinetics and Morphology of Ettringite Formation," Proc. 7th Int. Conf. Cem. Microsc., Ed. James Bayles, pp. 360-381.

Collepardi, M., Monosi, S., Moriconi, G., Pauri, M., [1984], "Influence of gluconate, lignosulphonate, and glucose on the C3A hydration in the presence of gypsum with or without lime," *Cement and Concrete Research*, Vol. 14, 1984, p. 105-112.

Collepardi, M., [1999], "Damage by Delayed Ettringite Formation – A Holistic Approach and New Hypothesis," *Concrete International*, Vol. 21, No. 1, pp. 69-74.

Collepardi, M., [2003], "A state-of-the-art review on delayed ettringite attack on concrete," *Cement and Concrete Composites*, Vol. 25, 2003, p. 401-407.

Copeland, L. E., Bodor, E., Chang, T. N. and Weise, C. H., [1967], "Reactions of Tobermorite Gel with Aluminates, Ferrites, and Sulfates" *Journal of The PCA Research and Development Laboratories* Vol. 9, No. 1, Portland Cement Association.

Daerr, G.M., Punzet, M., Ludwig, U., [1977], "On the Chemical and Thermal Stability of Ettringite on Dehydration I," Cem. Summ. Contrib. Semin., pp. 42-45.

Day, R.L., [1992], "The effect of secondary ettringite formation on the durability of concrete: a literature analysis," *Research and Development Bulletin RD 108T*, *Portland Cement Association*, Skokie Illinois, 1992. Also in Civil Engineering Report CE 92-2, *Department of Engineering, University of Calgary*, 113 p., PCA Project 92-05, May 1992.

Deng, M. and Tang, M., [1994], "Formation and Expansion of Ettringite Crystals," Cement and Concrete Research, Vol. 24, pp. 119-126.

Detwiler, R.J., Kjellsen, K.O., and Gjorv, O.E., [1991], "Resistance to chloride intrusion of concrete cured at different temperatures," *ACI Materials Journal*, Vol. 88, No. 1, Jan-Feb 1991, p. 19-24.

Detwiler, R.J., Fapohunda, C.A, and Natalie, J., [1994], "Use of supplementary cementing materials to increase the resistance to chloride ion penetration of concretes cured at elevated temperatures," *ACI Materials Journal*, Vol. 91, No. 1, Jan-Feb, 1994, p. 63-66.

Detwiler, R.J., Whiting, D.A., Gaida, J.W., [1997], "Comments on 'Durability aspects of precast prestressed concrete-Parts 1 and 2', by Sherman, M.R., McDonald, D.B., and Pfeifer, D.W.," *PCI Journal,* May-June 1997, p. 65-66.

Detwiler, R.J. and Powers-Couche, L.J., [1997], "Effect of sulfates in concrete on its resistance to freezing and thawing," *PCA R&D Serial No. 2128b*, 1997, 25 p.

Diamond, S., [1996], "Delayed ettringite formation-processes and problems," *Cement and Concrete Composites*, Vol., 18, No. 3, p. 205-215.

Diamond, S., [1999], "Unique response of LiNO3 as an alkali silica reaction preventive admixture," *Cement and Concrete Research*, Vol. 29, 1999, p. 1271-1275.

Diamond, S. and Leeman, M.E., [1995], "Pore size distributions in hardened cement paste by SEM image analysis," *Materials Research Society Proceedings*, Vol. 370, 1995, p. 217-226.

Diamond, S. and Ong, S., [1994], "Combined effects of alkali-silica reaction and secondary ettringite deposition in steam-cured mortars," *Cement Technology*, (Ed. E.M. Gartner and H. Uchikawa), Ceramic Transactions, Vol. 40, American Ceramic Society, Westerville, Ohio, 1994, p. 79-90.

Famy, C., [1999], "Expansion of heat-cured mortars," *Ph.D. Thesis*, University of London, September 1999, p. 256.

Famy, C., Scrivener, K.L., Brough, A.R., Atkinson, A., [2001], "Influence of the Storagge Conditions in the Dimensional Changes of Heat-Cured Mortars," Cem. Concr. Res. Vol. 31, pp. 795-803.

Famy, C., Scrivener, K.L., Atkinson, A., Brough, A.R., [2002], "Effects of an early or late heat treatment on the microstructure and composition of inner C-S-H products of Portland cement mortars," *Cement and Concrete Research*, Vol. 32, No. 2, 2002, p. 269-278.

Findeis, D., Gryzagoridis, J., Rowland, D., "Vibration Isolation Techniques suitable for portable Electronic Speckle Pattern Interferometry", *Proceedings of Nondestructive Evaluation and Health Monitoring of Aerospace Materials and Civil Infrastructure, A L Gyekenyesi et al*, Vol. 4707, pp159-167, SPIE, Washington, 2002.

Findeis, D., Gryzagoridis, J., "A comparison of the Capabilities of Portable Shearography and Portable Electronic Speckle Pattern Interferrometry", *Proceedings of Nondestructive Evaluation and Health Monitoring of Aerospace Materials and Civil Infrastructure,* P J Skull, v5393, pp41-49, 2004.

Fu Y. and Beaudoin, J.J., [1996a], "Microcracking as a precursor to delayed ettringite formation in cement systems," *Cement and Concrete Research*, Vol. 26, No. 10, 1996, p.1493-1498.

Fu Y. and Beaudoin, J.J., [1996b], "Letter to the Editor on the distinction between delayed and secondary ettringite formation in concrete," *Cement and Concrete Research*, Vol. 26, No.6, June 1996, p. 979-980.

Fu, Y., Ding, J., Beaudoin, J.J., [1997], "Expansion of Portland cement mortar due to internal sulfate attack," *Cement Concrete Research*, Vol. 27, No. 9, p. 1299-1306.

Glasser, F.P., [1996], "The role of sulphate mineralogy and cure temperature in delayed ettringite formation," *Cement and Concrete Composites*, Vol. 18, No.3, 1996, p. 187-193.

Glasser, F.P., Damidot, D., and Atkins, M., [1995], "Phase development in cement in relation to the secondary ettringite problem," *Advances in Cement Research*, Vol. 7, No. 26, April 1995, p. 57-68.

Grabowski, E., Czarnecki, B., Gillot, j.E., Duggan, C.R., Scott, J.F., [1992], "Rapid test of concrete expansivity due to internal sulfate attack," *ACI Materials Journal*, Sep-Oct 1992, p. 469-480.

Heinz, D., Kalde, M., Ludwig, U. and Ruediger, I., [1999], "Present state of investigation on damaging late ettringite formation (DLEF) in mortars and concretes," in *Ettringite-The Sometimes Host of Destruction, ACI Spring Convention*, Seattle, USA, SP-177, Ed. B. Erlin.

Heinz, D. and Ludwig, U., [1986], "Mechanism of subsequent ettringite formation in mortars and concretes after heat treatment," *Proceedings of the 8th International Congress on the Chemistry of Cement*," Rio de Janeiro, Brasil, Vol. V, Theme 4, September, 22-27, 1986, p.189-194.

Heinz, D. and Ludwig, U., [1987], "Mechanism of secondary ettringite formation in mortars and concretes subjected to heat treatment," in *Concrete Durability, Katharine and Bryant Mather International Conference, (J.M. Scanlon, Ed.),* SP-100, Vol. 2, American Concrete Institute, Detroit, p. 2059-2071.

Heinz, D, Ludwig, V., and Rudinger, I., [1989], "Delayed ettringite formation in heat-treated mortars and concretes," *Concrete Precasting Plant and Technology*, Vol. 11, 1989, p. 56-61.

Hung, Y.Y. [2000], "Digital Shearography and applications" *Trends in Optical Non-destructive Testing and Inspection,* pp287-308, Elsevier, (Editor: Pramond K. Rastogi and Daniele Inaudi).

Hung, Y.Y., Shang, H.M. and Yang, L.X., [2003], "Unified approach for holography and shearography in surface deformation measurement and nondestructive testing", *Opt. Eng*. 42 (5), p. 1197-1207.

Johansen V. and Thaulow N., [1997], "Heat curing and late formation of ettringite," ACI, Seattle, (Program on *Ettringite-The Sometimes Host of Destruction*, (B.Erlin, Ed.), ACI SP-177, 1999, p. 47-64), April 1997.

Johansen V., Thaulow N. and Skalny, J., [1993a], "Simultaneous presence of alkali-silica gel and ettringite in concrete," *Advances in Cement Research*, Vol. 5, No. 17, p. 23-29.

Kalousek, G.L., [1965], "Analyzing SO3-bearing phases in hydrating cements," *Materials Research and Standards*, Vol. 5, No.6, June 1965, p. 262-304.

Kalousek G.L and Benton, E.J., [1970], "Mechanism of seawater attack on cement pastes," *ACI Journal*, Proceedings, Vol. 67, No. 2, February 1970, p. 187-192.

Kelham, S., [1996], "The effect of cement composition and fineness on expansion associated with delayed ettringite formation," *Cement and Concrete Composites*, Vol. 18, No.3, 1996, p.171-179.

Kennerley, R.A., [1965], "Ettringite formation in dam gallery," *Journal of the American Concrete Institute*, Title No. 62-35, May 1965, p. 559-573.

Kjellsen, K.O., and Detwiler, R.J., [1992], "Reaction kinetics of Portland cement mortars hydrated at different temperatures," *Cement and Concrete Research,* Vol. 22, 1992, p. 112-120.

Kjellsen, K.O., Detwiler, R.J. and Gjorv, O.E., [1990], "Pore structure of plain cement pastes hydrated at different temperatures," *Cement and Concrete Research*, Vol. 20, No. 6, p. 927-933.

Kjellsen, K.O., Detwiler, R.J. and Gjorv, O.E., [1991], "Development of microstructure in plain cement pastes hydrated at different temperatures," *Cement and Concrete Research*, Vol.21, No. 1, January 1991, p. 179-189.

Klieger, P., [1958], "Effect of mixing and curing temperature on concrete strength," *ACI Journal*, Vol. 54, No. 12, p. 1063-1082, June 1958. Also Research Bulletin Dept., Bulletin 103, *Portland Cement Association.*

Klieger, P., [1960], "Some aspects of durability and volume change of concrete for prestressing," *Journal, PCA Research and Development Laboratories*, Vol. 2, No. 3, p. 2-12, September 1960. Also in Research Department Bulletin 118, *Portland Cement Association.*

Kurdowski, W., [2002], "Role of delayed release of sulphates from clinker in DEF," *Cement and Concrete Research*, Vol. 32, No. 3, p. 401-407.

Kuzel, H.-J., [1996], "Initial hydration reactions and mechanisms of delayed ettringite formation in Portland cements," *Cement and Concrete Composites*, Vol. 18, No.3, 1996, p.195-203.

Kuzel, H.-J. and Pöllmann, H., [1991], "Hydration of C3A in the presence of Ca(OH)2, CaSO4.2H2O and CaCO3," *Cement and Concrete Research*, Vol. 21, No.5, 1991, p. 885-895.

Lawrence, C.D., [1995a], "Delayed ettringite formation: an issue?," in *Materials Science of Concrete IV (J. Skalny and S. Mindess, Eds), American Ceramic Society*, Westerville, OH, USA, 1995, p. 113-154.

Lawrence, C.D., [1995b], "Mortar expansions due to delayed ettringite formation. Effects of curing period and temperature," *Cement and Concrete Research*, Vol. 25, No. 4, may 1995, p.903-914.

Lawrence, B.L., Myers, J.J. and Carrasquillo, R.L., [1997], "Premature concrete deterioration in texas department of transportation precast elements," presented at

ACI Spring Convention, Seattle, April 1997. Also in *Ettringite-The Sometimes Host of Destruction*," (B. Erlin, ed.), ACI SP-177, 1999, p. 141-158.

Lerch, W. and Ford, C. L., [1948], "Long-Time Study of Cement Performance in concrete – Chapter 3. Chemical and Physical Testing of Cements," Journ. Amer. Concr. Inst., Proceedings, Vol. 44, pp. 743-795..

Livingston, R. A., C. Ormsby, A. M. Amde, M. Ceary, N. McMorris and P. Finnerty (2006). "Field Survey of Delayed Ettringite Formation Related Damage in Concrete Bridges in the State of Maryland." *CANMET Conference on Durability of Concrete*, Montreal, CANADA: in press.

Livingston, R. A., M. Ceary and A. M. Amde (2002). "Statistical Sampling Design for a Field Survey of Delayed-Ettringite-Formation Damage in Bridges." *Structural Materials Technology V : An NDT Conference*, Cincinnati, OH, ASNT: 411-420.

Livingston, R. A. & Amde, A. M. (2001a). "Nondestructive Test Field Survey for Assessing the Extent of Ettringite-related Damage in Concrete Bridges." in *Nondestructive Characterization of Materials X* (eds. Green, R. E., Kishi, T., Saito, T., Takeda, N. & Djordjevic, B. B.), Elsevier Science Ltd., Oxford: 167-174.

Livingston, R.A., Amde, A.M. and Ramadan, E. (2001b). "Characterization of Damage in Portland Cement Concrete Associated with DEF." *Proc. of the 6th Int. Conf. CONCREEP 6 @ MIT* (eds. Ulm, Bazant, and Wittmann), Elsevier, Cambridge: 463 – 468.

Livingston, R. A., H. H. Saleh, E. O. Ramadan and A. M. Amde (2001c). Characterization of Damage in Portland Cement Concrete Associated with Delayed Ettringite Formation. *Creep, Shrinkage and Durabiity Mechanics of Concrete and Other Quasi-Brittle Materials*, Amsterdam, Elseveier: 463-468.

Ludwig, U., [1991], "Problems of the reformation of ettringite in heat cured mortars and concretes," *11th International Building Materials and Silicate Convention*, Weimar, Germany, Vol. 1, May 6-10, 1991, p. 164-177.

Marks, V.J and Dubberke, W.G., [1996], "A different perspective for investigation of Portlandcement concrete deterioration," *Transportation Research Record*, No. 1525, 1996, p. 91-96.

Maslehuddin, M., Shirokoff, J., and Siddiqui, M.A.B., [1996], "Changes in the phase composition in OPC and blended cement mortars due to carbonation," *Advances in Cement Research*, Vol. 8, No. 32, October 1996, p. 167-173.

Mather, K., [1978], "Tests and evaluation of Portland and blended cements for resistance to sulfate attack," *American Society for Testing and Materials*, *ASTM STP 663*, P.K. Mehta, Ed.,1978, p. 74-86.

McCoy, W.J., and Caldwell, A.G., [1951], "A new approach to inhibiting alkali-aggregate expansion," *Journal of the American Concrete Institute*, Vol. 41, p. 693-706.

Mehta, P.K., [1973], "Mechanism of Expansion Associated with Ettringite Formation," *Cement and Concrete Research*, Vol. 3, No. 1, pp. 1-6.

McGrath, P.F., and Hooton, R.D., [1999], "Re-evaluation of the AASHTO T259 90-day salt ponding test," *Cement and Concrete Research*, Vol. 29, 1999, p. 1239-1248.

Midgley, H.G., and Illston, J.M, [1983], "The penetration of chlorides into hardened cement pastes," *Cement and Concrete Research*, Vol. 14, No. 4, 1983, p. 546-558.

Mielenz, R.C, Marusin, S.L., Hime, W.G., and Jugovic, Z.T., [1995], "Investigation of prestressed concrete railway tie distress," *Concrete International*, Dec. 1995, p. 62-68.

Miller, F. M., and Tang, F. J., [1996], "The Distribution of Sulfur in Present-Day Clinkers of Variable Sulfur Content," *Cement and Concrete Research*, Vol. 26, pp. 1821-1829.

Mitchel, L.J., [1953], "Thermal expansion tests on aggregates, neat cements and concretes," *ASTM*, 1953, p. 963-977.

Monterio, P.J.M. and Mehta, P.K., [1985], "Ettringite formation on the aggregate-cement pasteinterface," *Cement and Concrete Research*, Vol. 15, No. 2, March 1985, p. 378-380.

Monterio, P.J.M., Mehta, P.K., [1986], "Interaction between carbonate rock and cement paste," *Cement and Concrete Research*, Vol. 16, No. 2, 1986, p. 127-134.

Neville, A.M., [1970], "*Creep of concrete: plain, reinforced and prestressed*," North-Holland Publishing Company, Amsterdam, 1970.

Neville A.M., [1996], "*Properties of concrete*," 4th Edition, New York, John Wiley and Sons Inc., 1996.

Newman, J. W., Amde, A. M., Ceesay, J. & Livingston, R. A. (2006), "Development of a Portable Laser Shearography system for Crack Detection in Bridges", *ASNT Smart Materials and Technology in prep.*

Oberholster, R.E., Maree, H., Brand, J.H.B, [1992], "Cracked prestressed concrete railway sleepers: alkali-silica reaction or delayed ettringite formation," *Proceedings of the 9th International Conference on Alkali-Aggregate Reaction in Concrete*, ACI London, Vol. 2, 1992, p. 739-749.

Odler, I., [1985], "Crack formation during heat curing of concrete," *Beton*, 6, 1985, p. 235-237.

Odler, I. and Chen, Y., [1995], "Effect of cement composition on the expansion of heat cured cement pastes," *Cement and Concrete Research*, Vol. 25, No.4, May 1995, p. 853-862.

Odler, I. and Chen, Y., [1996], "On the delayed expansion of heat cured Portland cement pastes and concretes," *Cement and Concrete Composites*, Vol. 18, 1996, p. 181-185.

Pettifer, K. and Nixon, P.J., [1980], "Alkali-metal sulphate-a factor common to both alkaliaggregate reaction and sulfate attack on concrete," *Cement and Concrete Research*, Vol. 10, No.2, March 1980, p. 173-181.

Pfeifer, D.W. and Landgren, J.R., [1991], "A Laboratory study for plant produced prestressedconcrete," *Prestressed Concrete Institute*, Technical Report No. 1, 1991.

Pfeifer, D.W. and Marusin, S., [1991], "Energy efficient accelerated curing of concrete," a state-of-the-art review, *Prestressed Concrete Institute*, Technical Report No. 1, 1991

Prince, W., Edwards-Lajnef, M., Aïtcin, P.-C., [2002], "Interaction between ettringite and a polynaphthalene sulfonate superplasticizer in a cementitious paste," *Cement and Concrete Research*, Vol. 32, No.1, p. 79-85.

Radzy, F. and Richards, C.W., [1973], "Effect of curing and heat treatment history on the dynamical mechanical response and the pore structure of hardened cement paste," *Cement and Concrete Research*, Vol. 3, No.1, 1973, p. 7-21.

Ramlochan, T., [2003], "The effect of pozzolans and slag on the expansion of mortars and concretes cured at elevated temperatures," *Ph.D. Thesis*, Dept. of Civil Engineering, University of Toronto.

Robertson, B. and Mills, R.H., [1985], "Influence of sorbed fluids on compressive strength of cement paste," *Cement and Concrete Research*, Vol. 15, 1985, p. 225-232.

Rosenberg, A.M., [1964], "Study of the mechanism through which calcium chloride accelerates the set of Portland cement," *Journal of the American Concrete Institute, Proceedings,* Vol. 61, No. 10, October, 1964, p. 1261-1269.

Roy, D.M. and Parker, K.M., [1983], "'*Microstructures and properties of granulated slag- Portland cement blends at normal and elevated temperatures*,' Fly ash, silica fume, slag and other mineral by-products in concrete," V.M. Malhotra, Ed., SP-79, American Concrete Institute, Detroit, 1983, p. 397-414.

Scrivener, K.L. and Taylor, H.F., [1993], "Delayed ettringite formation: a microstructural and microanalytical study," *Advances in Cement Research*, Vol. 5, No. 20, October 1993, p. 139-146.

Shao, Y., Lynsdale, C.J., Lawrence, C.D., and Sharp, J.H., [1997], "Deterioration of heatcured mortars due to the combined effect of delayed ettringite formation and freeze-thaw cycles," *Cement and Concrete Research*, Vol. 27, No.11, Nov. 1997, p. 1761-1771.

Shayan, A. and Ivanusec, I., [1996], "An experimental clarification of the association of delayed ettringite formation with alkali-aggregate reaction," *Cement and Concrete Composites*, Vol. 18, 1996, p. 161-170.

Shayan, A. and Quick, G.W., [1992a], "Relative importance of deleterious reactions in concrete: formation of AAR products and secondary ettringite," *Advances in Cement Research*, Vol. 4, No. 16, p. 149-157.

Shayan, A. and Quick, G.W., [1992b], "Microscopic features of cracked and uncracked concrete railway sleepers," *ACI Materials Journal*, Vol. 89, No.4, July-August 1992, p. 348-361.

Skalny J. and Odler, I., [1967], "The effect of chlorides upon the hydration of Portland cement and upon some clinker minerals," *Magazine of Concrete Research,* December 1967, Vol. 19, No. 61, p. 203-210.

Skalny, J. and Odler, I., [1972], "Pore structure of calcium silicate hydrates," *Cement and Concrete Research,* Vol. 2, No. 4, July-August 1972, p. 387-400.

Skalny, J. P., Johansen, V., Thaulow, N., and Palomo, A., [1996], "DEF as a form of sulfate attack," *Materiales de Construcción,* Vol. 46, No. 244, October-November-December 1996, p. 5-29.

Steinchen, W., Yang, L., [2003] "Digital Shearography: Theory and Application of Digital Speckle Pattern Shearing Interferometry" (*SPIE PRESS Monograph Vol. PM100*), Bellingham, WA, SPIE, p.330.

Sylla, H-M, [1988], "Reactionen im zementstein durch wärmebehandlung (Reactions in cement paste due to heat treatment)," *Beton*, Vol. 38, No. 11, 1988, p. 449-454.

Taylor, H.F.W, [1994], "Delayed ettringite formation," *Advances in Cement and Concrete* (M.W. Grutzeck and S.L. Sarkar, Eds.), American Society of Civil Engineers*,* New York, p.122-131.

Taylor, H.F.W, [1996], Guest Editorial, *Cement and Concrete Composites*, 1996, p. 157-159.

Tepponen, Pirjo and Ericksson, Bo-Erik, [1987], "Damages in concrete railway sleepers in Finland," *Nordic Concrete Research*, No. 6, 1987, p. 199-209.

Tikalsky, P.J , and Carrasquillo, R.L., [1989], "The Effect of Fly Ash on the Sulfate Resistance of Concrete," Research report 481-5, *Center for Transportation Research*, The University of Texas at Austin.

Thaulow, N. and Jacobsen, U.H., [1995], "The diagnosis of chemical deterioration of concrete by optical microscopy," Proceedings of the *Materials Research Society's Symposium on Mechanisms of Chemical Degradation of Cement-Based Systems*," Boston, USA, 27-30, Nov. 2995, p. 1-13.

Thaulow, N., Johansen, V. and Hjorth Jacobsen, V., [1996], "What caused Delayed Ettringite Formation?," *Ramboll Bulletin* No. 60, pp. 8.

Yang, R., [1998], "Mechanism of delayed ettringite formation," *Ph.D. Thesis*, Department of Engineering Materials, The University of Sheffield.

Yang, R., Lawrence, C.D. and Sharp, J.H., [1996], "Delayed ettringite formation in 4-year old cement pastes," *Cement and Concrete Research*, Vol. 26, No. 11, Nov. 1996, p. 1649-1659.

Yang, R., Lawrence, C.D. and Sharp, J.H., [1999a], "Effect of type of aggregate on delayed ettringite formation," *Advances in Cement Research*, Vol. 11, No. 3, p. 119-132.

Yang, R., Lawrence, C.D., Lynsdale, C.J. and Sharp, J.H., [1999b], "Delayed ettringite formation in heat-cured Portland cement mortars," *Cement and Concrete Research*, Vol. 29, No. 1, p. 17-25.

Young, J.F. and Mindess, S., [1981], "Concrete," Prentice – Hall, Inc, Englewood Cliffs, New Jersey.

Young, J. F., Mindess, S. and Darwin, D., [2002], "Concrete," 2nd Edition, Prentice Hall, Inc.

Zhang, Z., Olek, J., Diamond, S., [2002a], "'Studies on delayed ettringite formation in earlyage, heat-cured mortars,' I. Expansion measurements, Changes in dynamic modulus of elasticity, and weight gains. II. Characteristics of cement that may be susceptible to DEF," *Cement and Concrete Research*, Vol. 32, No.11, p. 1729-174